THESIS FOR THE DEGREE OF LICENTIATE OF ENGINEERING

Recycling of nickel metal hydride (NiMH) batteries

Characterization and recovery of nickel, AB_5 alloy and cobalt

Filip Holmberg

Industrial Materials Recycling
Department of Chemistry and Chemical Engineering
CHALMERS UNIVERSITY OF TECHNOLOGY
Gothenburg, Sweden 2017

Recycling of nickel metal hydride (NiMH) batteries
Characterization and recovery of nickel, AB_5 alloy and cobalt

FILIP HOLMBERG

Licentiatuppsatser vid Institutionen för kemi och kemiteknik
Chalmers tekniska högskola.
Nr 2017:09

Industrial Materials Recycling
Department of Chemistry and Chemical Engineering
Chalmers University of Technology
SE-412 96, Gothenburg
Sweden
Telephone: +46 (0) 31-772 1000
filip.holmberg@chalmers.se

Cover:
The cover image shows SEM micrographs of three components used in nickel metal hydride batteries, in the following order from back to front: nickel hydroxide particle (cathode), conductive metallic nickel powder (cathode and anode) and spent hydrogen storage alloy (anode).

Chalmers Reproservice
Gothenburg, Sweden, 2017

Recycling of nickel metal hydride (NiMH) batteries

FILIP HOLMBERG

Industrial Materials Recycling
Department of Chemistry and Chemical Engineering
Chalmers University of Technology

ABSTRACT

Nickel metal hydride (NiMH) batteries are used today for applications that can assist in the adaptation toward carbon-neutral energy sources (i.e. hybrid vehicles and smart grids). Recovery of metals such as nickel, cobalt and rare earth elements (REEs) from discarded NiMH batteries is important for economic and/or technological reasons. Recirculation of valuable materials back into society can be achieved by the production of pure concentrates of elements from waste, or by regenerating and reusing materials.

Recycling of NiMH batteries can be done through pyro- and hydrometallurgical methods, which produces pure and valuable metal fractions. The current work focuses on the separation of three different types of material from NiMH waste: (1) metallic nickel powder, (2) reusable hydrogen storage alloy (i.e. AB_5) and (3) cobalt-enriched surface compounds.

Bipolar NiMH batteries were investigated in this work, which are different in design compared to previous investigations on recycling of batteries. In these batteries the conductive nickel network is made up of nickel powder, instead of conventional nickel foam grids.

Previous investigations suggest that spent electrode materials are not completely degraded. Reusing parts of the discarded NiMH battery has however not yet been commercially realized. For the current work spent NiMH batteries were characterized separately. Corrosion products form on the anode particles during battery cycling, and in this work rare earth hydroxides (i.e. $REE(OH)_3$) were identified. The hydrogen storage alloy can potentially be reused if corrosion products are removed.

In the current work it was re-confirmed that nickel, even in powder form, can be recovered by dissolution of the waste matrix using hydrochloric acid. Cyanex 923 was briefly considered for treating the leachate solution. The extraction of REEs and aluminum from the leachate was affected by the amount of acid present, which was attributed to preferential extraction of acid. Controlling the acid in the dissolution step is therefore important in order to further treat leachate solutions.

The relatively novel recycling approach of recovering AB_5 alloy using carboxylic (malonic, maleic, acetic and citric) acid was considered. An interesting result was that $REE(OH)_3$ could be removed using acetic and citric acid, without dissolving much of the remaining spent AB_5 alloy. The practical uses were otherwise limited due to similar dissolution rates of the AB_5 alloy and other waste matrix.

A novel recycling approach of using ascorbic acid was suggested and tested. Separation of the cobalt layers from the cathode hydroxide particles is possible because these cobalt layers have different oxidation states (higher than 2) compared to the waste matrix. The ascorbic acid treatment does not dissolve the anode material. Ascorbic acid can therefore potentially be used as a pre-step to chemically separate the anode material from the cathode material in a mixed electrode waste flow.

LIST OF PUBLICATIONS

This thesis is based on the work contained in the following paper:

Paper I:

Holmberg F., Gutknecht T., Cao, Y., Ekberg C., Steenari B.M. *Selective dissolution of cobalt from spent nickel metal hydride (NiMH) batteries using ascorbic acid*, Manuscript.

Contribution Report:

Major experimental work, data treatment, evaluation and major part of writing the manuscript

Table of contents

ABBREVIATIONS

Battery cycling	continuous charge and discharge of battery cells
Ni(s)	metallic nickel
AB_5 alloy	hydrogen storage alloy. In this work this refers to the AB_5 type
$Ni(OH)_2$	the cathode active material consisting of nickel hydroxide that has been doped with Co and Zn. The particles of this material have been coated with cobalt and this is also included in the abbreviation. Conductive nickel network is not included in this abbreviation.
REE	rare earth element. In this work REE refers to lanthanum, cerium, praseodymium and neodymium
$REE(OH)_3$	rare earth element (La, Ce, Pr, Nd) hydroxides
SHE	standard hydrogen electrode potential
S/L	solid to liquid ratio (g/L)
O:A ratio	organic phase (volume) per aqueous phase (volume)
D	distribution ratio
At%	atomic percent
Leachate	the produced aqueous solution containing elements that have been dissolved from a solid sample
TBP	tributyl phosphate
Cyanex 923	commercial blend of four tri-alkylphosphine oxides
ICP-OES	inductively coupled plasma optical emission spectroscopy
XRD	X-ray diffraction
EDS	energy dispersive X-ray spectroscopy
SEM	scanning electron microscopy
D2EHPA	bis(2-ethylhexyl)phosphoric acid
TOA	tri-octylamine
Cyanex 272	bis(2,4,4,-tri-methylpentyl)phosphinic acid
PC-88A	2-ethylhexyl 2-ethylhexyphosphonic acid
TBP	tri-butyl phosphate
Alamine 336	tri-octyl/decylamine
Tween 80	surfactant
PAM	polyacramide

1. INTRODUCTION

The nickel metal hydride (NiMH) battery was commercialized at the end of the 1980s and has since then been used in various applications [1-5]. Today, niche markets are energy back-up and smart grid applications [6]. NiMH technology is a part of the present technologically diverse battery market that is growing to meet the needs for adaptation to lower carbon footprint energy sources.

In the European Union (EU) the legislation demands general recycling of batteries in order to avoid pollution by environmentally hazardous elements [7]. All types of batteries, from small button to large industrial batteries, are collected, sorted and recycled.

Recycling of disposed NiMH batteries sustains the global markets with economic and technologic important metals, i.e. nickel, cobalt and rare earth elements (REEs). These elements are used in various applications, from common stainless steels to high tech alloys (i.e NiMH alloy) [8]. Examples of recycling companies that treat discarded NiMH batteries are Nickelhütte Aue GmbH and Umicore [9, 10]. Both pyro and hydrometallurgical methods are currently used today in order to produce pure metal fractions from NiMH waste.

Sustainable production of metals and components through recycling is needed in order to decrease the life cycle impact of these commodities. To increase sustainability of recycling it is necessary to selectively recover metals and components, while minimizing the consumption of energy and chemicals.

NiMH components do not completely degrade throughout the battery lifetime and can potentially be reused in new batteries. Reusing NiMH materials would add additional value to the waste, as producing NiMH materials consumes high amounts of chemicals, energy and/or uses highly toxic compounds. However, reusing spent NiMH electrode materials in new batteries has still not been practically demonstrated.

The aim of the present work was to contribute to the development of selective and sustainable recycling methods for NiMH electrode materials, thus making important parts of the electrodes reusable. The first goal was to characterize the materials in respect to degradation of materials, in order to evaluate the recycling option of reusing material. Further goals of the practical work were to investigate the selective recovery of (1) metallic nickel, (2) reusable NiMH alloy and (3) cobalt.

2. BACKGROUND

2.1 Economic and environmental values of metals in nickel metal hydride (NiMH) batteries

Batteries are important products for the overall goal of making our energy consumption more sustainable by storing energy from carbon-neutral energy sources. There are, however, economic and environmental costs that are associated with the production of materials that are used in batteries. The present work focuses on NiMH batteries and the emphasis on such material costs are therefore included here.

Most NiMH battery components consist of inorganic materials. It is energy efficient to design the battery as compact as possible. NiMH batteries therefore contain high concentrations of metals. As an example, these batteries may contain 17.9 wt% nickel, 4.4 wt% cobalt and 17.3 wt% REE [11].

The most economically important metals used in NiMH batteries are nickel and cobalt. The metal exchange market prices of 99.8-99.9 wt% purity nickel and cobalt are currently approximately 13000 and 33400 USD/tonne (respectively, in 2017) [12]. The energy consumption associated with the production of a concentrate of nickel from sulfide (0.5-7 $wt\%_{Ni}$) and laterite (1-3 $wt\%_{Ni}$) ores are high (60-1300 and 125-400 GJ/ton, respectively) [13]. The different energy consumptions are related to the

concentration of nickel in the ore. As can be expected, the subsequent refinement methods to produce pure nickel (99 wt%) are much less energy demanding (10-38 GJ/ton).

Cobalt is a byproduct from primary production of copper and nickel ores, which are used for the production of 35% and 55%, respectively, of global cobalt production [14].

Although REEs are not of immediate economic concern their general availability has been frequently discussed in relation to the development of important technologies and growth of clean energy economies [8, 14, 15]. Examples of applications where REEs are important are batteries and magnets. Battery alloys, such as the ones used in NiMH batteries, have been reported as a significant market for the consumption of REEs in the last decade [16, 17]. According to Binnemans et al. [16] global recycling of REEs is low (< 1% in 2011). Recycling rates for REEs need to be improved as the primary production of REEs (La, Ce, Pr, Nd) is an energy intensive process (687 GJ/ton) [18, 19].

An assessment by Majeau-Bettez et al. [20] showed that the production of NiMH batteries contribute significantly more (> 55%) to the overall environmental impact of NiMH batteries compared to the use phase. Unsurprisingly, the metal depletion potential was the highest score for the considered environmental impacts.

Treating NiMH waste that has high concentrations of nickel and REEs can have a significant impact on the life cycle energy consumption for these metals. Consequently, the environmental impacts of NiMH components, which are rich in these metals, should also decrease. Managing NiMH waste also recirculates economic and technologically important metals back into society.

2.2 Fundamentals of the NiMH battery

The fundamental components for a NiMH battery are the active anode (hydrogen storage AB_5 alloy) and cathode ($Ni(OH)_2$) electrode materials, separator and electrolyte (KOH/LiOH). The NiMH battery is discharged by the coupled anode ($M=AB_5$) and cathode reactions,

$MH + OH^- \rightleftarrows M + H_2O + e^-$ Eq. 1 (anode) $E° = -0.83$ V

$NiOOH + H_2O + e^- \rightleftarrows Ni(OH)_2 + OH^-$ Eq. 2 (cathode) $E° = 0.52$ V

$MH + NiOOH \rightleftarrows M + Ni(OH)_2$ Eq. 3 (total cell reaction) $E° = 1.35$ V

As can be seen in Eq. 1 and Eq. 2 water carries hydrogen ions between the electrodes. Hydrogen is reduced during charge and oxidized during discharge which results in a zero net consumption of water (Eq. 3). The reduced hydrogen does not combine into hydrogen gas but diffuses into the AB_5 alloy until released during discharge (Eq. 1).

There are also other reactions that occur inside a NiMH battery during practical operation that need to be addressed when designing these batteries. In principle, as soon as any current is applied in the cell several temperature, concentration, voltage and current gradients are created [21]. These variations promote some competing reactions to occur depending on the charge/discharge conditions [21-23]. The reactions that are of concern during the charge and discharge processes are shown in Figure 1.

The cathode and anode interact with each other not only via the electrolyte but also through the gas phase [22]. Gas pressure may increase, due to evolution of oxygen and hydrogen at the cathode and anode (respectively) [24]. Excess anode capacity does not allow hydrogen gas to be evolved at the anode during overcharge, because the cathode has already been completely charged. The excess anode also allow recombination of oxygen and hydrogen gases at the anode surface; a reaction that produces water. Using a starved electrolyte design allows some porosity in the separator and gases are able to

pass between the electrodes. As a precaution the closed cells are also equipped with a safety vent. Although releasing the overpressure may be necessary, this quickly dries out the cell.

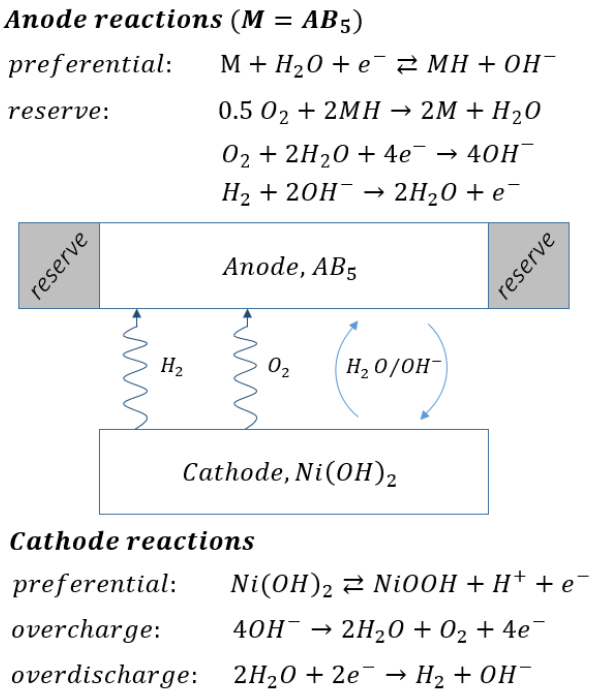

Figure 1. The principal reactions during charging and discharging of the sealed NiMH battery cell [24].

2.2.1 Hydrogen storage AB_5 alloy used in the anode

There are many different formulations of the hydrogen storage alloy used in NiMH batteries. One of the common types is the hexagonal AB_5 with $CaCu_5$ crystal structure (see Figure 2). The amount of A (e.g. La, Ce, Pr, Nd) atoms are proportionally less than B (e.g. Ni, Co, Mn, Al) elements [25]. The type of element and/or amount used for A and B can vary between producers.

The starting materials for the AB_5 alloy are pure metal ingots, except for the ingot containing REEs (La, Ce, Pr and Nd). A mixture of REEs is acceptable to use since these elements have similar chemical properties. The similar chemical properties of REEs is due to the lanthanide contraction where the atomic and ionic radii, respectively, are relatively constant from lanthanum to lutetium [26]. Avoiding the need for elemental separation during primary production result in a much cheaper AB_5 alloy.

Producing AB_5 alloys involves the following steps: mixing of ingots, melting in inert atmosphere, rapid cooling and finally reducing particle size by either mechanical crushing or hydrogen sorption/desorption cycles [27]. In order to produce a material with strictly homogeneous composition it is also useful to post-anneal the as-cast ingot before the particle size reduction [28]. This process has been reported to proceed for 10 h at 1000 °C, according to Fetcenko et al. [25].

Clean surfaces of metals are needed for dissociative chemisorption and associative desorption of hydrogen, according to Schlapbach et al. [29]. The necessary surface properties of the AB_5 alloy particles have also been discussed by Ye et al. [21]. The surface has to form a dense layer that inhibits corrosion in the alkaline electrolyte during battery applications. However, it also needs to remain catalytically active to create and break O-H bonds in the water molecules. Additionally, some hydrogen permeability is needed in the AB_5 bulk/surface interface as hydrogen atoms are moved between the interface during battery cycling. Finally, it is also important that the surface is electrically conductive. As pointed out by Ye et al. [21] there is little knowledge of the reactions that take place on the particle surfaces.

It is generally accepted that high-rate discharge of the negative electrode is influenced by the reaction kinetics at the AB_5 alloy surface [30]. A large reaction surface and a uniform particle size are important for the high-rate performance [31]. These two properties lead to a minimization of various gradients in the cell [21].

Producing the AB_5 alloy material used for NiMH batteries from ingots is an energy intense process. It is therefore of interest to reuse this material in new batteries.

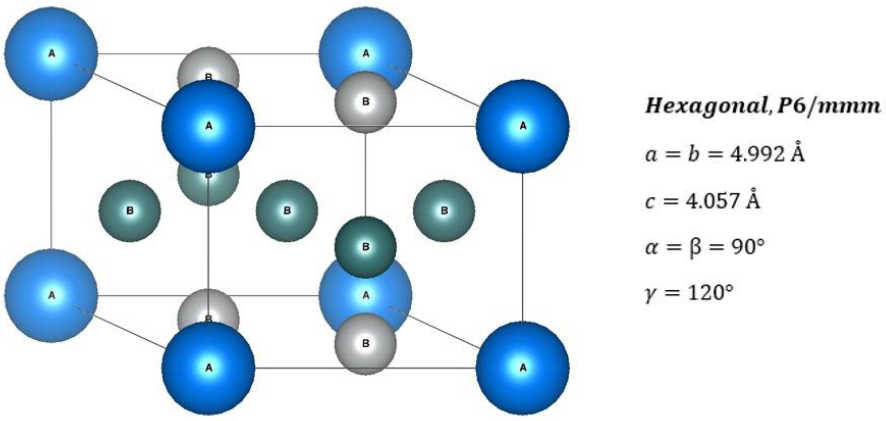

Figure 2. The principal crystal structure of hydrogen storage alloy AB_5 hexagonal P6/mmm. Constituents of A and B may vary in elements and amounts, and between producers. Here, an example of formulation is A = La, Ce, Pr, Nd (blue) and B = Ni, Co, Al, Mn (gray and green).

2.2.2 Nickel hydroxide $Ni(OH)_2$ used in the cathode

The aim of this section is to review the properties of nickel hydroxide used for the NiMH cathode active material.

Due to the low conductivity of nickel hydroxide efforts have been made to improve its conductivity. A specific focus has been how the nickel hydroxide material behaves during cycling. The simplified sequence of phase transitions (see Figure 3) was first described by Bode et al. [32]. Since then the understanding of the complexity of nickel hydroxide has increased and a good review has been published by Hall et al. [33].

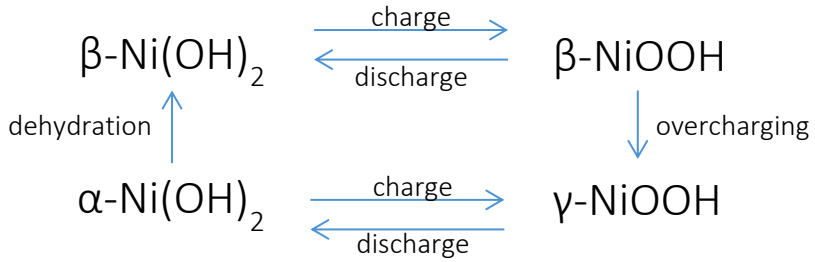

Figure 3. Phase transitions of nickel hydroxide in alkaline media and battery applications [34]. According to Hall et al. [33] the α-$Ni(OH)_2$ is better described as α-$Ni(OH)_2 \cdot xH_2O$ ($0.41 \geq x \geq 0.7$). Dehydration refers to the removal of intercalated water between the $Ni(OH)_2$ planes.

As can be seen in Figure 3, different phase transitions in each charge and discharge state are possible [35]. The crystal parameters of these phases can be seen in Table 1. The crystal lattice parameter (c) for α-$Ni(OH)_2$ (8.0) and γ-NiOOH (6.9) are large compared to β-$Ni(OH)_2$ (4.6) and β-NiOOH (4.8). Preferably, the cathode electrode should only operate in β-$Ni(OH)_2$/β-NiOOH cycling, because the lattice volume change between this pair is lower compared to that of the α-$Ni(OH)_2$/γ-NiOOH pair. According to Chen et al. [36] the lattice volume increases by 44 vol% during the transition of β-NiOOH to γ-NiOOH.

The increased cathode volume due to cycling between the two oxidized/reduced forms of nickel hydroxide can cause the electrolyte balance in the cell to shift, and electrolyte is redistributed toward this electrode. As a consequence the internal resistance of the cell increases [37, 38]. According to Shinyama et al. [39] this is one of the dominating factors for battery failure.

Table 1. Parameters for crystal structures of different phases of nickel hydroxide [40, 41].

Phase	a = b (Å)	c (Å)
β-$Ni(OH)_2$	3.13	4.6
α-$Ni(OH)_2$	3.02	8.0
β-NiOOH	2.81	4.84
γ-NiOOH	2.82	6.9

Partial substitution of nickel ions with zinc and cobalt ions is a common procedure to improve the nickel hydroxide performance in batteries. In particular, it is believed that zinc suppresses formation of γ-NiOOH, and that cobalt increases conductivity of the material by formation of CoOOH during the charging process [36, 42, 43]. It has also been reported that co-precipitation of cobalt minimizes oxygen evolution [44]. Oxygen evolution may cause oxidation of the metallic anode components, e.g. AB_5 alloy.

To manufacture a spherical form of nickel hydroxide to be used in NiMH batteries it is necessary to control the growth of particles during synthesis. A popular method is to feed a stirred reactor with nickel salt solution and an alkaline chemical. The addition of dopants (Co and Zn) is easily achieved by adding salts of these elements into the nickel solution. Complexing agents temporarily enhance solubility that assist the Ostwald growth process to produce spherical particles [45, 46]. After filtration the collected particles are dried and can be used without further treatment. A summary of suggested process parameters used by various authors can be seen in Table 2. The resulting tapping density of the produced particles refers to how efficiently the particles can be packed.

Table 2. A summary of process parameters for the synthesis of $Ni(OH)_2$ particles used in NiMH batteries.

Metal salts	Temp. (°C)	pH	Atm.	Base	Chem. additive	time (h)	Drying (°C)	Size (μm)	Tapping density (g/cm³)	Ref.
SO_4^{2-}	60	max 11.4	N_2	5 M NaOH	10 M NH_4OH	10-20	n/a	n/a	1.8	[47]
SO_4^{2-}, NO_3^-, Cl^-	50-60[1]	11[1]	n/a	NaOH	Not used	n/a	120[1]	2-30	2.2	[48]
$C_2H_3O_2^-$, NO_3^-, Cl^-, SO_4^{2-}	80	n/a	Ar	n/a	NH_4OH	3	80	n/a	n/a	[43]
$C_2H_3O_2^-$, SO_4^{2-}	50	9-13	N_2	4 M NaOH	Tween 80	14	n/a	5-100	n/a	[49][2]
SO_4^{2-}	50	n/a	n/a	4 M NaOH	PAM	14	120	27	2.3	[50, 51][2]
SO_4^{2-}	50-55	11-11.5	n/a	NaOH	NH_4OH	60	105	n/a	n/a	[46]
SO_4^{2-}	n/a	n/a	n/a	NaOH	n/a	n/a	n/a	13	2.3	[52]
SO_4^{2-}	55	12-13	n/a	NaOH	NH_4OH	n/a	80	8	2.1	[53]

n/a not stated or not described in detail.
[1]stated as optimum parameters.
[2]non spherical particles were produced.

Cobalt is also applied as a coating on the nickel hydroxide particle surface in order to increase the conductivity, which results in higher utilization of the electrode material. Utilization refers to the amount of β-NiOOH that is discharged compared to the theoretical amount (289 mAh/g) [43]. Oshitani et al. [54] first reported a method to coat the particles with cobalt, and since then other methods to coat the particles have been suggested [55-58]. Most authors seem to be in agreement that the final

compound is CoOOH, although the reduction-oxidation reactions that would produce these surface layers do not appear to be well understood. Compared to less conductive NiOOH (10^{-1} mho/cm) the CoOOH has higher conductivity (50 mho/cm) [59].

2.2.3 Metallic powders nickel and cobalt

Metallic nickel is used to increase the electron transfer between particles in both electrodes, as well as to the current collector. The active materials are pressed into foam nickel substrates or mixed with nickel fibers [24], i.e. Ni(s). These conductive networks are important for the discharge performance, and nickel fibers can be used for ultra-high power discharge.

Cobalt metal powders can also be added to the cathode formulation. It has been reported that the metallic cobalt re-precipitates as CoOOH during the first charge/discharge cycle, which then improves the life-cycle stability of the cell [60].

There are several methods to produce cobalt powders. The common industrial processes are the Sheritt process, solid phase reduction, the amalgam technique and electrolytic deposition [61, 62]. The carbonyl process (Mond Process) can be used to produce cobalt powders. The reaction with cobalt and carbon monoxide occurs at 150-170 °C [61]. This process is however commercially restricted for cobalt due to low capacity and poor quality of the obtained powder [62]. In the Sheritt process a sulfide concentrate is leached under pressure at 90 °C with ammonium sulfate. High pressure hydrogen is injected and cobalt is recovered as a metallic precipitate.

In the production of nickel powders used in NiMH batteries the carbonyl process is the most important commercial production method [62]. Nickel tetra carbonyl is formed by allowing carbon monoxide to pass over metallic nickel at 50 °C [63]. Nickel tetra carbonyl is liquid at room temperature. The decomposition into metallic nickel occurs in heated atmospheres at around 230 °C. By controlling the process parameters it is possible to recover particles with various shapes (i.e. fibrous or spheres) and size (less than a few microns). More information about the process can be found in the original research paper by Mond et al. [64] and other references [65, 66].

2.3 Degradation mechanisms of battery cells and materials

NiMH batteries are eventually discarded when the required standard for application is no longer met. The overall degradation of the cell is a complex process that involves different phenomena, e.g. loss of electrolyte, increased internal resistance, corrosion of the AB_5 alloy, pulverization and contamination between the electrodes. There are numerous scientific papers that discuss NiMH battery degradation [21-23, 30, 31, 37-39, 67-78].

To simplify this review, the main degradation aspects of the electrode materials are separately considered in the following sections. However, it should be emphasized that battery degradation includes all the separate processes described above. For this reason references will reoccur in the following subsections.

2.3.1 Loss of electrolyte

One of the main causes of NiMH battery degradation is that the cell dries out, i.e. the electrolyte liquid is lost. The purpose of the electrolyte is to provide ionic conductivity and the optimal concentration is approximately 6 M KOH [68]. Above this concentration the discharge capacity of the anode electrode decreases.

During charge and discharge of the battery the electrolyte redistributes between the electrodes, causing the separator to dry out. As a consequence, the internal resistance of the cell increases [37, 38]. As previously mentioned, increased internal resistance is believed to be one of the dominating factors for battery failure [39]. In agreement with this notion Li et al. [38] replenished the electrolyte of spent batteries and demonstrated that the discharge capacity could be partially restored to 10% of the original values. This demonstration indicates that there are other causes for battery failure. However, it is reasonable that a lack of electrolyte plays an important role by promoting unwanted reactions in the electrodes, due to increased temperature caused by increased internal resistance.

2.3.2 Pulverization

Pulverization refers to particle size reduction through mechanical (i.e. grinding) or chemical treatment. The effect of chemical treatment is that the lattice volume contracts or expands unevenly, which results in parts of the particle bulk cracking. An example of chemical treatment that results in pulverization is hydrogen intercalation into lattices of strong hydride forming elements (i.e La, Ce, Pr, Nd) [79].

Both cathode and anode materials are pulverized during continuous charge/discharge of the battery. It is the phase transitions that occurs during cycling that are the main cause of this degradation process.

Pulverization of the cathode electrode material increases with increasing number of cycles [38, 69]. Li et al. [38] noticed an increase of γ-NiOOH phase formation in the cathode electrode during cycling. As mentioned previously, this phase is associated with high (44%) lattice volume change.

Pulverization of the AB_5 alloy has been observed by many authors [23, 30, 38, 69, 71]. According to Bäuerlein et al. [23] both the chemical composition of the alloy and the amount of intercalated hydrogen affects the increase of lattice volume during charge. Pulverization is caused by mechanical stress within the alloy, which builds up during cycling. As a final result, the alloy particles crack. Since consecutive cycling reduces the AB_5 alloy particle size, the AB_5 alloy surface area also increases. Both preferable electrochemical and corrosion reactions are promoted as a consequence of these physical changes. Interestingly, it has been demonstrated that a decreased AB_5 alloy particle size increases the discharge capacity of the anode electrode [23]. Although the cycle stability of the anode is also decreased, spent AB_5 alloy can potentially be reused for high-discharge rate applications.

2.3.3 Corrosion

Corrosion of the AB_5 alloy material has been in focus for research into the causes of battery failure. Authors [23, 37, 74] generally illustrate the corrosion of the AB_5 alloy as being similar to the following reaction (M = AB_5),

$$2M + H_2O \rightarrow MH + MOH \qquad \text{Eq. 4}$$

It was suggested that the initial corrosion is enhanced by the lack of protective corrosion products on the alloy particles [37]. Interestingly, it has also been reported that pre-treating the alloy in alkali solution at elevated temperature improves the life-cycle of the AB_5 alloy by the formation of protective corrosion layers [71]. These reports suggest that formation of metal oxide/hydroxide layers are important for inhibiting further corrosion. However, the thickness and composition of these layers can potentially retard e.g. hydrogen diffusion rates [23].

The reported compositions of the corrosion layers that form on the alloy particles during cycling appear to be similar [37, 69, 71, 72]. Zhou et al. [69] detected three phases with different degrees of oxidation; (1) low oxidized core of AB_5 particles, (2) partially oxidized with very little manganese and aluminum content and (3) heavily oxidized with mostly REE and manganese. Ikoma et al. [71] observed that $REE(OH)_3$ and manganese oxides were formed at the alloy surface and that nickel and cobalt existed in metallic form near the surface. It was proposed that manganese initially dissolved and then re-deposited as an oxide on the alloy surface. Similar observations of corrosion products were made by others [23, 72]. Furthermore, Maurel et al. [72] reported that grains of MnO(OH) (s), $Mn(OH)_2$ (s) and CoOOH (s) were randomly scattered over the alloy surface and covered the $REE(OH)_3$ needles. Based on the analysis work of Young et al. [78] it can be approximated that the thickness of the surface layers are in the order of 50-100 nm. According to Schlapbach et al. [29] it is corrosion products like the ones mentioned above that inhibit the critical function of the AB_5 alloy to absorb and desorb hydrogen.

Removing corrosion products is important for the possibility to reuse the AB_5 alloy, in order to allow sufficient hydrogen diffusion rate to and from the AB_5 bulk.

2.3.4 Cross contamination between cathode and anode

Contamination of metals from one electrode onto the other has been reported to occur during battery cycling.

Leblanc et al. [37] suggested that measurements of aluminum in the cathode can be used as an indicator of corrosion of the AB_5 alloy. Since that report was published this method has been adopted by others [23, 72]. Of course, this method of quantifying AB_5 corrosion is only valid if all the oxidized aluminum can be found in the positive electrode. Some authors state that as aluminum is dissolved it will end up trapped in the $Ni(OH)_2$ lattice [37, 69, 74, 75]. Aluminum is an unwanted contaminant that is known to stabilize the unwanted α-$Ni(OH)_2$ structure during cycling [69].

Contamination of manganese in the cathode electrode has also been observed [23]. According to the investigation performed by Gerlou-Demourgues et al. [80] substitution of nickel with manganese can also lead to the formation of α-$Ni(OH)_2$.

The anode is also susceptible to contamination of elements from the cathode. Zhou et al. [69] reported contamination from the cathode, through observations of zinc on the spent AB_5 alloy material. This element does not appear to have a detrimental effect on the anode electrode. Instead, it may even inhibit further corrosion [74].

2.4 Hydrometallurgical recycling methods to treat NiMH waste

2.4.1 Dissolution

Dissolution of spent NiMH waste is a method to produce an aqueous solution (i.e. a leachate), which will be subsequently treated using separation and recovery methods. It is also the first opportunity for chemical separation. Selective separation is economically interesting because it reduces the need for subsequent treatment.

Interestingly, only mineral acids (hydrochloric, sulfuric and nitric acid) have been considered for complete dissolution of the waste, in previous investigations (see Table 3).

Table 3. Optimal leaching conditions with respect to the dissolution of nickel and cobalt. Mixed refers to mixed cathode and anode material. For the sake of comparison values have been adapted from references through both tables and graphs. Differences in reported REEs leaching results are due to differences in consideration of the reaction yields (i.e. dissolution or oxidation).

Electrode(s)	Acid	Temp. °C	time	S/L (g/mL)	Ni	Co	REE	Ref.
Mixed	1.5 M H_2SO_4 + 4 vol% H_2O_2	50	1 h	1/50	100%	n/a	n/a	[81]
Anode, cathode	2 M H_2SO_4	20	2 h	1/10	76.6%	97.6%	> 90%	[82]
Mixed	3 M H_2SO_4	75	5 h	1/10	> 95%	>95%	> 95%	[83]
Mixed	3 M H_2SO_4	95	4 h	13/100	> 95%	>95%	< 5%	[52]
Mixed	2 M H_2SO_4	95	4 h	5/100	97%	100%	96%	[84]
Mixed	3 M HCl	95	3 h	1/10	97.4%	100%	99.1%	[85]
Mixed	1.5 M H_2SO_4	30	1 h	1/20	97%	95-100%	87%	[86]
Anode	3 M H_2SO_4	95	4 h	1/10	99.5%	99.5%	94.5%	[87]
Mixed	2 M H_2SO_4	20	2 h	1/10	> 76.6%	>97.6%	> 91.8%	[88]
Mixed	12 M HCl	40	2 h	15/100	n/a	n/a	n/a	[89]
Mixed	4 M HCl	95	3 h	1/10	98%	100%	99%	[90]
Mixed	4 M H_2SO_4	80	3 h	n/a	100%	98%	36%	[91]
Anode, cathode, mixed	pH ≥1: H_2SO_4, HCl, HNO_3	30	5.5	1/50	n/a	n/a	n/a	[92]
Mixed	8 M HCl	30	n/a	3.7/10	n/a	100%	100%	[93]

n/a – not available or not presented in detail.

Some general observations can be from the work presented in Table 3. Firstly, mineral acids (hydrochloric, sulfuric and nitric acid) have been extensively studied and it is expected that these acids will efficiently dissolve the mixed electrode materials. Secondly, it is possible to separate REE sulfates from sulfate solutions [52]. Thirdly, the S/L ratio can generally be kept high (1-3.7/10) in both hydrochloric and sulfuric acid solutions. A high S/L is preferable, as the dissolution step produces less

secondary liquid waste that needs to be treated. No other acidic media than the above mentioned ones have been found to have been extensively studied.

It is worth further mentioning the work by Larsson et al. [92] because these authors investigated in detail the dissolution behavior of electrode materials in hydrochloric, sulfuric and nitric acid. At high pH (≥ 1), treatment in these acids will result in different outcomes. In nitric acid all material is dissolved after 14 hours at pH 1. Dissolution of metallic nickel is expected because nitric acid is an oxidizing acid. In de-aerated hydrochloric and sulfuric solutions, the dissolution of metallic nickel is suppressed.

Interestingly, de-aereated conditions do not seem to be necessary in practice. The required time for dissolution of the waste matrix was approximately 5.5 h in aerated solutions, using either sulfuric or hydrochloric acid at pH 1 [92]. In the work by Larsson et al. [92] the metallic nickel was of the foam type, and its dissolution did not appear to be complete even after 44 h in hydrochloric acid. Therefore, it may be possible to practically separate the Ni(s) component even in aerated solutions.

2.4.2 NiMH metal separation by solvent extraction

Solvent extraction techniques have been used to treat leachate solutions that have been produced by dissolution of NiMH waste into acidic solutions. In a solvent extraction separation of elements dissolved in an aqueous leachate, an immiscible organic phase is brought into contact with the leachate solution. The organic phase contains an extracting agent, which is able to form a complex with the metal ion that is more soluble in the organic phase than in the aqueous phase. Thus, the metal ion is extracted, i.e. transported to the organic phase.

Several extracting agents have been proposed for the extraction and separation of elements from leachate solutions [52, 81, 84-87, 89, 90, 93-98]. Some of these suggested systems have been optimized for practical recycling applications. A summary of some of these systems are given in Table 4. As can be seen from this table there are several extraction agents that can be used to separate nickel, cobalt and REEs from sulfate and chloride aqueous solutions.

Table 4. Recovery rates (%) of rare earth elements (REE), cobalt and nickel according to suggested extraction systems.

Leachate anion	REE (%)	Cobalt (%)	Nickel (%)	Extracting agent system	Ref.
SO_4^{2-}	93,6	96	96	D2EHPA, Cyanex 272	[84]
	97,8	98,1	98,1	D2EHPA, Cyanex 272	[52]
	98,9	98,5	98,4	PC-88A	[87]
	99,5	99,5	99,6	Quaternary ammonium salts	[97]
Cl^-	98	98	96	D2EHPA, TOA	[85]
	98,9	93,6	97	TBP, Alamine 336, PC-88A	[89]
	99,9	99	99	Cyanex 923	[93]

Recovery of metals from a loaded solvent can be made by stripping (i.e. back-extraction) [99]. For stripping it is important to make extracted metals soluble in the aqueous phase, and approaches are dependent on the system at hand. Examples of methods to strip metals are to vary the pH, amount of aqueous phase, temperature and/or use counter-ions (e.g. nitrates). Stripping of metals can result in elemental separation and therefore the stripping step is appropriately applied before recovering the metals as solid compounds.

2.4.3 Recovery of metals

Recovery of metals from leachate solutions produced through hydrometallurgical treatment of NiMH waste has been investigated using different techniques. These methods include precipitation, calcination and electrowinning of metals. Electrowinning refers to the extraction of metals from compounds through the electrolysis of solutions containing metal ions [100]. Applying a current that matches the reduction potential of a metal ion can reduce the metal ion into its elemental state.

Tzanetakis et al. [90, 95] investigated electrowinning of nickel and cobalt from aqueous chloride media at pH 3. Depending on the current efficiency the composition of the nickel (76-83%) and cobalt (11-14%) varied. Lupi et al. [101] also reduced nickel and cobalt, but from sulphate solutions at pH 4.3.

Recovery of metals can be made by adding precipitation agents into the leachate solutions. Metal ions form insoluble complexes and precipitate out of solution. Once nickel, cobalt and REE have been separated (using i.e. solvent extraction separation) these purified metal fractions may be recovered using oxalic acid [84, 85, 89, 97]. To transform these solids into oxides, the recovered material can be calcined at 850-900 °C [84, 85]. Nayl [97] reported that the calcination of oxalates of REE, cobalt and nickel can be performed also at lower temperatures (700, 500 and 400 °C, respectively). Precipitation using alkaline solutions has also been discussed by others [52, 83, 86, 91, 94, 96, 102-104].

3. THEORY

3.1 Oxidation of metals

The current work discusses the recovery of Ni(s) and AB_5 alloy using acidic media. It is difficult to recover metallic NiMH components due to the generally low reduction potentials, which are shown in Table 5.

Consider the half cell reactions of the least reactive system of Ni(s) and water,

$$Ni(s) \rightleftarrows Ni^{2+}(aq) + 2e^- \qquad \text{Eq. 5}$$

$$2H^+(aq) + 2e^- \rightleftarrows H_2(g) \qquad \text{Eq. 6}$$

Here, the reduction of hydrogen (Eq. 6) represents the splitting of water and is not associated with acid consumption. The Nernst equation can be used to calculate the cell potential of Eq. 5 and Eq. 6 [105],

$$E = E_0 + 2.3\frac{RT}{nF}log(Q^{-1}) \qquad \text{Eq. 7}$$

where the constants R, T and F represents the gas constant (8.3141 J mol^{-1} K^{-1}), temperature (K) and Faradays constant (96.485 J mol^{-1} V^{-1}), respectively. The variable n is the number of electrons transferred per mole reaction. E_0 is the standard reduction potential. The reaction quotient Q is defined as,

$$Q = \frac{a_C^c\, a_D^d}{a_A^a\, a_B^b}\ when\ aA + bB \rightleftarrows cC + dD \qquad \text{Eq. 8}$$

For an ideal gas, ideal solution or pure solid/liquid, the activity (a) can approximated by its partial pressure (P/P_0, P_0 = 1 bar), molar concentration (M/M_0, M_0 = 1 mol/L) or by unity, respectively [106]. The hydrogen partial pressure is per definition at unity, in order to compare cell potentials with the standard hydrogen electrode (SHE).

To determine oxidation of metals it is conventional to choose metal concentrations of 10^{-6} M [105]. The cell potential of nickel and water in the least acidic system available (pH ≈ 7) can be calculated,

$$E = E_{H^+} - E_{Ni^{2+}} + 2.3\frac{RT}{nF}\left(\log\left(a_{Ni(s)}\right) + 2\log(a_{H^+}) - \log(a_{Ni^{2+}}) - \log\left(a_{H_2}\right)\right) = [\text{Table 5}] =$$

$$= +0\,V - (-0.26)\,V + \frac{0.059\,V}{2}(\log(1) - 2pH(=7) - \log(10^{-6}) - \log(1)) =$$

$$= 0\,V + 0.26\,V - 0.236\,V = 0.024\,V$$

The cell potential is positive which means that nickel will oxidize in any aqueous media at pH ≤ 7.

The AB_5 alloy contains elements (Co, Al, Mn, REEs) with reduction potentials below that of nickel. Therefore it is reasonable to also assume that the AB_5 alloy component will also oxidize in acidic media.

It can be concluded that the recovery of AB_5 alloy and Ni(s) using acidic media relies completely on the difference in dissolution rates of the NiMH battery components.

Table 5. Standard reduction potentials for elements found in NiMH batteries vs the standard hydrogen electrode [105, 107].

Oxidized ⇄ Reduced	E° (V) vs SHE
$Li^+ + e^- \rightleftarrows Li$	-3.04
$K^+ + e^- \rightleftarrows K$	-2.93
$La^{3+} + 3e^- \rightleftarrows La$	-2.38
$Pr^{3+} + 3e^- \rightleftarrows Pr$	-2.35
$Nd^{3+} + 3e^- \rightleftarrows Nd$	-2.32
$Ce^{3+} + 3e^- \rightleftarrows Ce$	-1.72
$Al^{3+} + 3e^- \rightleftarrows Al$	-1.66
$Mn^{2+} + 2e^- \rightleftarrows Mn$	-1.19
$Zn^{2+} + 2e^- \rightleftarrows Zn$	-0.76
$Co^{2+} + 2e^- \rightleftarrows Co$	-0.28
$Ni^{2+} + 2e^- \rightleftarrows Ni$	-0.26
$2H^+ + 2e^- \rightleftarrows H_2$	-0.059pH [105][1]
$O_2 + 4H^+ + 4e^- \rightleftarrows H_2O$	+1.23

[1]Not to be confused with the hydrogen reduction associated to acid consumption.

3.2 Recovery of nickel

3.2.1 Recovery of metallic nickel using hydrochloric solutions

Recovery of Ni(s), i.e. the conductive nickel particle network used in the electrodes, from NiMH waste using acidic solutions can be achieved if competing surface processes limit the oxidation of Ni(s). In the system considered here, the most important process that can protect the metal surface is adsorption of hydrogen.

Nickel is expected to dissolve into acidic media, e.g. hydrochloric acid, through two general reactions,

$$Ni(OH)_2 + 2HCl\,(aq) \rightarrow NiCl_2(aq) + 2H_2O(l) \qquad \text{Eq. 9}$$

$$Ni(s) + 2HCl\,(aq) \rightarrow NiCl_2(aq) + H_2(g) \qquad \text{Eq. 10}$$

These reactions (Eq. 9-10) are also expected to occur for other metals found in the NiMH waste.

Hydrogen adsorbs strongly only to nickel surfaces, and the nickel hydride bond can be approximated to -96 kJ/mol [108, 109]. The strong nickel-hydride bond constitutes chemisorption (≤ -40 kJ/mol), which is a binding strength that is characterized by less reversibility compared to physisorption (≥ -40 kJ/mol) according to McCafferty [110]. That is to say, the hydride bond will block further acidic attacks. As thermodynamics do not consider the kinetics of processes, one can only speculate that strong chemisorption will results in a slow hydrogen desorption rate from metallic nickel surfaces.

The Ni(s) used in the current work is in the form of powder, and therefore has a high specific surface area (m^2/g). A high surface area can potentially compensate slow desorption rates of hydrogen, which

can result in a dissolution of Ni(s). Therefore it is not known if the nickel-hydride bond is sufficiently strong to allow Ni(s) powder to be extracted using acidic media.

From practical considerations, hydrochloric acid is preferred over other conventional acids (sulfuric and nitric acid). The practical properties of conventional acids can be seen Table 6. The NiMH waste consists of predominantly nickel in the form of Ni(s), AB_5 alloy and nickel hydroxide. In order to reduce leachate volumes it is necessary that the nickel solubility is high in the leaching solution.

Between the different acids in Table 6, hydrochloric acid has the second highest solubility of nickel. The chloride (-I) anion cannot be further reduced due to a completed outer electron configuration shell ($3p^6$). Since no reduction of the chloride can occur, the nickel hydride cannot be oxidized. However, sulfates and nitrates do have reduction potentials above SHE, which suggests that these acids can oxidize the nickel hydride. Therefore hydrochloric acid is preferred over sulfuric and nitric acid.

Table 6. Solubility of nickel salts produced by dissolution of nickel compounds into mineral acids [111].

Mineral acid	Salt	Solubility (water, 20 °C) [g/100 g_{water}]	Ligand reduction [107]
H_2SO_4	$NiSO_4$	40.1	$SO_4^{2-}/\ SO_3^{2-}$ +0.17 V
HCl	$NiCl_2$	60.8	*None*
HNO_3	$Ni(NO_3)_2$	94.2	$NO_3^-/\ NO_2^-$ *+0.93 V*
			$NO_3^-/\ NO$ *+0.96 V*
			$NO_3^-/\ N_2O_4$ *+0.80 V*

3.2.2 Distribution into the organic phase in solvent extraction

Separation of elements and compounds using solvent extraction is a technique that is used in pharmaceutical and biochemical industries, analytical chemistry, metallurgy and industrial recycling of inorganic waste [112].

By contacting a non-miscible organic phase with an aqueous phase (i.e. leachate), neutral complexes distribute between the phases. A schematic representation of the solvent extraction technique is illustrated in Figure 4. In the current work the extraction agent Cyanex 923 is used, and its extraction of metals found in NiMH batteries is discussed in the following section.

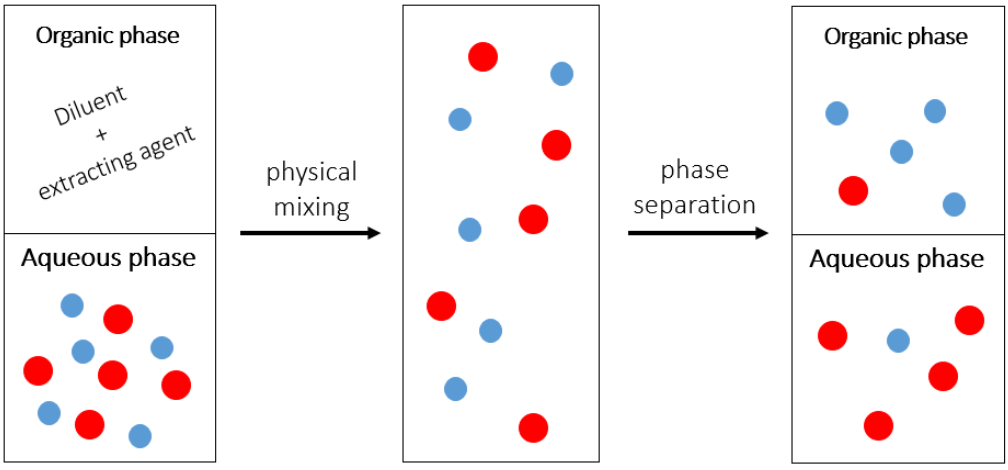

Figure 4. Illustration of the solvent extraction technique. One metal (blue) is preferentially distributed in the organic phase over another (red), after physical mixing and phase separation. The difference in distribution results in elemental separation.

The distribution of a metal A can be quantified using the distribution ratio at equilibrium,

$$D_A = \frac{[A]_{org}}{[A]_{aq}} \qquad \text{Eq. 11}$$

If D_A >> 1 the metal is mainly distributed in the organic phase. Separation of metals from a mixed leachate solution occurs when the distribution ratios of the metals are different.

3.2.3 Extraction of chloride complexes with Cyanex 923

Nickel is the most abundant metal in NiMH batteries and extracting agents are relatively expensive. It is therefore economically beneficial to extract all other elements except nickel from leachate solutions.

The commercial mixture of tri-alkylpshosphine oxides sold under the name Cyanex 923 can be used to extract, for example, lanthanides and zinc from aqueous phases. This extracting agent is especially useful for chloride based leachates.

The chloride-Cyanex 923 extraction system for separation of metals from NiMH waste was investigated by Larsson et al. [113] at great lengths. In a first step zinc was extracted and separated from the other metals by low (8 vol%) concentration of Cyanex 923. Extraction of remaining metals other than nickel (Al, REE, Co and Mn) was then made by increasing the extractant concentration to 70 vol%. Recovery of metals in groups from the organic phase was possible by contacting the organic phase with different aqueous phases (i.e. stripping). In the first strip step cobalt and manganese were recovered with a nitrate solution (0.1 M $Na(NO_3)_2$). The other elements (Al and REE) were subsequently recovered with hydrochloric acid (1 M).

The extraction of metal chlorides with Cyanex 923 (B) follows the solvating mechanism [113],

$$M^{x+}(aq) + xCl^{-}(aq) + yB(org) \rightleftarrows MCl_xB_y(org) \qquad \text{Eq. 11}$$

The aqueous metal chloride complex is associated with water, and it is more accurately described as $MCl_x(H_2O)_z$. The water molecules are not co-extracted. Importantly, the extraction of i.e. lanthanum is enhanced by increased chloride ion concentrations in the solution [93]. A complete neutralization of the H^+-ions from the acid in the dissolution of NiMH waste in 8 M HCl solution will create a chloride-rich solution and thus promote extraction of the REEs.

In media that is too acidic the extraction of REEs may be low. According to Alguacil et al. [114] acid can also be extracted by Cyanex 923 and that reduces the amount of ligand that is available for binding to REEs,

$$H^{+}(aq) + Cl^{-}(aq) + B(org) \rightleftarrows HClB(org) \qquad \text{Eq. 12}$$

The practical implication of Eq. 12 is that stripping of aluminum and REEs will be affected by the co-extracted acid. Any aqueous solution used for stripping metals (i.e. Co and Mn) from the loaded organic phase will also strip the acid. Consequently, aluminum and REEs are also stripped from the organic phase. For this reason alone, controlling the addition of acid in the prior dissolution step is important in order to avoid excess acid remaining in the leachate.

3.3 Recovery of reusable anode using carboxylic acids

Carboxylic acids were chosen for this work to investigate the recovery of reusable anode (containing AB_5 alloy) material from NiMH waste. Here the intention was to dissolve other components, such as nickel hydroxide and $REE(OH)_3$, but leave the AB_5 alloy relatively undissolved.

Trial experiments indicated that the spent AB_5 alloy component was not immediately oxidized in carboxylic acid solutions, which otherwise occurred in mineral acids. Smith et al. [115] suggested that the AB_5 alloy can be recovered selectively from a mixture of AB_5 alloy and nickel hydroxide, by selective dissolution of nickel hydroxide in carboxylic acid(s). In the work for the current thesis a demonstration of the dissolution of NiMH waste in carboxylic acids has not yet been found.

Carboxylic acids have the functional group COOH, which results in the ability of these acids to deprotonate in aqueous solutions and form metal complexes. Deprotonation of carboxylic acids depends on the pH of the solution,

$$R\text{-}(COOH)_x + xH_2O = R\text{-}(COO^-)_x + xH_3O^+ \quad \text{Eq. 13}$$

Deprotonation is suppressed at low pH values, which relates to the weak acid character of carboxylic acid. As a practical example, in a 1 M carboxylic acid solution at pH 1 only 10 mol% of the acid is deprotonated. This means that the acid solution will contain both COOH and COO^- functional groups.

The stability constants for some carboxylic acids and metals from a critical survey by Martell et al. [116] are presented in Table 7. This table shows the stability constants for deprotonation of some carboxylic acids and their complex formation for nickel and lanthanum (major waste constituents). The fact that stability constants have been quantified suggests that nickel and lanthanum carboxylates are soluble to some degree.

Ultimately, the dissolution rates cannot be approximated by stability constants and need to be investigated experimentally.

It is expected that dissolution of NiMH components in carboxylic acids is slow. Lone pair electrons on the functional COOH group can interact with metallic surfaces through adsorption [110]. Inhibition of carboxylic acids on metallic surfaces in mineral acids has been previously demonstrated using e.g. malonic, ascorbic, citric and succinic acid [117-120]. The ability to donate electrons is an important parameter for inhibition, and the greater the pK_a the greater tendency for electron donation [110]. The pK_a of the carboxylic acids used in the current work can be seen in Table 7.

The effect of adsorption processes can result in a slow dissolution. Potentially, the adsorption onto metallic surfaces, i.e. AB_5 alloy, is stronger than onto hydroxide surfaces, thus resulting in a slower dissolution of the AB_5 alloy.

Table 7. Equilibrium quotients (e.g. stability constants) for the formation of metal complexes in different carboxylic acids. Values are adapted from Martell et al. [116] for the range of 20-25 °C and 0.1-0.5 M.

Carboxylic acid	pK_a (1,2,3)	Formula	Equilibrium quotient	Log K (Ni^{2+})	Log K (La^{3+})
Acetic	4.6	$C_2H_4O_2$	$K = [ML]/[M][L]$ $K = [ML_2]/[M][L]^2$ $K = [ML_3]/[M][L]^3$	0.7	1.8 2.8 3.5
Citric	2.9, 4.4, 5.7	$C_6H_8O_7$	$K = [ML]/[M][L]$	5.4 3.3 $[MHL]/[M][HL]$ 1.8 $[MH_2L]/[M][H_2L]$	7.6 10.2 $[ML_2]/[M][L]^2$ 2.2 $[MHL_2]/[ML][HL]$
Malonic	2.7, 5.3	$C_3H_4O_4$	$K = [ML]/[M][L]$ $K = [MHL]/[M][HL]$ $K = [ML_2]/[M][L]^2$	3.2 1.0 4.9	3.7 5.9
Maleic	1.8, 5.8	$C_4H_4O_4$	$K = [ML]/[M][L]$ $K = [ML_2]/[M][L]^2$	2.0	3.5 5.4

3.4 Recovery of cobalt using ascorbic acid

Cathode materials used in NiMH batteries are surface engineered with a conductive cobalt enriched surface layer. It is believed that this layer still exists on (spent) cathode surfaces after battery cycling, which consists of cobalt in oxidation states higher than 2. Ascorbic acid has both reducing and acidic properties, and was chosen for the investigation of removing the cobalt layers selectively. It is expected that the acidic property will react also with other battery components. To achieve selective dissolution of cobalt it is therefore important that the simultaneous reduction and dissolution of cobalt is faster than the dissolution of other components.

A practical challenge of selective dissolution in acids is the general dissolution reactions of both electrode materials (Eq. 9-10). Since those reactions involve oxidation of the metals, it appears more likely that a selective dissolution of cobalt-enriched surface layers will happen when using an acidic reducing agent, namely ascorbic acid, than when using a common mineral acid.

Ascorbic acid can both dissociate its proton and become oxidized. According to Du et al. [121] the dissociation of hydrogen ions and oxidization to dehydroascorbic acid are coupled, which can be seen in Figure 5.

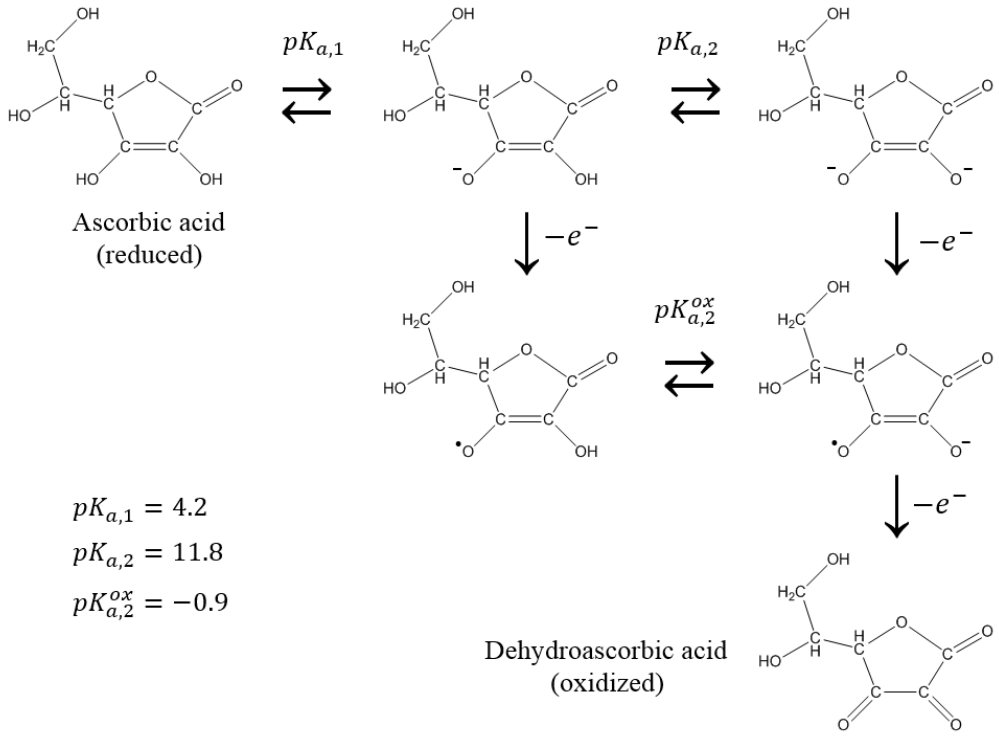

Figure 5. The oxidation of ascorbic acid to dehydroascorbic acid is coupled to hydrogen dissociation in aqueous solutions. The image has been adapted and reconstructed from Du et al. [121].

If no oxidation of ascorbic acid occurs the formation of ascorbate ions is only dependent on the pH of the solution. Speciation modelling of ascorbic acid in aqueous solution show that at pH 7 the dominant species for ascorbic acid is $AscH^-$ (99.9%) and there are low concentrations of the other forms $AscH_2$ (0.1%) and Asc^{2-} (0.005%) [121].

The reduction potential of ascorbic acid has been reported to be in the range of –0.283 and -0.066 V, in the corresponding pH range of 2-7 [122]. These reducing potentials do not raise any suspicion that metals associated with NiMH batteries will be reduced from metal ions to elemental state in ascorbic acid solutions. Common oxidation states of the metals used in NiMH batteries (see Table 5) does not allow a significantly large positive cell potential to be formed between the metal ion and ascorbic acid.

The rate of redox reaction between ascorbic acid and cobalt is important for selective dissolution. Ascorbic acid has not been tested previously for recycling NiMH materials. The ascorbic acid oxidizing rate is therefore evaluated by broadening the discussion.

Buettner et al. [123] found that aerated and room-temperature aqueous solutions of ascorbic acid in 50 mM phosphate buffers (pH 7) experienced up to 30% loss of an original 125 µM ascorbate within 15 min. When care was taken to remove transition metals the loss of ascorbate was decreased to 0.05%/15 min. This reaction was not described in detail, but it is indicated that the oxidation rate of ascorbic acid in the presence of transition metals is fast. In addition, the ascorbate ion can also oxidize by reaction with soluble oxygen to produce superoxide through the following reaction,

$$C_6H_6O_6{}^{2-} + O_2 \rightarrow C_6H_6O_6{}^{\cdot -} + O_2{}^{\cdot -} \qquad \text{Eq. 14}$$

The observed pseudo-first-order rate constants of autooxidation of $AscH^-$ is k = 10^{-6} $M^{-1}s^{-1}$ and that of Asc^{2-} is k = 10^2 $M^{-1}s^{-1}$ [121]. This mean that the oxidation rate of ascorbic acid in the presence of oxygen is most dependent on the presence of Asc^{2-} ions.

There are reasons to suspect that simultaneous reduction and dissolution of solid cobalt (iii) into solution should also be fast. According to Li et al. [124] the dissolution of cobalt from mixed lithium cobalt oxide in ascorbic acid solutions is completed after 20 minutes of dissolution at room temperature (20 °C).

4. EXPERIMENTAL

4.1 Experimental outline

This work focuses on characterization of the NiMH electrode materials and the feasibility of recovering three different components, and these goals are listed in the following order:

(1) Characterization of unspent and spent cathode and anode.

(2) Recovery of Ni(s) from the conductive nickel network.

(3) Recovery of reusable anode material. Specifically, this is a mixture of AB_5 alloy and Ni(s).

(4) Selective recovery of cobalt from cobalt-enriched surface layers on cathode materials.

These recovery processes involve the use of different chemical systems, which are discussed separately. A schematic overview of the experimental work is shown in Figure 6.

The materials used for the manufacturing of the cathode electrode are powders of Ni(s), metallic cobalt and nickel hydroxide. The anode is made only from Ni(s) and AB_5 alloy. The respective electrode mixtures had been pressed onto polymeric carrier sheets.

Batteries were charged and discharged (i.e. cycled) by the battery producer Nilar AB [6]. The batteries were considered spent when the internal resistance was twice that of the initial resistance, below 80% of capacity and/or due to miscellaneous aspects causing battery failure.

Unspent materials were assembled in the same process as the cycled batteries. However, unspent materials were not subjected to electrolyte (25-30% KOH).

A total of 5 different types of samples were produced, namely unspent cathode and anode, spent anode and cathode, and spent mixed electrode materials. One spent cathode and one spent anode batch were produced by collecting the respective separated material from at least 3 batteries. These batches were used to produce mixed electrode samples.

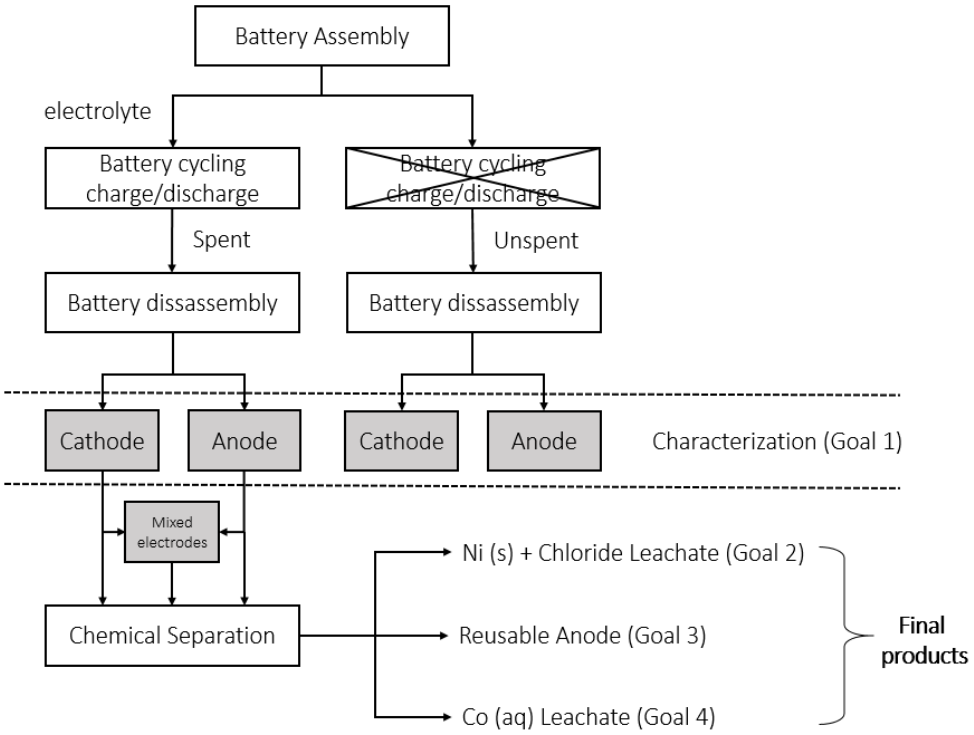

Figure 6. Process flow diagram for experimental work and samples presented in this thesis. Unspent materials originate from batteries that have been assembled and disassembled. Spent materials refers to batteries with charge and discharge properties that are considered below standards for battery applications.

4.2 Battery disassembly

Discharged bipolar NiMH batteries of the size 12 V and 10 Ah were provided by Nilar AB. A schematic overview of this type of module is shown in Figure 7. The modules had been cycled differently for various application purposes.

Prior to disassembly the spent batteries were discharged in the laboratory using a 50 Ω resistor until less than 2 V and 3 mA could be measured using a conventional multimeter. The active materials were manually separated from the casing, separator, terminal and current collector into separate anode and cathode fractions. Depending on the use phase of the battery the disassembled anode fractions can react with oxygen in normal atmosphere and self-ignite, and therefore this fraction was immediately immersed into water (>18 MΩ/cm, Milli-Q, Millipore).

Water was used to rinse the fractions in order to remove the remaining KOH-rich electrolyte. During this procedure the electrode substrate (polymeric carrier sheets) was removed. The produced materials were dried at 55 °C and normal atmosphere until no further weight loss could be detected.

A reference battery with no addition of electrolyte was built, disassembled and used without further work up procedures.

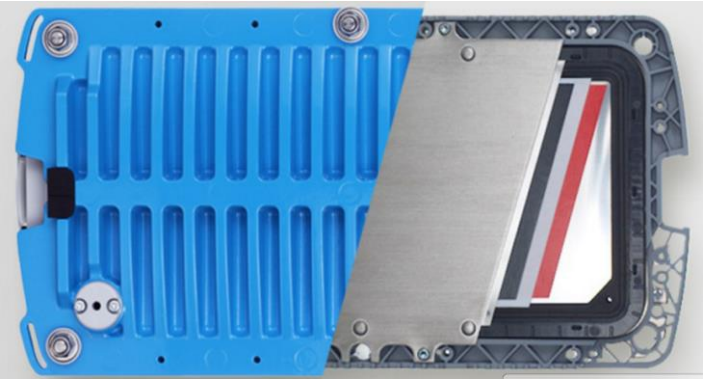

Figure 7. Schematic overview of NiMH battery module illustrating the bipolar stack design [6]. The illustrated components (left to right) are casing, terminal, current collector, anode, separator, cathode, separator, inner and outer stack frame.

4.3 Characterization

Characterization of spent cathode and anode materials was done to investigate the chemical and physical state of the spent materials in order to develop specific treatment methods. In addition, characterization of unspent and spent materials was necessary to identify degradation, in order to evaluate the feasibility of recovery and reuse of the AB_5 alloy. Several characterization techniques were used to investigate degradation of the electrode material and are listed in Table 8.

Table 8. Investigated chemical and physical property with respective analysis technique. Four types of materials were characterized separately: unspent cathode, spent cathode, unspent anode and spent anode. Analysis techniques are described in Appendix I.

Property/ Degradation aspect	Analysis method
Foreign crystalline compounds	XRD
Cross-contamination between cathode and anode	ICP-OES
Morphology and pulverization	SEM
Specific surface area (m^2/g) for pore formation and pulverization	BET

No further work up procedures were made related to X-ray diffraction (XRD), scanning electron microscopy (SEM) and the Brunauer-Emmett-Teller (BET) method, except conventional preparation methods (e.g. mounting of sample and desorption of water). Analysis techniques are described in Appendix I.

For elemental composition determination of solid samples the inductively coupled plasma optical emission spectroscopy (ICP-OES) analysis technique was used. Samples were dissolved in aqua regia, which was prepared from hydrochloric acid (37 wt%, Sigma Aldrich) and nitric acid (65 wt%, Merck) at a ratio of 3:1. Complete digestion was achieved by prolonged dissolution time (minimum 18 h) and periodical addition of hydrogen peroxide (30 wt%, Sigma Aldrich). The liquids were then heated to 70 °C for two hours and allowed to cool down. Finally, the solutions were transferred into volumetric flasks and the volume was corrected for with pure water (>18 MΩ/cm, Milli-Q, Millipore).

The above described method was used to determine elemental concentrations of all types of samples in this work.

Samples were diluted in 0.7 M suprapure nitric acid (65 wt%, Merck) and compared to external calibration, prepared from standard stock solutions (1000 ppm, Ultra Scientific), using ICP-OES. Determined metal concentrations were used as references for characterization purposes and/or dissolution experiments.

4.4 Recovery of nickel

Recovery of nickel was investigated by dissolution of materials in hydrochloric acid solution, with subsequent leachate treatment carried out using solvent extraction. The experimental details are described in the following subsections, respectively. The effect of acidity on nickel dissolution was studied. One solvent extraction system was tested for leachate treatment by varying the O:A ratio at two recommended extraction concentrations [93]. Determination of appropriate O:A ratio following metal extraction was also necessary, in order to study the effect of acidity on the same extraction.

The amount of acid present in solution can affect both the dissolution of nickel and the subsequent treatment of the leachate solution, using solvent extraction. The aspect of acid concentration was therefore a focus for the goal of recovering Ni(s). A list of the nickel recovery experiments performed is shown in Table 9.

Table 9. Experiments used to investigate recovery of Ni(s) from mixed electrode materials using hydrochloric acid.

Practical goal	Investigation	Sample
Ni (s) recovery	a) Dissolution rates at pH 1 b) Characterization of undissolved material	Mixed electrode material
Ni (s) recovery	Nickel dissolution rates at 1-8 M HCl	a) Mixed electrode material b) Unspent Ni(s)
Leachate treatment	Metal extraction by variation of O:A	Chloride leachate
Leachate treatment	Effect of acidity on metal extraction	

4.4.1 Dissolution rates of metals at pH 1

Dissolution rates of metals from mixed electrode materials (0.5 g cathode and 0.6 g anode) were studied using hydrochloric acid solutions corresponding to pH 1. The materials were immersed into solutions and the suspensions were stirred using plastic propellers (Metrohm). Acid was continuously added to the solution to compensate the decrease of acidity due to dissolution of metals.

The aqueous potential was measured using a pH glass electrode (Metrohm), calibrated with buffer solutions corresponding to pH 1, 4 and 7 (Radiometer Analytical, Metrohm). No compensation for changes in ionic strength were made. Reported pH values should therefore only be regarded as approximate.

The initial solution was prepared from sodium chloride salt (VWR) and the aqueous potential was preset to pH 1 and kept constant by addition of titrant (1 M HCl). The titrant was prepared from pure water (>18 MΩ/cm, Milli-Q, Millipore) and hydrochloric acid (37 wt%, Sigma Aldrich). Addition of titrant was measured and controlled through a Titrando (905, Metrohm) titrator which was connected to a computer. The aqueous potential was measured continuously and kept constant.

Samples were taken periodically in small volumes (1.5 mL), and immediately filtered (PP, 0.45 µm). Recorded volumes and concentrations determined using ICP-OES allowed calculations of the amounts of dissolved metal (%), with the comparison to metal concentrations in samples established previously (section 4.2).

Characterization using XRD and SEM was carried out on undissolved mixed materials (5 g) that had been produced by separate experiments using 5 M HCl solution, which had been terminated after 5 h. The solid materials were washed in three steps using fresh hydrochloric acid (pH 1), followed by three steps

of pure water (>18 MΩ/cm, Milli-Q, Millipore) rinsing. The washed material was collected and dried in a normal atmosphere at 55 °C until no further weigh loss could be recorded.

4.4.2 Nickel dissolution rates at 1-8 M HCl

Investigations of nickel dissolution rates from mixed electrode samples in 1-8 M HCl solutions were carried out at room temperature (20 °C). Magnetic stir bars were used to mix the suspensions in vials. Unspent powders of nickel metal, supplied by the battery manufacturer Nilar AB, were also used in these experiments.

According to previous research the appropriate S/L ratio for dissolution of NiMH batteries is 1/10 [82, 83, 85, 87, 88, 90]. The amount of ligand (here chloride ion) to form metal complexes in solution is a 4 times excess for complete dissolution, assuming a 1:2 metal:ligand ratio. Samples were immersed in acidic solution at S/L ratio of 1/20 (nickel powder) and 1/10 (mixed 0.5 g cathode and 0.5 g anode).

Acid solutions were prepared from pure water (>18 MΩ/cm, Milli-Q, Millipore) and hydrochloric acid (37 wt%, Sigma Aldrich).

Small aliquots (0.5 mL) of samples were withdrawn periodically from the stirred solutions and immediately filtered using a 0.45 µm filter (PP). No compensation for withdrawn volumes was made. Nickel concentration in reference samples had been previously determined according to the procedure in section 4.2. The amount of dissolved nickel was calculated assuming a constant S/L ratio.

4.4.3 Leachate treatment with solvent extraction

Organic phases and leachate solutions were added to vials, and the vials were sealed and shaken at 1500 vpm (vibrations per minute) using a shaking machine (IKA Vibrax VXR Basic) for 2 h. The temperature was kept constant (25 °C) by a connected water bath. Subsequently, the vials were centrifuged at 3500 rpm for 10 minutes (radius equal to 9 cm corresponding to 1231 g-force) with a Labofuge 200 (Heraeus). Aqueous samples were collected before and after the extraction, and prepared according a typical procedure (section 4.2) and analyzed using ICP-OES.

Extraction of metals from chloride leachate solutions was investigated with varied O:A ratios, using two different concentrations of extractant Cyanex 923, with 8 vol% used to separate zinc and 70 vol% used to extract all metals, except nickel.

Stock solutions with 8% or 70 vol% Cyanex 923 (95%, Cytec), respectively, containing the phase modifiers 10 vol% tri-butyl phosphate (97%, Sigmal Aldrich, i.e. TBP) and 10 vol% n-decanol (99%, Sigma Aldrich) in diluent solvent 70 (Statoil) were prepared. The organic phases were pre-equilibrated with pure water (>18 MΩ/cm, Milli-Q, Millipore).

The chloride leachate solution was prepared by dissolution of mixed electrode material in 8 M HCl. The acid solution was prepared with pure water (>18 MΩ/cm, Milli-Q, Millipore) and hydrochloric acid (37 wt%, Sigma Aldrich).

Acid neutralization of the 8 M HCl solution was carried out in a series of stepwise additions of mixed electrode material. The solid-liquid dispersion was allowed to react under magnetic stirring and cooling (ice bath) until hydrogen gas evolution could no longer be observed. The aqueous potential was measured with a glass pH electrode (Metrohm). Additional material was added until no further change in aqueous potential could be measured. When the potential was stable the acid neutralization process was complete.

The 8 M chloride leachate solution produced was filtered (0.45 µm, PP) and sampled. The results from ICP-OES analysis of sampled leachate are presented in Table 10.

Table 10. Concentrations (10^{-3} mol/L) of leachate solutions after dissolution of mixed electrode materials in 8 M HCl solutions. The aqueous potential was measured to 310 mV.

Metal	10^{-3} mol/L
Al	78
Ce	60
Co	227
La	179
Mn	104
Nd	31
Ni	2902
Pr	11
Zn	57

The effect of acidity on the extraction of metals was investigated using 8 M chloride leachate solutions at different acidities (i.e. aqueous potentials) and 70 vol% Cyanex 923. An O:A ratio of 1.4 was used and had been previously determined as sufficient for metal extraction, but below the point of loading. Under these conditions the metal extraction becomes dependent on the acidity of the solution.

The leachate solution presented above (Table 10) was further diluted in steps using the same stock solution of 8 M HCl that had been used for the leachate preparation. Between each step the aqueous solution was sampled and the aqueous potential was measured with the same electrode mentioned above.

4.5 Recovery of anode material (including AB_5 alloy)

Recovery of reusable anode material was investigated by dissolution experiments where 4 carboxylic acids (malonic, maleic, acetic and citric acid) were used. Here, the main goals were to chemically separate the anode material from the cathode material by dissolution of the cathode, and to remove corrosion products from the anode.

To be precise, anode samples consist of both AB_5 alloy and Ni(s), which can potentially be reused as a mixture. Corrosion products only need to be removed from the AB_5 component in order to reuse the AB_5 and Ni(s) mixture as anode material.

Chemical separation relies on different dissolution rates of the cathode and anode. There are no theoretical indications that the AB_5 alloy is immune to oxidation in acid solutions. Determining dissolution rates of both cathode and anode material is therefore essential for the evaluation of chemical separation. The results from experiments on separate material types can be used to evaluate the dissolution of electrode mixtures.

Characterization of undissolved samples containing anode components is important for the determination of selective removal of corrosion products from the AB_5 alloy surface.

A list of experiments done in this work for the recovery of reusable anode is shown in Table 11, and the details of the experiments are described in the following subsections. The same results from experiments using 4 different carboxylic acids were used to evaluate chemical separation of cathode/anode and removal of corrosion products. 1 M maleic acid was further chosen for separation of cathode/anode by increasing the dissolution time and temperature, in order to increase the amount of metal dissolution from the cathode.

Table 11. Experiments for the recovery of reusable anode material using carboxylic acids.

Practical goal	Dissolution condition	Sample	Investigation 1.	
Chemical separation	4 carboxylic acids	cathode anode	Dissolution rates	Investigation 2.
	maleic acid / 10 h	cathode anode		
	maleic acid / 50 °C	cathode anode mixed electrodes		Characterization of undissolved material
Corrosion products removal	4 carboxylic acids	Anode		

4.5.1 Dissolution experiments using carboxylic acids

Dissolution experiments were carried out on cathode and anode samples (respectively). The samples were suspended in 1 M carboxylic acid (malonic, maleic, acetic and citric) solution at a S/L of 1/10 through magnetic stirring at room temperature (20 °C). The same experiment was also prolonged to 10 h in the case of maleic acid.

Spent cathode and anode samples, respectively, and a mixture thereof (0.5 g cathode and 0.5 anode) were immersed in 1 M maleic acid at 50 °C for 75 minutes. The S/L ratio was 1/10 for the separate fractions, and 2/10 for the mixed sample. The temperature was kept constant using a double-walled glass vial connected to a heating bath, and a plastic propeller was used for stirring.

Fresh 1 M acid solutions were prepared prior (< 48 h) to the experiments by dissolving appropriate amounts of malonic, maleic respectively citric acid salts (Sigma Aldrich) in pure water (>18 MΩ/cm, Milli-Q, Millipore), in a volumetric flask. A volumetric flask was also used for the dilution of concentrated acetic acid (99%, Sigma Aldrich).

The pH was measured using a pH glass electrode (Metrohm) before and after dissolution experiments that were conducted at room temperature. Buffer solutions at pH 1, 4 and 7 (Radiometer Analytical, Metrohm) were used for calibration. Variations of aqueous potentials due to ionic strength were not considered, and therefore reported pH values can only be regarded as approximated values.

Small aliquots of samples (0.75 mL) were withdrawn periodically from solutions and immediately filtered using a 0.45 µm PP-filter. Metal concentrations were determined by ICP-OES measurements, according to procedures described in section 4.2. Dissolution of metals (%) was calculated by the assumption of constant S/L ratio and previously determined metal concentrations of reference samples. No compensations for withdrawn volumes were made.

In dissolution experiments for the anode samples the experiment was terminated, and undissolved material was rinsed using respective fresh 1 M carboxylic acid in three steps. Three steps of pure water (>18 MΩ/cm, Milli-Q, Millipore) rinsing followed. The residual material was dried in a normal atmosphere for 24 h at 55 °C, and analyzed using XRD and SEM. EDS analysis was carried out on undissolved mixed electrode samples from experiments at 50 °C using the same sample work up procedure.

4.6 Recovery of cobalt using ascorbic acid

Separation of cobalt enriched surface layers from the spent cathode materials were investigated using ascorbic acid. The feasibility of selective dissolution of cobalt was initially investigated, and most subsequent experiments were carried out to further investigate the effects of reactions observed in the initial experiments.

The undissolved material remaining after each experiment was characterized to evaluate the effect of acid treatment on the anode material.

The list of experiments in Table 12 follows the order of presented results. The details of the experimental work are described in the following subsections.

Table 12. Separation of cobalt enriched surface layers from cathode material

Sample	Ascorbic treatment	Practical goal	Investigation	Analysis technique
Spent cathode	1 M / 4 h	feasibility	Dissolution rates	ICP-OES
	pH 2-5	Decoupling of redox/acidic properties		
	1 M / 2 h	Scale up and sample homogeneity	S/L ratio	
		non-destructive method confirmation	Morphology	SEM
Cathode a) unspent b) spent c) treated	a) untreated b) untreated c) 1 M / 2 h	Removal of cobalt surface enrichment	Surface species	XPS
Spent anode	1 M / 4 h	non-destructive method confirmation	Dissolution rate and residual characterization	ICP-OES, XRD, SEM

4.6.1 Dissolution experiments using ascorbic acid

Dissolution experiments using ascorbic acid were carried out on spent cathode and anode samples, respectively, at an S/L ratio of 1/10. Solutions were stirred with magnetic stir bars and the room temperature was monitored (20 °C) and kept constant. The same conditions were adopted for experiments with varied S/L ratios or pH.

Fresh acid solutions (1-1.5 M) were prepared (< 48 h) prior to the experiment by dissolution of L-ascorbic acid salt (Sigma Aldrich) in pure water (>18 MΩ/cm, Milli-Q, Millipore). For the investigations of the effect of pH, 1.5 M buffer solutions of acid respective conjugate base (sodium L-ascorbate, Sigma Aldrich) were mixed, based on approximations according to Henderson-Hasselbalch [106]:

$$pH = pK_a + log\frac{[base]_{initial}}{[acid]_{initial}} \quad \text{Eq. 15}$$

Measurements of pH, sampling, calculations and further sample work up procedures for characterization of undissolved material were similar to those previously described (sections 4.4.1 and 4.2).

5. RESULTS AND DISCUSSION

5.1 Characterization

Identification of crystalline compounds by XRD analysis was used as a first indication of how the electrode materials had changed during the battery use phase. Figure 8a-b shows the cathode material, both unspent (black) and spent (red), and anode electrode fractions, respectively. The XRD peaks of the cathode material did not indicate the presence of any foreign crystalline phases within samples, only phases of β-nickel hydroxide (doped with cobalt and zinc) and metallic nickel that are consistent with JCPDS Card No: 00-059-0459 [125] and 01-070-1849 [126], respectively. No difference was noticed between the spent and unspent cathode samples. According to the manufacturer, these samples contain both metallic nickel and cobalt. Due to the similar scattering properties of these metals it was not possible to differentiate between these elemental phases.

Results from XRD analyses of unspent and spent anode samples can be seen in Figure 2b. The two phases that were identified in unspent samples correspond to metallic nickel and AB_5 alloy, due to the consistency with JCPDS Card No: 01-070-1849 [126] and 04-009-7537 [127], respectively. The spent anode sample showed a similar diffraction pattern, however the corrosion product that corresponds to $REE(OH)_3$ (e.g. JCPDS Card No: 01-074-0665 [128]) was also detected. It is reasonable to assume that the corrosion product includes a mixture of four REEs (La, Ce, Nd and Pr). These elements are chemically alike due to the lanthanide contraction phenomena [26], and all these REEs are used in the alloy formulation.

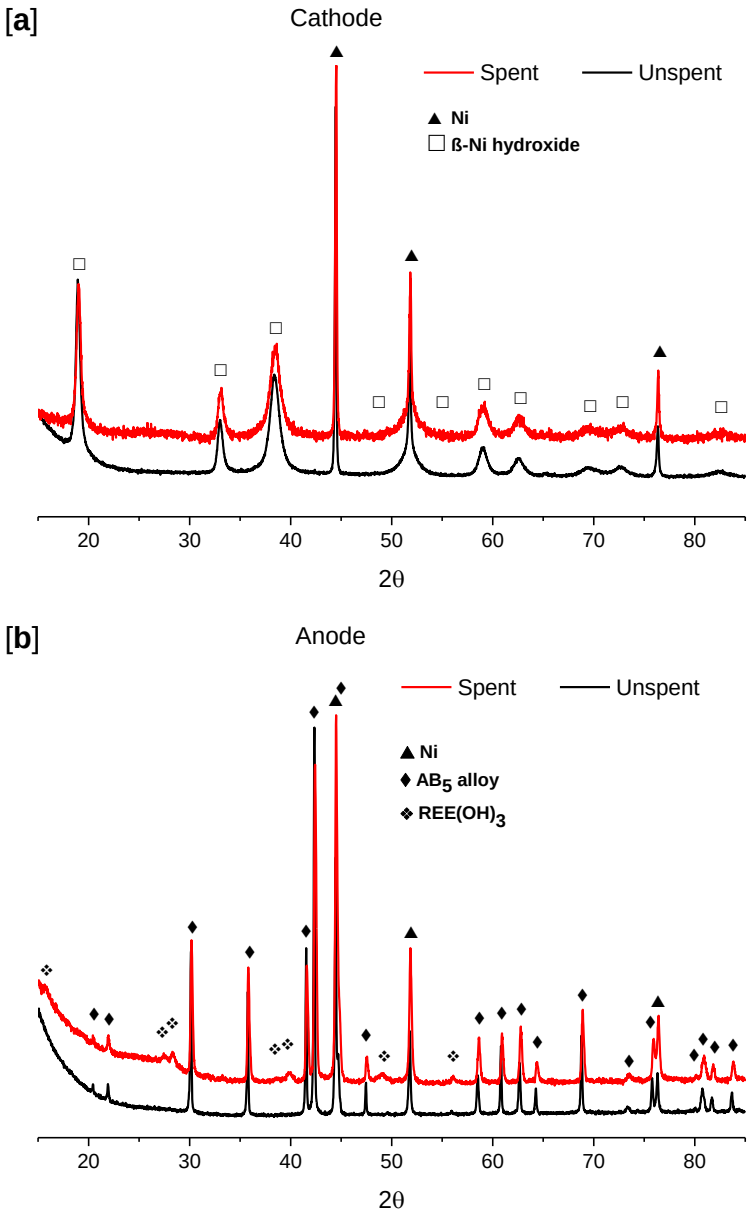

Figure 8. XRD lines for (a) cathode and (b) anode. Both spent (red) and unspent (black) diffraction patterns are shown. X-ray diffraction spectral lines of (a) unspent (red) and spent (black) cathode samples and (b) unspent (red) and spent (black) anode samples. The suggested phases Ni, β-nickel hydroxide, AB_5 alloy and $REE(OH)_3$ are consistent with JCPDS Card No: 01-070-1849 [126], 00-059-0459 [125], 04-009-7537 [127] and 01-074-0665 [128], respectively.

SEM analysis was done to observe changes in particle size, shape and morphology of both electrode materials during battery cycling. Cathode particles appeared to not have been changed by battery cycling, as can be seen by comparing SEM images of unspent and spent samples in Figure 9a-b, respectively. Independent of sample type (unspent and spent) there was a mixture of completely spherical and cracked and shattered particles.

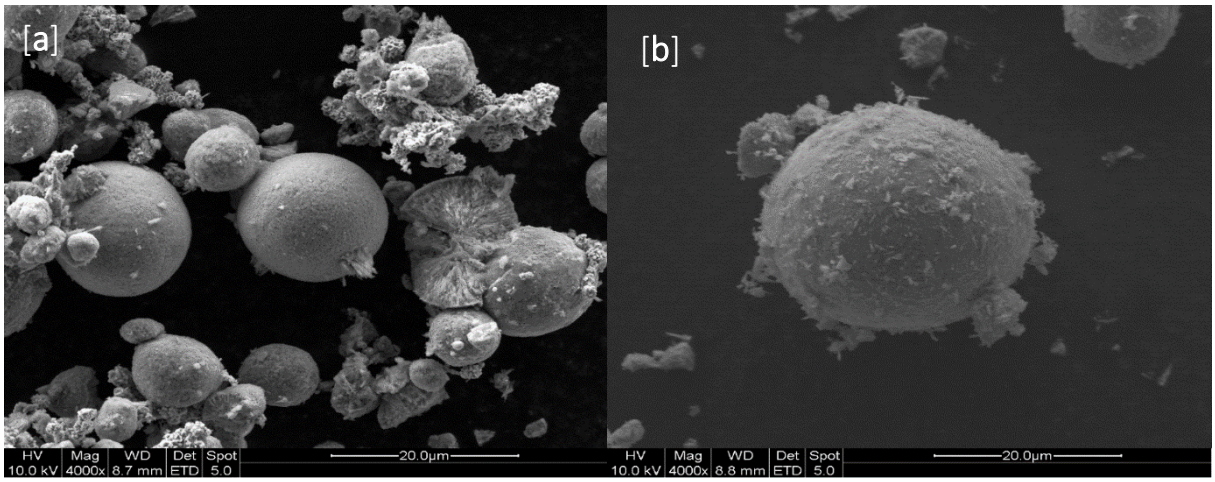

Figure 9. SEM images of (a) unspent and (b) spent cathode material.

AB_5 alloy particles from unspent and spent anode samples are shown in Figure 10. AB_5 particles in spent samples were generally smaller, and had crevices, compared to equivalent unspent particles. Furthermore, on the AB_5 alloy particles a needle shaped configuration could be detected, as can be seen in Figure 11. Based on the literature and the XRD analysis these compounds are identified as $REE(OH)_3$, which formed as a result of alloy corrosion in the electrolyte [69, 71, 72].

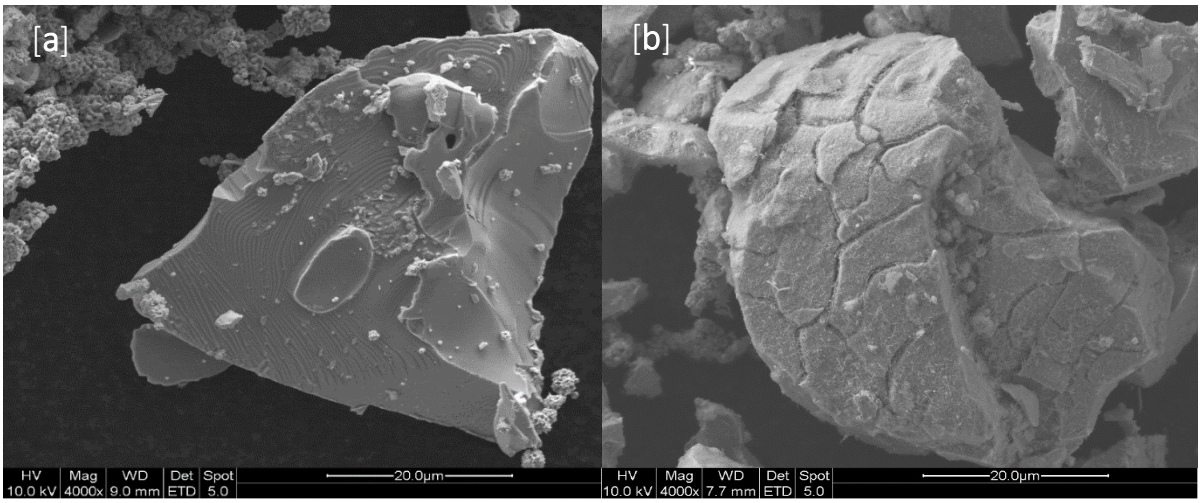

Figure 10: SEM images of (a) unspent and (b) spent anode material.

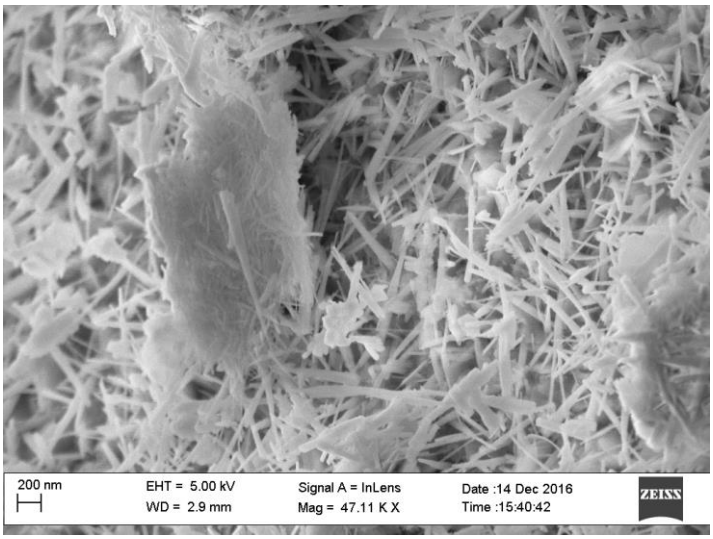

Figure 11. High resolution SEM image of spent anode material.

The metal composition of both spent electrode materials as determined by ICP-OES is shown in Table 13. In the cathode nickel, cobalt, zinc and low concentrations of aluminum and manganese were observed. Aluminum and manganese were not detected in the equivalent unspent cathode samples and are believed to be present in the spent cathode due to cross contamination from the anode. This is not unexpected and contaminants on the spent cathode material have been observed by others [23, 37]. For the spent anode samples, no zinc could be detected.

Table 13. Composition of spent cathode and anode electrode samples.

	Spent Cathode $mg \cdot g^{-1}$	Spent Anode $mg \cdot g^{-1}$
Al	2.1 ± 0.1	14.5 ± 0.1
Ce		44.4 ± 0.3
Co	41.9 ± 0.1	55.0 ± 0.4
La		166.2 ± 1.0
Mn	0.5 ± 0.1	37.0 ± 0.2
Nd		28.7 ± 0.2
Ni	605.2 ± 2.1	564.9 ± 3.7
Pr		10.3 ± 0.1
Zn	20.7 ± 0.1	
Total	670.4 ± 2.5	921.0 ± 6.0

The detected metal content of the cathode (670.4 mg/g) is an expected result, as the main components are metal (Ni, Co and Zn) hydroxides. If the cathode reference sample would only consist of pure nickel hydroxide, the amount of nickel should correspond to 633 mg/g. The deviation from this value (37.4 mg/g) is probably most affected by the presence of Ni(s) powder that has been mixed into the cathode electrode.

The degree of oxidation of the spent anode appears to be low as only 79 mg/g of the reference sample weight was not accounted for, which indicates that most of this weight fraction is oxygen. The amount of oxidation of the anode can be approximated to 5.5 wt% based on the following assumptions: homogeneous oxidation of elements, their common oxidation states and the formation of only hydroxides. This approximation is, however, dubious.

The surface area of both materials was determined using BET measurements. The results from these measurements are shown in Table 14.

Table 14. Surface area of electrode samples using BET method kept isothermal at 77 K and with N_2.

Electrode	Battery	Surface Area ($m^2 \cdot g^{-1}$)	Increase Factor
Cathode	Unspent	6.12 ± 0.10	4.6
	Spent	28.34 ± 8.28	
Anode	Unspent	0.20 ± 0.01	12.3
	Spent	2.42 ± 0.91	

The cathode surface area increased from 6.12 to 28.34 $m^2\ g^{-1}$ from the unspent to spent battery. The nickel hydroxide material can undergo several phase transitions (α, β, γ) that result in increased surface area, leading to pulverization and/or pore formation. Therefore, this is an expected result.

For the anode material the specific surface area had increased from 0.20 to 2.42 $m^2\ g^{-1}$. This is expected, because pulverization of the anode material is expected to have occurred with changes in lattice volume during intercalation of hydrogen into the AB_5 alloy lattice [23].

From the results of the characterization presented here some conclusions can be drawn about the degradation of the two spent electrode materials. Degraded qualities will effect strategies to recycle the materials.

For the cathode material it was not possible to detect any foreign crystalline compounds in the samples, which indicates that the material has not been changed by the battery cycling. However, low amounts of the contaminants aluminum and manganese were detected in the analysis of elemental composition. The presence of these two elements can affect the preferred cycling between β-$Ni(OH)_2$/β-NiOOH. BET measurements showed that the cathode had degraded through increased surface area. A change in void size distribution and/or pore formation can affect electrolyte diffusion, which indirectly can cause increased internal resistance. Thus, charge/discharge characterisistics are degraded. Analysis with SEM did however not raise suspicions of severe size or morphology changes during cycling.

In the anode material the original AB_5 alloy and Ni(s) crystal structures were detected using XRD, and also a foreign $REE(OH)_3$ phase. Through SEM analysis this phase was observed as needle-shaped configurations on the AB_5 alloy surface. Several different corrosion scales that reside underneath these needles have been observed by others [69, 71, 72]. All corrosion products can interfere with the functions of the alloy surface. Specifically, the functions are to catalytically react with the electrolyte and transport hydrogen to and from the alloy bulk [21]. Thus, it is only reasonable to assume that corrosion products such as $REE(OH)_3$ affect the charge/discharge rate of the anode electrode.

The elemental composition of the anode was analyzed using ICP-OES. The experimentally calculated weight of metals in the spent anode material was close to 1000 $mg \cdot g^{-1}$, which suggested that only a part (79 $mg \cdot g^{-1}$) is oxygen and/or hydroxide. No contamination of zinc could be observed on the spent anode material. The amount of corrosion products was not substantial, and was estimated to be approximately ≈ 5.5 wt%.

An increase in surface area was noted for the spent anode material using the BET method. Increased surface area will increase both preferred and parasitic reactions on the AB_5 alloy surface. Removal of corrosion products from the spent AB_5 alloy can potentially produce a material that can be used in applications where high discharge-rates are preferred. Therefore, it is interesting to further investigate treatment methods that recover reusable AB_5 alloy from spent anode materials.

5.2 Recovery of nickel

5.2.1 Effect of acidity on nickel recovery

Results from dissolution experiments of mixed electrode materials at pH 1 are shown in Figure 12a, and are in agreement with those obtained by Larsson et al. [113]. From analysis of elemental composition > 90% of Al, Co, Mn, La and Zn were dissolved after 5 h. At this time less (80%) of the nickel was dissolved. After 30 h of dissolution the amount of dissolved Al, Co, Mn, La and Zn had not changed much compared to the change in the amount of dissolved nickel (100%). This indicates that nickel is mainly dissolving during the period between 5-30 h. Lanthanum is only found in the AB_5 alloy and zinc is only found in the nickel hydroxide. Therefore one can expect that the dissolution rate of AB_5 alloy > $Ni(OH)_2$ (s) in hydrochloric acid solutions at pH 1.

According to the added titrant rate (Figure 12b) the dissolution rate of the waste appears to be divided into a fast (0-5 h) and a slow regime (5-30 h). These two regimes have very different dissolution rates and indicate that the different components AB_5 alloy, nickel hydroxide and Ni(s) are dissolving at different rates.

The dissolution rate of the remaining 17% nickel (approximately) after 5 h acid treatment is slower compared to those of the other elements. Nickel exists in mixed electrode materials in three main forms, namely Ni(s), AB_5 alloy and nickel hydroxide. It is expected that Ni(s) is only a small fraction of the samples. Therefore, the 17% nickel that is dissolving slowly is attributed to Ni(s). This is a reasonable conclusion since hydrogen desorbs slowly from nickel surfaces.

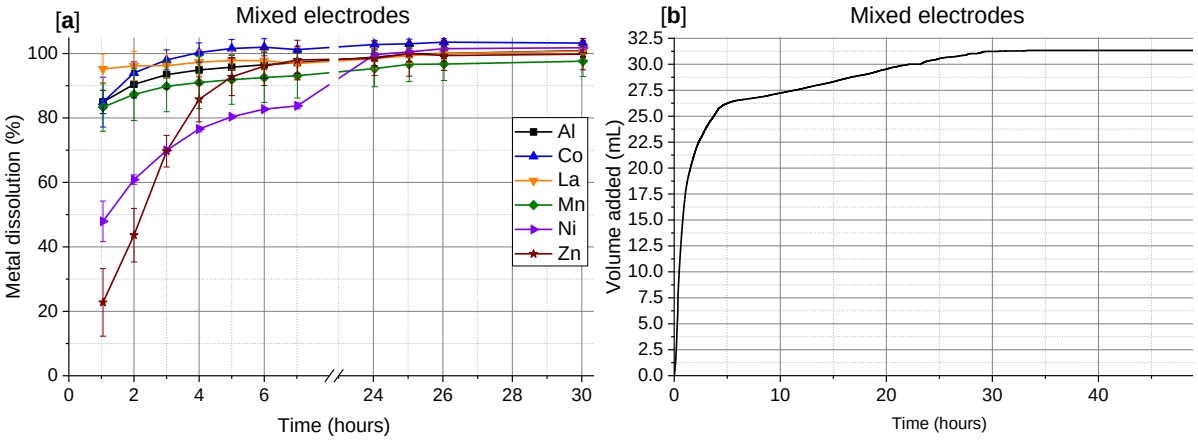

Figure 12. Dissolution of 1.1 g mixed electrode fraction in pH 1 HCl solution at 25 C. The results show (a) dissolved amount of elements (%) and equivalent (b) 1 M volume acid addition to maintain pH.

Undissolved material after 5 h of dissolution of mixed electrode materials in hydrochloric acid at pH 1 was characterized. An interesting observation during the practical work was that the undissolved material was magnetic and could easily be collected with the use of a magnet. The nickel content of these collected residuals was high (96.6 ± 1.0 wt%) and they also contained some cobalt (0.3 ± 0.1 wt%). No other elements could be quantified ≥ 0.1 wt%. The unaccounted amount (≈ 3 wt%) is believed to be related to oxygen present. Analysis results from XRD and SEM can be seen in Figure 13 and Figure 14, respectively.

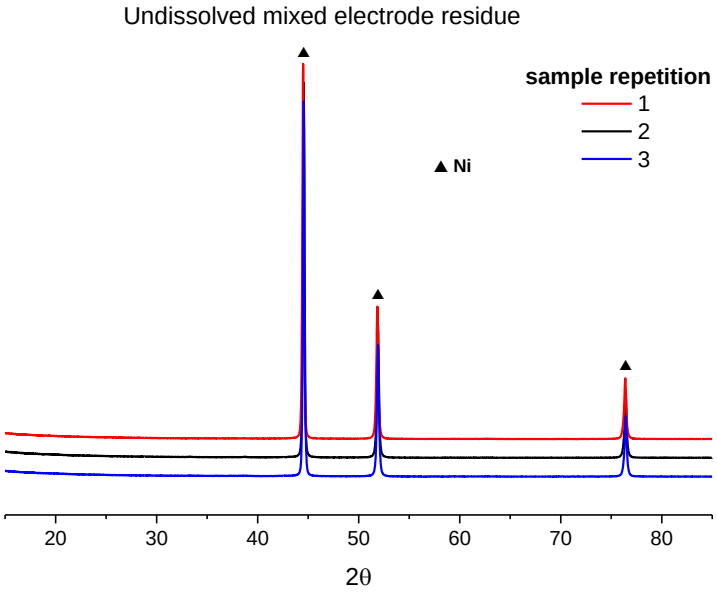

Figure 13. Results from XRD analysis of residual material collected from three replicates (red, black and blue) obtained from dissolution of mixed electrode material, using pH 1 hydrochloric acid solutions at 25 C, after 5 h. The suggested phase Ni is consistent with JCPDS Card No: 01-070-1849 [126].

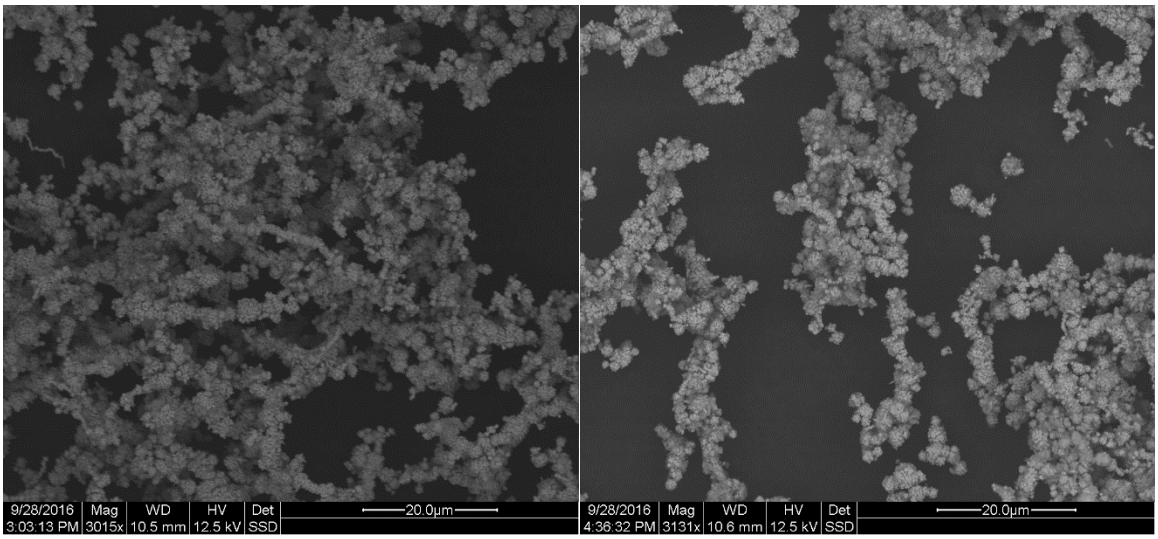

Figure 14. SEM images using Quanta 200 FEG ESEM of unused nickel powder (left) and spent nickel powder (right) collected after dissolution experiments at pH 1.

Results from dissolution of mixed electrode materials in 1-8 M hydrochloric acid solutions are shown in Figure 15a-b. The dissolution rates of the AB_5 alloy and $Ni(OH)_2$ (s) components are illustrated with the amount of dissolved lanthanum and zinc, respectively. Dissolution rates of these two components are complete after 0.5 h in 2-8 M hydrochloric acid solutions. The corresponding dissolution rate of nickel can be seen in Figure 15b. It is an expected result that the dissolution rate of nickel is different compared to that of lanthanum and zinc, since some of the nickel originates from the Ni(s) component.

The dissolution rate of nickel from pure Ni(s) powder samples in hydrochloric acid solutions (1-8 M) can be seen in Figure 16. Interestingly, the dissolution rate of nickel in 1-4 M hydrochloric acid is similar and in 8 M solution almost complete dissolution of nickel is achieved after 5 h immersion time.

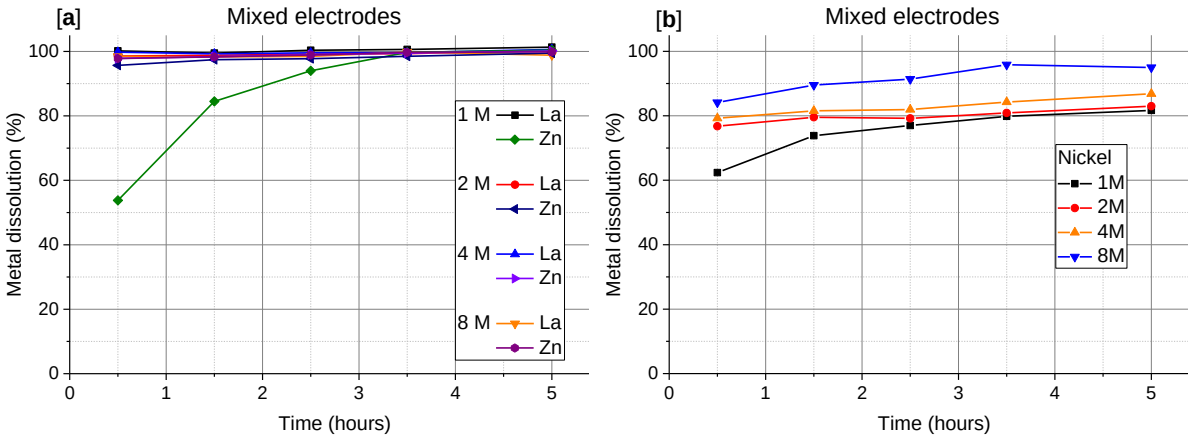

Figure 15. Dissolution of (a) lanthanum, zinc and (b) nickel from 0.5 mixed electrode material initially in 1-8 M hydrochloric acid solutions.

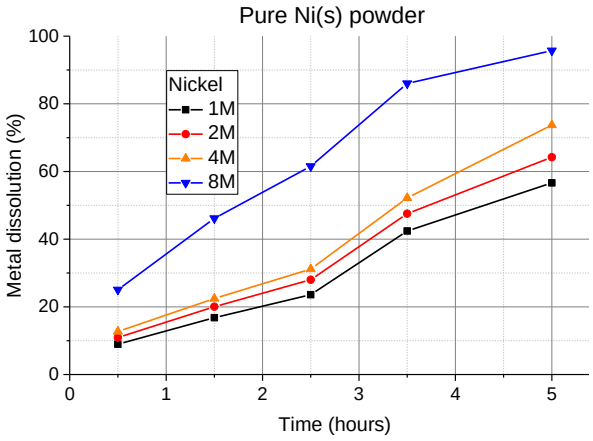

Figure 16. Dissolution of nickel from 0.25 g pure Ni(s) powder samples initially in 1-8 M hydrochloric acid solutions.

Recovery of Ni(s) can be made by dissolving mixed electrode materials in hydrochloric acid. In a practical recycling process the mixed electrode materials are immersed in e.g. 8 M hydrochloric acid in order to dissolve the materials. The dissolution rate of components follows the decreasing order AB_5 alloy ≈ $Ni(OH)_2$ (s) >> Ni(s) in 2-8 M hydrochloric acid concentration and AB_5 alloy > $Ni(OH)_2$ (s) >> Ni(s) in 1-0.1 (i.e. pH 1) M acid concentration. That is to say, the acid is rapidly consumed by the AB_5 alloy and $Ni(OH)_2$ (s) components. Therefore one should expect to recover the majority of Ni(s) powder component even when mixed electrode materials are immersed in 8 M hydrochloric solutions.

5.2.2 Extraction of metals using Cyanex 923 and the effect of acidity

When the logarithmic distribution ratio of a metal exceeds zero the metal is more concentrated in the organic phase compared to the aqueous phase. The separation of one metal from others is increased when the differences in distribution ratios between the metals are increased.

The distribution ratio of zinc from the leachate solution increases with increasing O:A ratio, as can be seen in Figure 17. The distribution ratio of zinc is at least 1.75 higher order of magnitude compared to distribution ratios of the other metals (Al, REE, Mn and Co) at O:A = 3. Thus, zinc can be separated from the other metals. The extraction and separation of zinc from similar leachate solutions, by keeping a low concentration (8 vol%) of Cyanex 923, is in agreement with the results of others [93].

Variation of general metal extraction with respect to O:A ratio can be seen in Figure 18. All metals except nickel were extracted, because the concentration of Cyanex 923 was high (70 vol%). Above a 3.5 O:A ratio the extraction of metals does not increase. As anticipated, Cyanex 923 can be used to extract and separate metals from nickel [93].

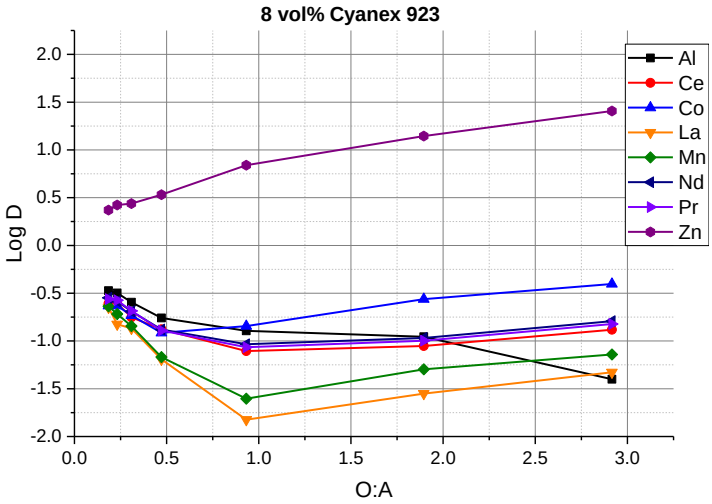

Figure 17. Extraction of zinc and other metals from 8 M chloride leachate solution using 8 vol% Cyanex 923 in Solvent 70. Nickel was not extracted.

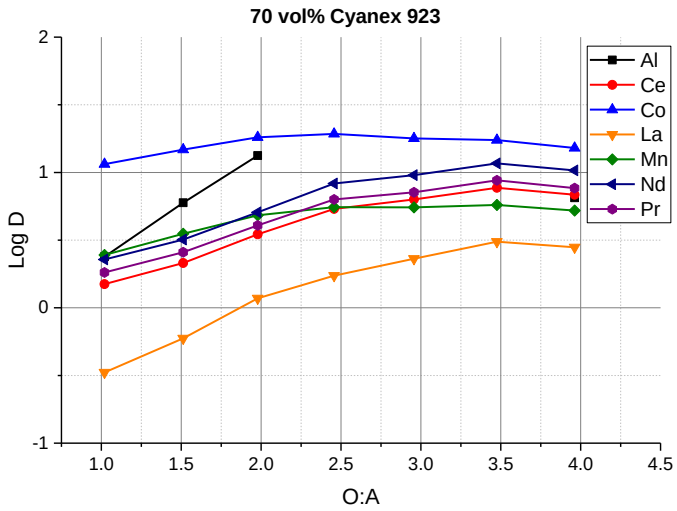

Figure 18. Extraction of metals from 8 M chloride solutions using Cyanex 923 (70 vol% in Solvent 70). Zinc was quantitatively extracted and nickel was not extracted.

The results from experiments at different aqueous potentials can be seen in Figure 19. For the sake of reference, 440 mV corresponds to approximately 0.12 M HCl concentration. At a measured aqueous potential up to 440 mV the extraction of all metals does not vary with the amount of HCl concentration. The Log (D_{La} = -0.25) corresponds to approximately 40% extraction of lanthanum. Above 440 mV the extraction of aluminum and REEs decreases. It was described by Larsson et al. [93] that the extraction of REEs and aluminum benefits from a high chloride concentration but not from increased acidity. The amount of available extracting agent (Cyanex 923) that can extract REEs and aluminum are instead consumed by the extraction of acid. Therefore, the results obtained from these experiments are expected.

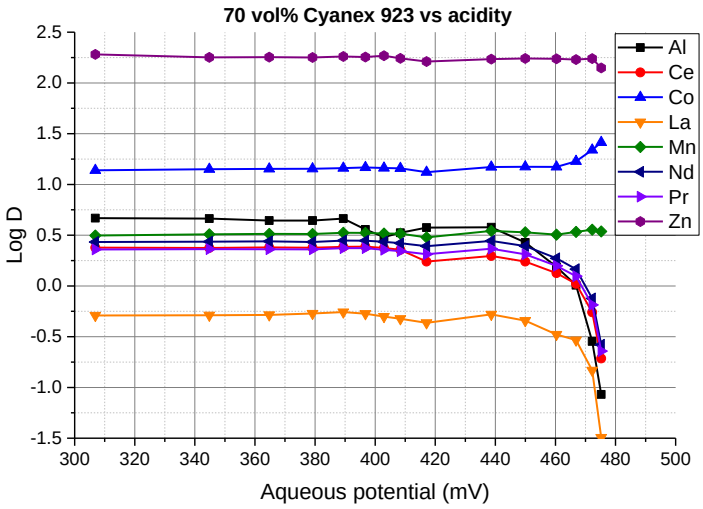

Figure 19. Extraction of metals from 8 M chloride solutions, at varied aqueous potentials. An 8 M chloride solution has been diluted with 8 M hydrochloric acid, which resulted in an increase of aqueous potential registered with a glass electrode. The organic phase consists of Cyanex 923 (70 vol% in Solvent 70). The experiments were carried out at a constant O:A ratio of 1.4.

Experimental results from varied O:A ratio experiments confirm the Cyanex 923-chloride system as appropriate for the separation of zinc, aluminum, cobalt, manganese and REEs from nickel.

The experimental results presented here demonstrate that controlling the acidity is important for maintaining extraction of REEs and aluminum from 8 M chloride solutions using Cyanex 923. A concentration of 0.12 M HCl was identified as a threshold value for acceptable REE and aluminum extraction at 70 vol% Cyanex 923. This threshold implies that 15 mL 8 M HCl is the tolerated level of acid overshooting when producing 1 L of leachate solution. This accuracy (15 mL) can be achieved on an industrial recycling scale. However, further work is needed to determine the target level.

5.3 Recovery of reusable anode using carboxylic acids

5.3.1 Chemical separation of anode and cathode

A summary of the amounts of dissolved metals from cathode respectively anode materials after 4 h treatment in carboxylic acids (acetic, citric, maleic and malonic acid) are shown in Figure 20. From these results one can expect no chemical separation of the electrode materials to be achieved without losses of anode. Possibly, the investigated dissolution period (4 h) was not sufficient for complete dissolution of the cathode material.

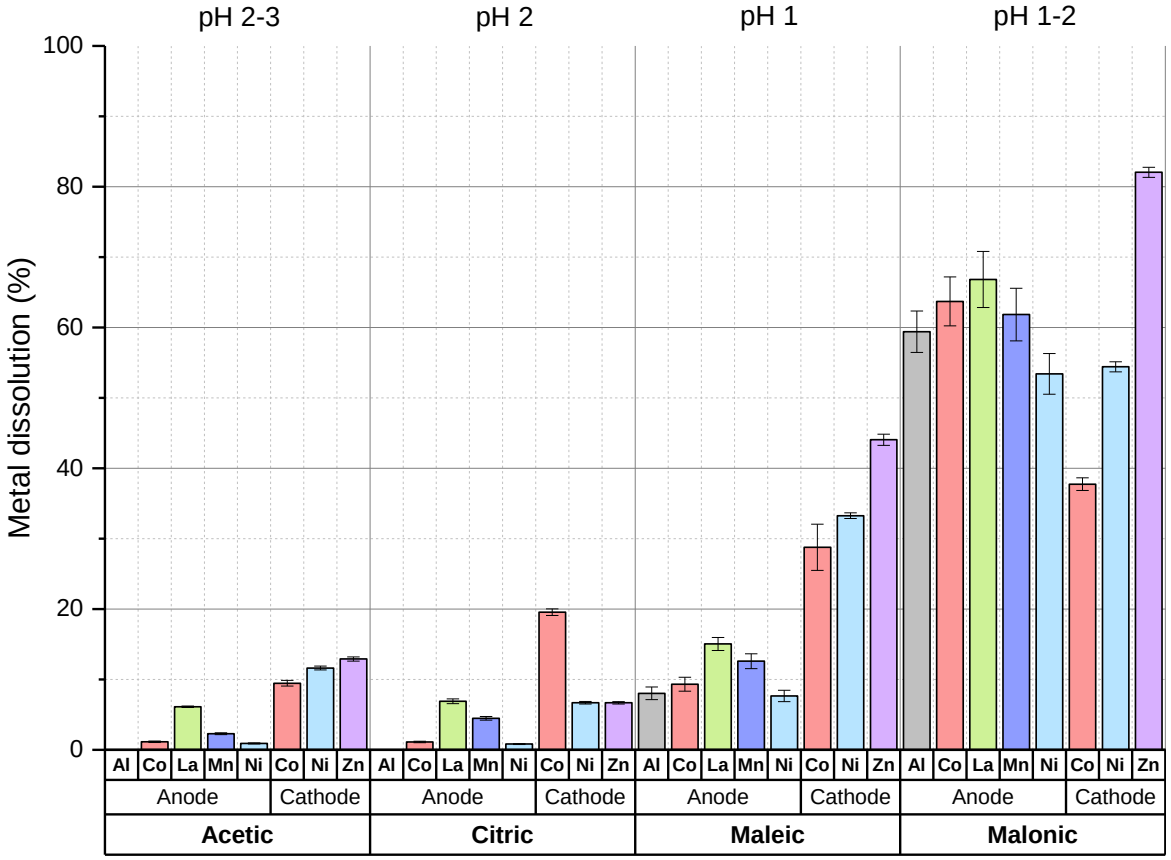

Figure 20. Summary of the amount dissolved of the main constituent metals (%) in the electrode materials in the respective 1 M carboxylic acids, after 4 h dissolution at room temperature (20 °C). The pH values before and after the experiments were similar and approximated with the indicated values.

In trial experiments at 50 °C only maleic acid appeared useful (between the 4 carboxylic acids) with respect to achieving separation of cathode and anode material, and maleic acid was selected for further experimental tests.

Dissolution rates of metals from cathode and anode material in 1 M maleic acid solutions are shown in Figure 21a-b, respectively. The amount of dissolved metals from cathode as well as from anode increases with time. After 10 h the dissolution of the cathode material was still not complete. However, it is indicated in Figure 21a by the dissolution curve that the amount of metals released from the cathode appear to converge. Therefore, separation of cathode and anode is possibly coupled to a limited solubility of zinc, cobalt and nickel.

Dissolution of all metals from anode samples was high (≥ 30%) after 10 h, as can be seen in Figure 21b. This indicates that the AB_5 alloy material was dissolving.

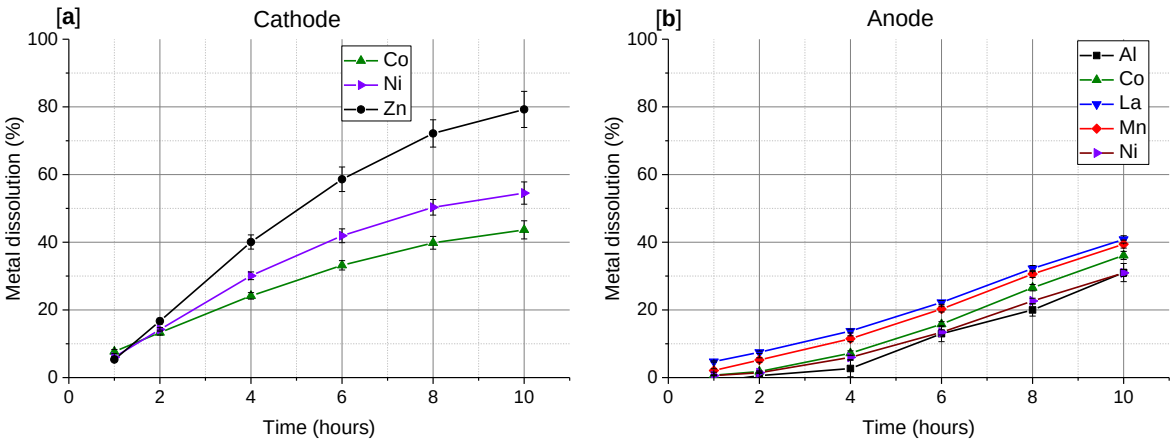

Figure 21. Dissolution of 0.5 g (a) anode and (b) cathode samples in 50 mL 1 M maleic acid solutions at 20 °C.

The effect of elevated temperature (50 °C) on the dissolution rates of metals from cathode and anode in 1 M maleic acid is shown in Figure 22a-b, respectively. With respect to room temperature (20 °C), the amount of dissolved metals from both cathode and anode were increased.

Zinc had been dissolved completely (100%) after 60 min in 1 M maleic acid at 50 °C, which is an important observation to make from the results shown in Figure 22a. The amount of dissolved nickel and cobalt are approximately the same (70%). The current dissolution experiment can potentially still constitute a separation of the cathode and anode material. Nickel exist as powder, and cobalt exists as both powder and cobalt-enriched surface layers. The amount of these three compounds in the cathode samples have not been determined. However, these should only exist at low amounts. Thus, the remaining undissolved 30% of nickel and cobalt can possibly be attributed to these three components. Based on these assumptions it is indicated that the nickel hydroxide has reacted completely with maleic acid.

It can be estimated that 50% of the AB_5 alloy had been dissolved from the anode sample immersed in 1 M maleic acid at 50 °C, as shown in Figure 22b. A lower fraction of the nickel was dissolved (40%). This is expected, because metallic nickel powder also exists in the anode samples.

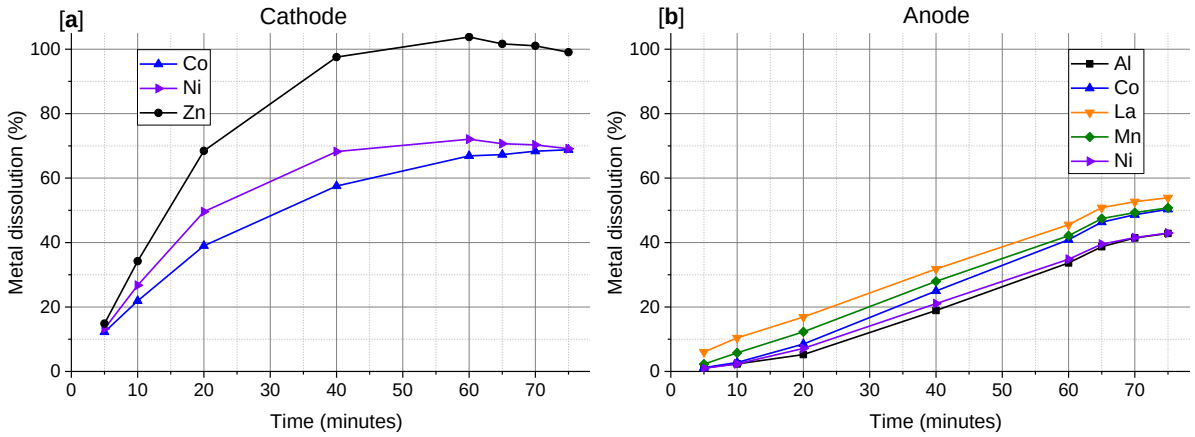

Figure 22. Dissolution of 0.5 g (a) anode and (b) cathode samples in 50 mL 1 M maleic acid solutions at 50 °C.

Samples treated with 1 M maleic acid at 50 °C for 75 min were characterized with XRD, and the results are shown in Figure 23. In agreement with the conclusion drawn from the dissolution investigation (Figure 22a-b) diffraction peaks corresponding to $Ni(OH)_2$ (s) could not be detected. Instead, only crystalline phases corresponding to anode constituent materials AB_5 alloy and Ni(s) were detected.

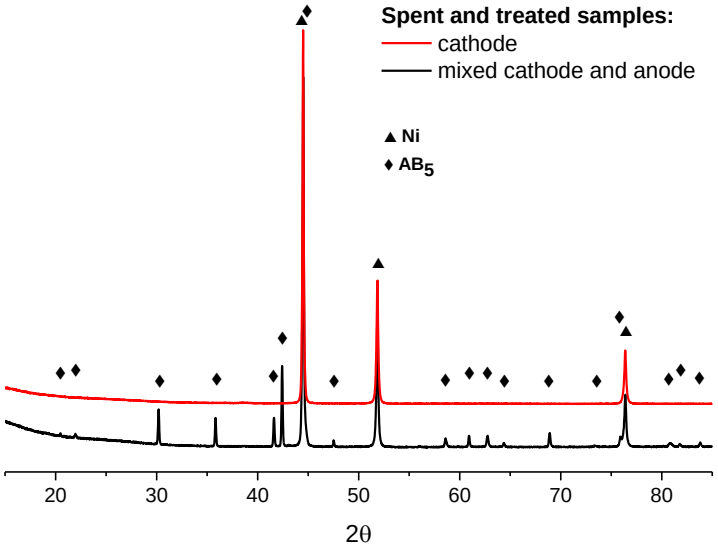

Figure 23. Results from XRD analysis of collected solid residual material from dissolution experiments with 1 M maleic acid solution at 50 °C for 75 minutes. Note that the diffraction peaks corresponding to the anode components AB_5 alloy and Ni(s) originate from a mixed cathode and anode sample. The phases Ni and AB_5 alloy are consistent with JCPDS Card No: 01-070-1849 [126] and 04-009-7537 [127], respectively.

A SEM image and EDS map of mixed cathode and anode sample that had been treated with 1 M maleic acid for 75 min at 50 °C is shown in Figure 24. The coupled SEM/EDS analysis illustrates that patch-wise corrosion layers (purple) rich in nickel (red) and carbon (blue) covered the AB_5 alloy particles. These layers possibly consist of nickel complexes that were not dissolved during dissolution experiments. There are no signs of $REE(OH)_3$ needle formation on the AB_5 alloy particles. Signs of pitting corrosion were generally observed on the AB_5 alloy particles.

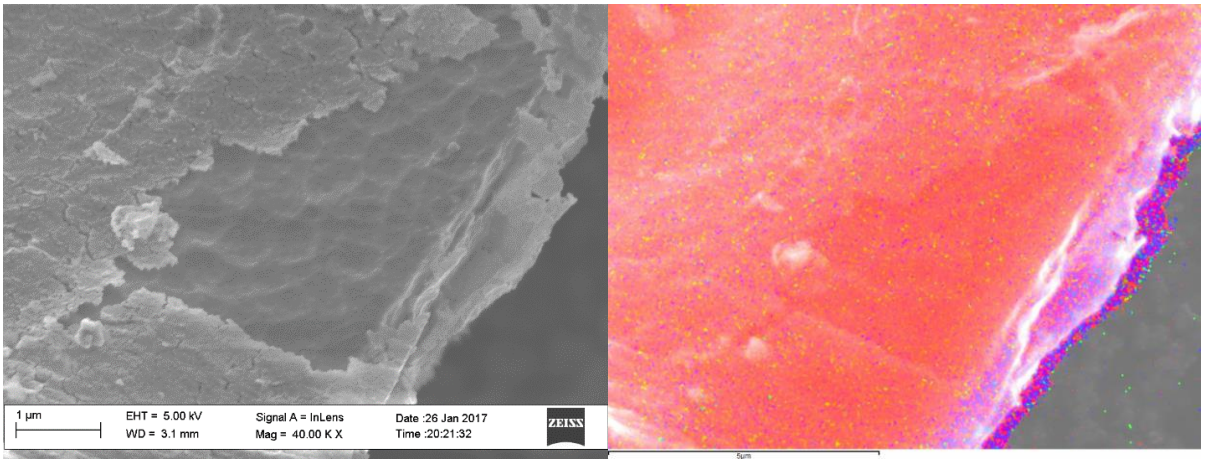

Figure 24. SEM images taken with Ultra 55 FEG SEM showing an anode particle separated from mixed electrode material, using 1 M maleic acid at 50 °C for 75 min. Images (left and right) are of the same surface area from one particle and illustrate patch wise surface layers. EDS analysis uses the following colors: nickel (red), oxygen (green), carbon (blue) and nickel-carbon (purple).

An industrial and practical method, using carboxylic acids, does not appear to be feasible for the chemical separation of cathode and anode. These acids would only be practically useful in the case where the dissolution behaviors (rates and amounts) of cathode and anode are very different in the same solution. Such differences in properties were not observed for any of the investigated carboxylic acids (malonic, maleic, acetic and citric acid).

It was demonstrated that increasing the temperature from 20 °C to 50 °C for the 1 M maleic acid solution could achieve a chemical separation of cathode and anode material. However, the anode was

significantly dissolved (50%). Dissolution of AB_5 alloy is coupled to the electrochemical oxidation where hydrogen ions are reduced and hydrogen gas evolves. This is a general drawback for the chemical separation of NiMH electrode materials using acidic solutions.

5.3.2 Separation of corrosion products from AB_5 hydrogen storage alloy

Dissolution rates of elements from anode samples using 1 M carboxylic acids (malonic, maleic, acetic and citric acid) are shown in Figure 25 and Figure 26, respectively. The dissolution of the main anode constituent elements nickel and lanthanum decreases in the order of malonic > maleic > acetic ≈ citric acid. The practical pH of the solutions did not vary before and after the experiment, and has been presented previously in Figure 20.

As previously pointed out it can be roughly approximated that 5.5 wt% of the sample was corrosion products, i.e. lanthanide hydroxides. Due to the high (> 50%) amounts of dissolved metals it is therefore indicated that the AB_5 alloy was dissolving as well in the malonic acid solutions.

The amounts of dissolved metals from anode material were different with respect to the different solutions used (maleic, acetic and citric acid), as shown in Figure 25a-b and Figure 26a-b. The amount of dissolved metals into maleic acid were low (< 20%). Interestingly, the amount of dissolved metals into acetic and citric acid was even lower (< 10%), and also appeared to converge. Previous investigations of the corrosion products on the spent AB_5 alloy surface suggest that many different oxidized compounds (Ni, Co, REE, Mn) can exist. Therefore, the observed different dissolution rates indicate that some of the corrosion products may have been removed.

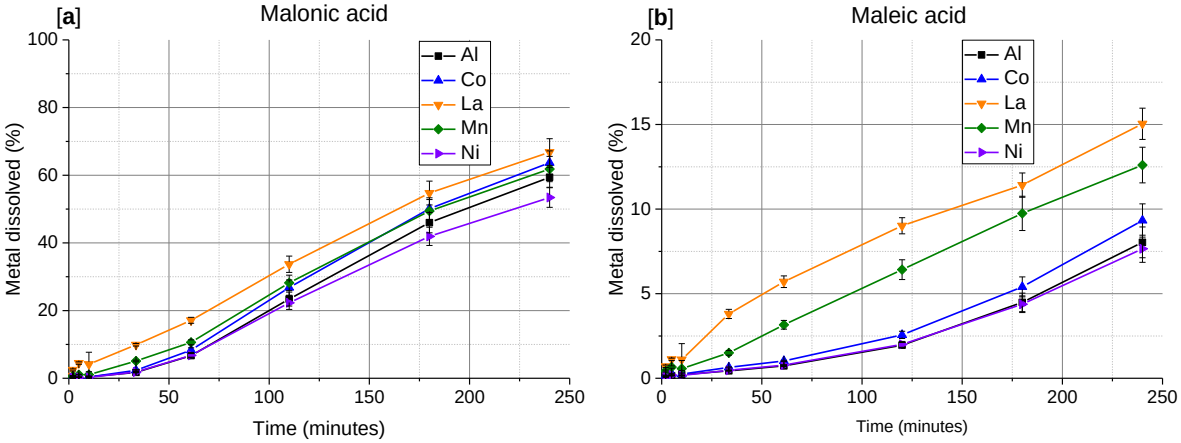

Figure 25. Dissolution of 0.5 g anode material in 50 mL 1 M (a) malonic and (b) maleic solutions.

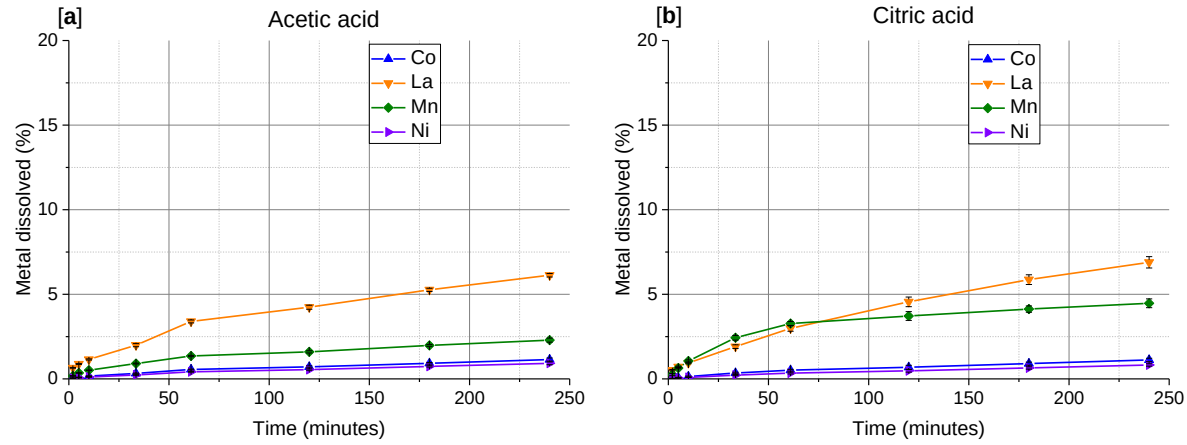

Figure 26. Dissolution of 0.5 g anode material in 50 mL initially 1 M (a) acetic and (b) citric acid solutions.

The results from the characterization of the collected anode samples (subjected to 4 h treatment in malonic, maleic, acetic and citric acid) using XRD can be seen in Figure 27a. For all samples the same crystalline phases corresponding to the AB_5 alloy and Ni(s) were detected. For the sake of comparison, the highest relative intensities of $REE(OH)_3$ phases, which occur between 27-29, 39-41 and 48-50 2θ angles are shown in Figure 27b. As far as can be seen from XRD analysis the $REE(OH)_3$ has been removed by the treatment of malonic, maleic, acetic and citric acids.

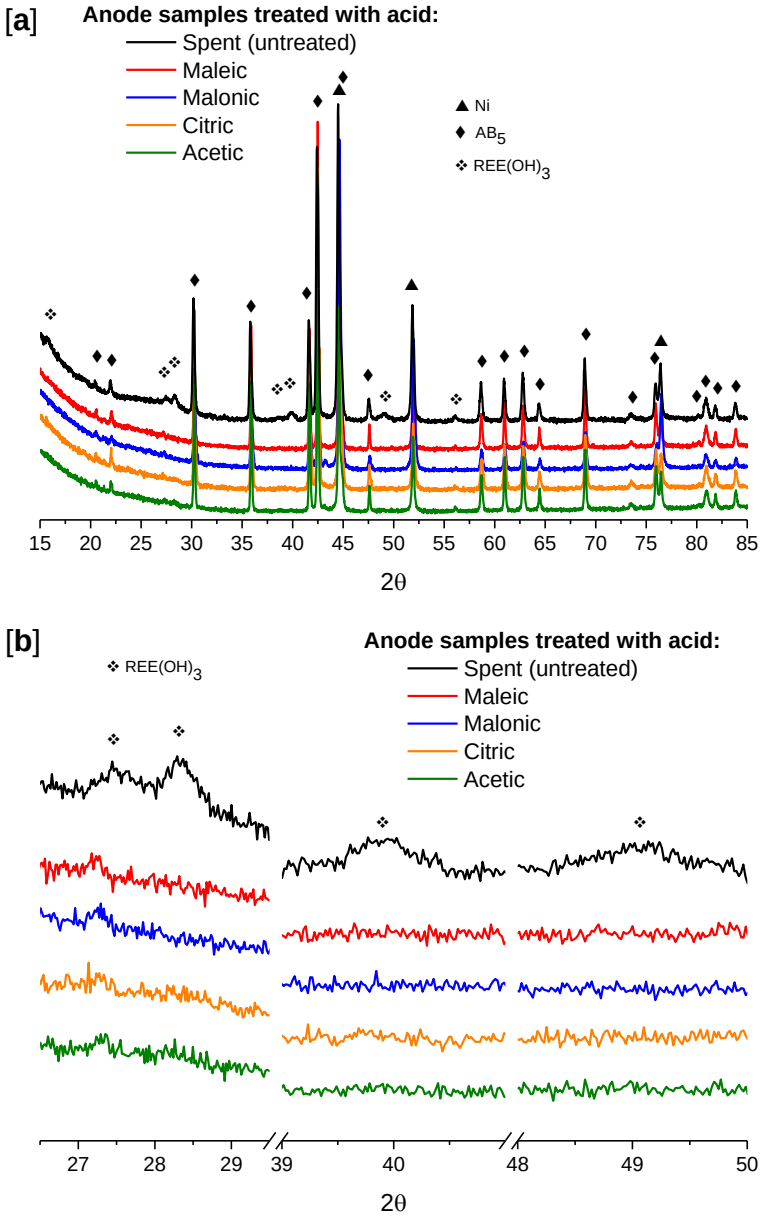

Figure 27. XRD diffractograms of spent and untreated anode and anode samples subjected to 4 h treatment in different 1 M carboxylic acids (a). The resolution of relative intensities at some 2Θ intervals has been increased (b). The phases Ni, AB_5 alloy and $REE(OH)_3$ are consistent with JCPDS Card No: 01-070-1849 [126], 04-009-7537 [127] and 01-074-0665 [128], respectively.

SEM analysis was conducted on anode samples that had been treated with 1 M carboxylic acids for 4 h and the results are shown in Figure 28a-b (malonic acid) and Figure 29a-b (acetic respectively citric acid). The effect of treatment with maleic acid that can be expected has been previously presented in Figure 24. The images that are shown here represent the most important observations that were made during analysis.

In all analyzed samples the characteristic irregular anode particle shape that resembles the shapes of unspent AB_5 alloy particles was detected. This indicates that neither treatment completely destroyed the particle shape.

In samples subjected to the aggressive leaching solution (malonic acid) the surfaces of particles were visually alike. Particles subjected to malonic acid appeared to have been subjected to uneven corrosion, e.g. pitting corrosion (Figure 29a). In addition, the surfaces of the examined particles had patch-wise surface layers (Figure 29b). In comparison to the EDS analysis of samples treated with maleic acid at 50 °C (Figure 24) these patch-wise surface layers are visually similar. Therefore it is reasonable to assume that the patch-wise surface layers seen here are also nickel-carbon enrichments.

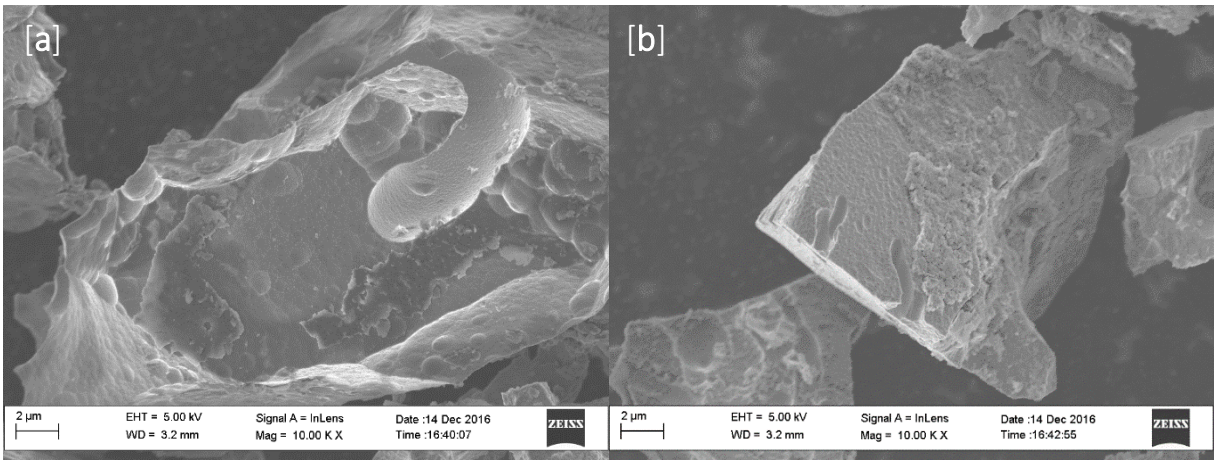

Figure 28. SEM images taken with Ultra 55 FEG SEM. Anode particles treated with 1 M malonic acid for 4 h. In the left hand Figure (a) patch-wise corrosion products are observed. In the right hand Figure (b) pit formation (i.e. pitting corrosion) is seen.

For the least aggressive treatment media (acetic and citric acid) the visual appearances of particles were similar regardless of treatment solution. Most of the AB_5 alloy particles in these samples were covered with irregular disc-like crystals (see Figure 29a-b). These surfaces do not resemble the surface of unspent AB_5 alloy. It is therefore believed that the observed surface layers are acetate or citrate metal complexes, respectively, or remaining undissolved corrosion products from battery cycling (i.e. nickel/cobalt oxides).

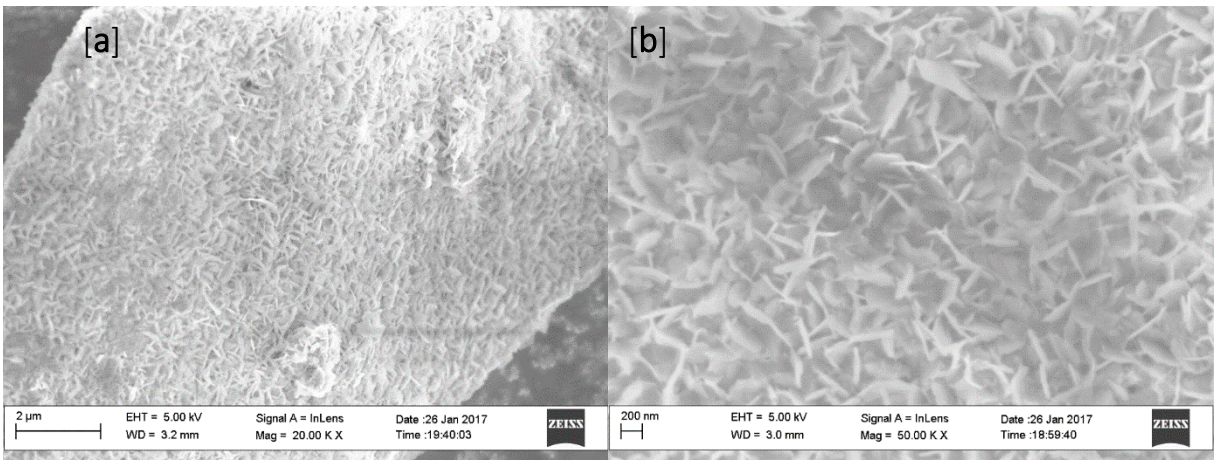

Figure 29. SEM images taken with Ultra 55 FEG SEM of anode particle treated with (a) acetic and (b) citric acid for 4 h. The surface morphologies of observed particles were comparably similar regardless of the acid (acetic and citric) used to treat the anode samples. The image to the right (b) is at high resolution.

It was not possible to recover an AB_5 alloy material completely free from inorganic and/or organic corrosion product from spent anode material using the carboxylic acids chosen for the current work.

Carboxylic acids contain oxygen in the functional group (COOH) that can interact with the surfaces of the solid samples. These interactions can result in kinetically slow surface processes. In fact, the dissolution rates of the anode material (in carboxylic acids) presented in the current work are generally low compared to previous investigations (in mineral acids) [113]. Therefore, the attempt to use carboxylic acids to slow down the dissolution of AB_5 was to some extent successful.

The practical usefulness of the investigated carboxylic acids is, however, limited. An interesting conclusion that can be drawn is that acetic and citric acid can be used to remove the $REE(OH)_3$ compounds from the surface without significantly dissolving the AB_5 bulk. This was not observed for the two other acids (malonic and maleic acid). From electrochemical considerations it is predicted that the AB_5 alloy will eventually also react with acetic and citric acid, due to the hydrogen evolution potential. Therefore, it is probable that the relatively selective removal of $REE(OH)_3$ is associated with slow dissolution rates of the remaining corrosion products.

5.4 Recovery of cobalt using ascorbic acid

5.4.1 Cathode material

5.4.1.1 Leaching of cathode

The results from preliminary dissolution experiments in 1 M ascorbic acid are shown in Figure 30. Dissolution of cobalt was approximately 63% after 60 minutes. At this time the dissolution of nickel (1.4%) and zinc (3.1%) were both low. Relatively selective dissolution of cobalt using ascorbic acid was expected, due to the reducing properties of ascorbic acid and the elevated oxidation state of cobalt at the cathode surface.

It is difficult to determine the cause of selective dissolution of cobalt in these experiments. Interestingly only a fraction of the cobalt was dissolved. The total concentration of cobalt in cathode material is low (4.2 wt%) and it is suspected that cobalt exists in the following three different components: elemental cobalt powder, cobalt hydroxide and surface enriched cobalt in oxidation states higher than 2. It is therefore difficult to estimate the amount of cobalt that exists on the surface of the nickel hydroxide material. Since the cathode material is complex, further experiments are needed to elaborate on the observed selective dissolution phenomena.

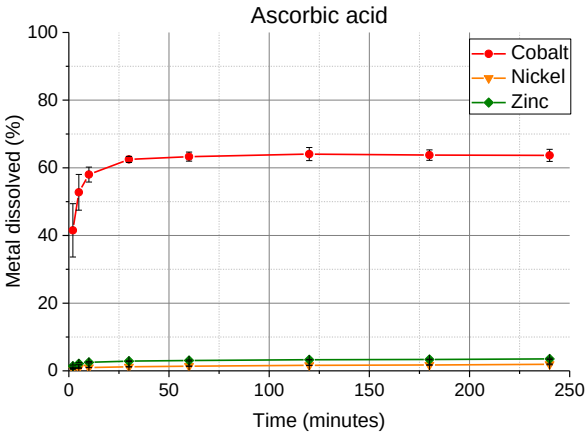

Figure 30. Dissolution of the main elements cobalt, nickel and zinc from cathode samples using 1 M ascorbic acid solutions, at 20 °C and S/L ratio of 1/10.

The effect of pH on the dissolution of metals from cathode samples was investigated, and the results have been summarized in Figure 31 and Figure 32. Aluminum and manganese that had been observed in spent cathode samples were also considered in these experiments. The results show that the solution pH has only a slight effect on the dissolution rate and amount (60-70%) of dissolved cobalt. The effect

of pH on the dissolution of other elements (Al, Ni and Zn) was similar, but the amount of dissolved metals was generally low (> 2-4.5%). Interestingly, the dissolution behavior of manganese is similar to that of cobalt with one exception; manganese dissolves completely (100%).

The hypothesis that a redox reaction responsible for selective cobalt dissolution was a general statement in section 4.5. The hypothesis was confirmed by decreasing the acidity of leaching solutions in which ascorbic acid still had a negative reduction potential.

A variation in pH did not have a significant effect on the dissolution of nickel hydroxide particles, as can be seen in Figure 31. Nickel and zinc are constituents of the spent nickel hydroxide bulk particles, and the dissolution of these metals was low (> 2-4.5%). Other researchers suggest that aluminum is intercalated into the nickel hydroxide bulk [37, 69, 74, 75]. In the current results (Figure 31) it is also suggested that aluminum is intercalated in the nickel hydroxide bulk, since aluminum dissolves with similar rates to the bulk-constituent metals nickel and zinc.

Both cobalt and manganese dissolved fast, and manganese completely, in ascorbic acid. Thus, it is reasonable to assume that both these metals exist at the surface of the cathode material. The reduction potential of the pairs Mn^{3+}/Mn^{2+} (1.54 V) and Co^{3+}/Co^{2+} (1.92 V) are both positive [107], and the reduction potential of ascorbic acid is negative in acidic solutions. Dissolution of these metals is therefore thermodynamically reasonable.

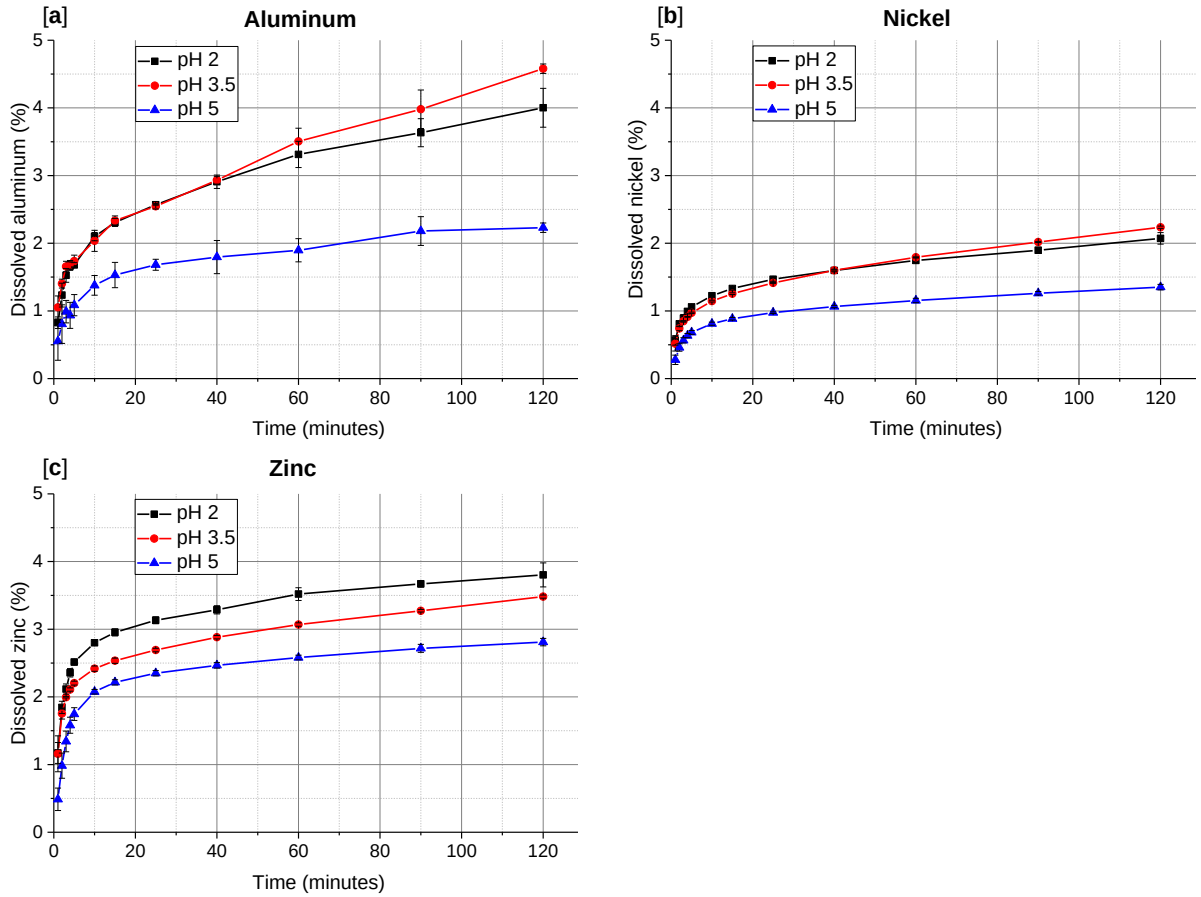

Figure 31. Dissolution of (a) aluminum (b) nickel and (c) zinc in 50 mL 1.5 M ascorbic acid/sodium hydrogen ascorbate solution at 20 °C, from 0.5 g cathode material. The acidities (pH) of the initial and final solutions were similar and have been approximated to the indicated pH values.

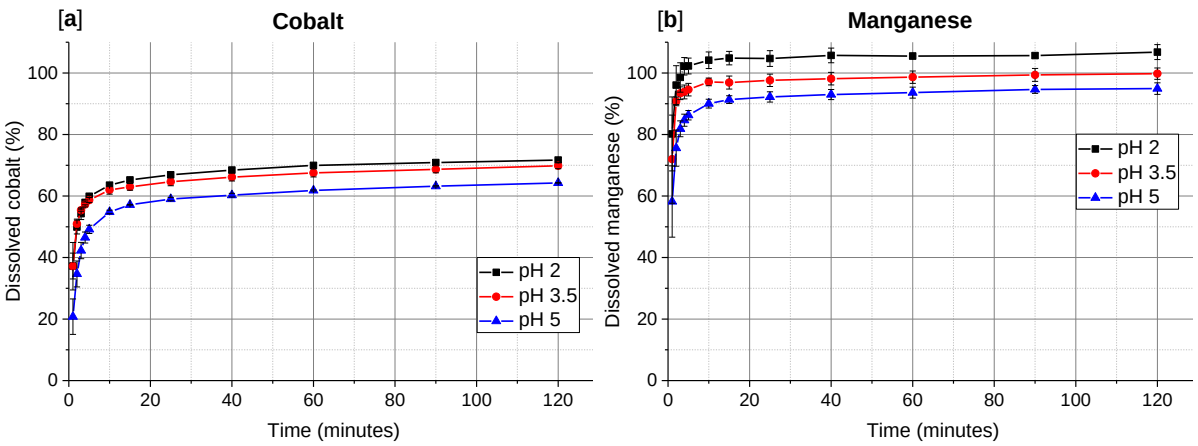

Figure 32. Dissolution of (a) cobalt and (b) manganese in 50 mL 1.5 M ascorbic acid/sodium hydrogen ascorbate solution at 20 °C, from 0.5 g cathode material. The acidities (pH) of the initial and final solutions were similar, and have been approximated to the indicated pH values.

Results from investigation of S/L ratio on the dissolution of cobalt and manganese are shown in Figure 33. Both the amount of manganese and the targeted cobalt are homogeneously distributed in the cathode material, as indicated by the similar amount of dissolved material. Existence of manganese in spent cathode material is a result of AB_5 alloy corrosion. It is therefore only logical that also manganese resides at the surface of the nickel hydroxide particles.

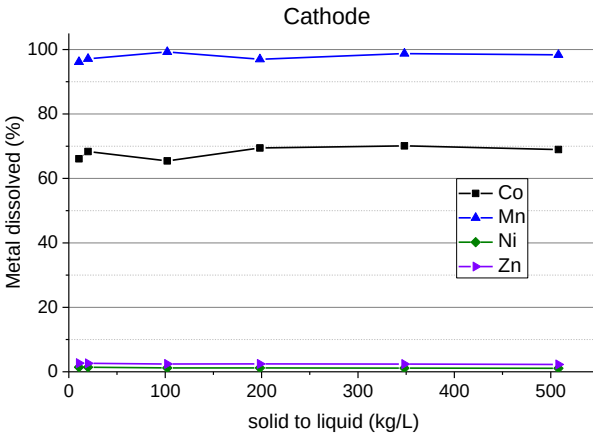

Figure 33. Dissolution cobalt, manganese, nickel and zinc in initially 1 M ascorbic acid solutions for 2 h at 20 °C, while varying the solid to liquid ratio (kg cathode/Liter solution).

With the results presented above it is indicated that ascorbic acid is useful for producing a concentrated cobalt solution from NiMH electrode waste. However, there are yet some aspects that need to be further investigated. In solutions with the highest amounts of dissolved metals (249 mmol/L Co, 10 mmol/L Mn, 56 mmol/L Ni and 3 mmol/L zinc) precipitation occurred during storage of the solution. Elemental analysis of the residual and filtered solutions showed reduced concentrations of all metals: cobalt (30.3%), manganese (7.6%), nickel (19.3%) and zinc (27%). From a recycling point of view this is an interesting result. It suggests that cobalt-enriched surface layers can be extracted relatively separately and then conveniently recovered as a solid compound.

5.4.1.2 Characterization of undissolved cathode materials

Cathode material was analyzed with SEM after ascorbic acid treatment (1 M for 2 h) and images of these samples are shown in Figure 34. These images show that spherical particles are still observed after treatment with ascorbic acid. In agreement with previous characterization of unspent and spent cathodes there are also observations of particles that have been shattered and/or cracked. Therefore the treatment using ascorbic acid cannot be regarded as a destructive method with respect to the shape of the particles.

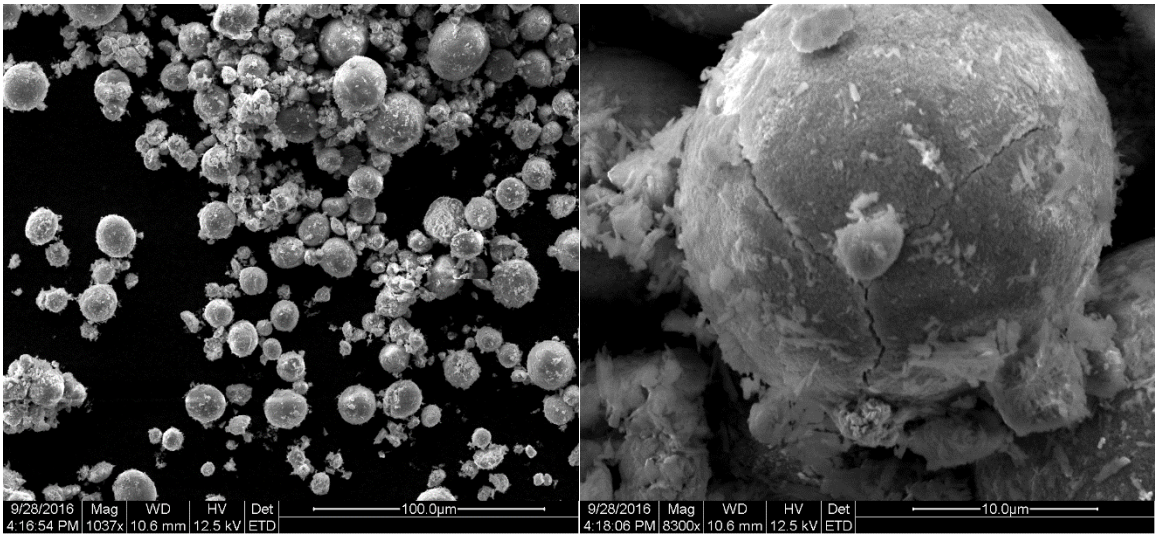

Figure 34. SEM images of cathode particles from analysis using Quanta 200 FEG ESEM. Both images show particles that have been treated with 1 M ascorbic acid for 2 h. The image to the right is at higher resolution.

A survey XPS spectrum was produced by analysis of several different cathode samples. In Figure 35 the results from analysis of unspent and spent cathode samples, and spent cathode sample, treated with 1 M ascorbic acid (2 h) can be seen. For the current result only the indicated peak Co $2p_{3/2}$ is of interest, which occurs at approximately 779.6 eV. The oxidation state of cobalt that is associated with this peak is discussed in more detail in the following paragraph, in which the results of narrow scans are presented. For now it is pointed out that this peak (779.6 eV) corresponds to certain cobalt compound(s). The peak position shows that such cobalt compound(s) only exist on samples that have not been treated with ascorbic acid.

Other peaks seen in Figure 35 are expected to be associated with other elements in the sample matrix (i.e. Ni) or impurities obtained from sample work up (Si, C, Na etc.).

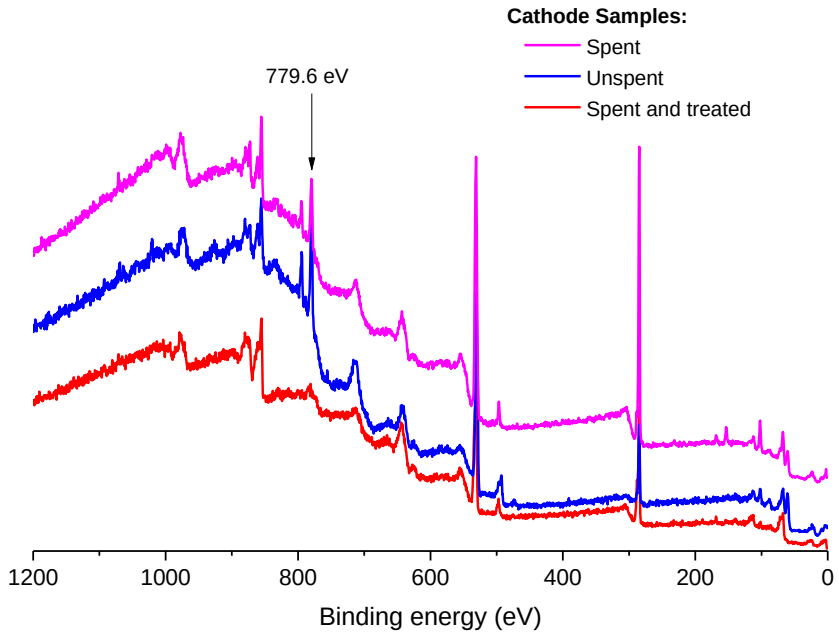

Figure 35. XPS survey spectrum of the three different sample types spent, unspent, and spent and treated cathode samples. Treated sample refers to treatment using 1 M ascorbic acid for 2 h.

At the immediate surface of both unspent and spent cathode particles a main peak at approximately 779.6 eV was detected, as can be seen in the narrow scan shown in Figure 36a. Binding energies at this energy correspond to cobalt $2p_{2/3}$. According to the literature, at this binding energy (779.5 eV) several cobalt compounds may give rise to the $2p_{2/3}$ spectral line, namely CoOOH, Co_2O_3 and Co_3O_4 [129]. Nonetheless, for these three compounds cobalt is at an elevated oxidation state, namely +2.7 (Co_3O_4) or +3 (CoOOH and Co_2O_3). As can be seen in these narrow scans, the cobalt compounds with oxidation states higher than 2 have been removed by treating the spent cathode samples in 1 M ascorbic acid solution for 2 h.

Narrow acquisition scans around 860 eV for spent and unspent cathode, and treated spent cathode samples are shown in Figure 36b. These results are presented in order to point out the presence of nickel at the surface, which is the most abundant metal in the cathode samples. Different nickel compounds ($Ni(OH)_2$, NiOOH and NiO) are associated with the peak broadening around the main peak (Ni $2p_{3/2}$, at 855.5 eV) [130]. It can be concluded that the surface speciation of nickel also varies, which can be expected due to complex surfaces. Interestingly, the nickel surface speciation does not appear to have changed during the ascorbic acid treatment.

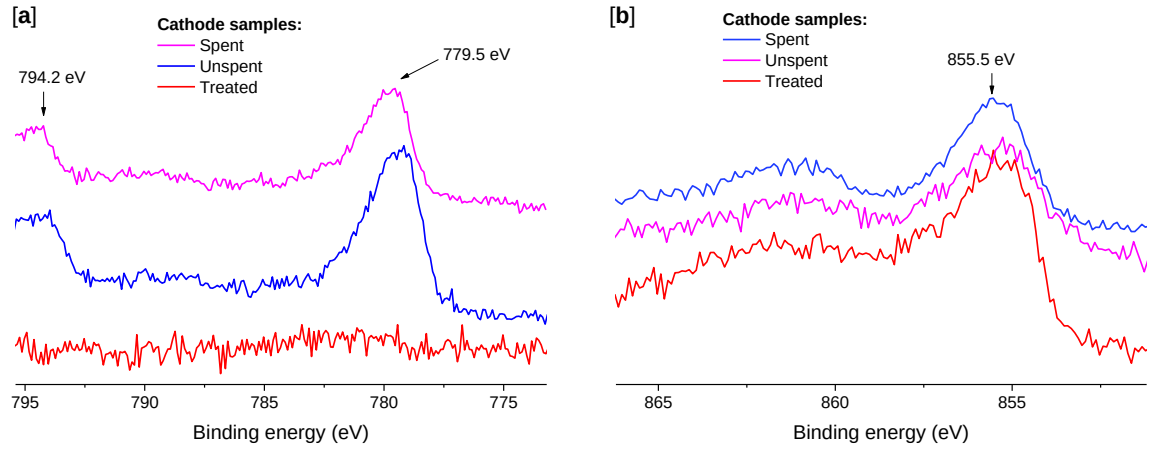

Figure 36. Narrow scans of different cathode samples, namely spent and unspent cathode samples, and spent samples treated with ascorbic acid (i.e. "treated"). In (a) spectral lines associated with Co $2p_{2/3}$ (779.5 eV) and Co $2p_{1/2}$ (794.2), on cathode samples. It can be seen that the sample treated with 1 M ascorbic acid (2 h) does not have any Co 2p peaks in this range (eV). In (b) spectral lines at around 855.5 eV correspond to Ni $2p_{3/2}$.

Detection of the contaminants aluminum and manganese was not possible with XPS. Aluminum is difficult to detect due to its low concentration (2 mg/g) in the material and the only peaks (2s and 2p) that could be expected in the measured range overlap with peaks corresponding to nickel 3s and 3p. Although the manganese peak of $2p_{3/2}$ also overlaps with the nickel auger line the Mn $2p_{1/2}$ should be detectable if the concentration is sufficiently high. However, the concentration is low (0.5 mg/g) in these samples. Therefore it is concluded that no significant manganese enrichment on the cathode surface could be detected using this method. Due to limited practical means of detecting manganese at such low concentrations its existence can only be speculated.

To verify that cobalt is enriched on the surfaces of spent cathode samples it was of interest to also analyze the depth profile. The result of this analysis is shown in Figure 37 and it can be seen that the concentration of nickel and cobalt varies with the depth. At the immediate top surface the concentration of cobalt is higher (25 at%) compared to deeper into the bulk, in which cobalt converges to < 10 at%. This confirms that cobalt is more located at the surface region.

With the presented XPS results it can be concluded that the cobalt-enriched surface on spent cathode materials can be removed by ascorbic acid. This also confirms the results obtained from dissolution experiments. Because the cobalt-enriched surface can be selectively dissolved, the ascorbic acid treatment may also be a practical means of evaluating the thickness of these layers.

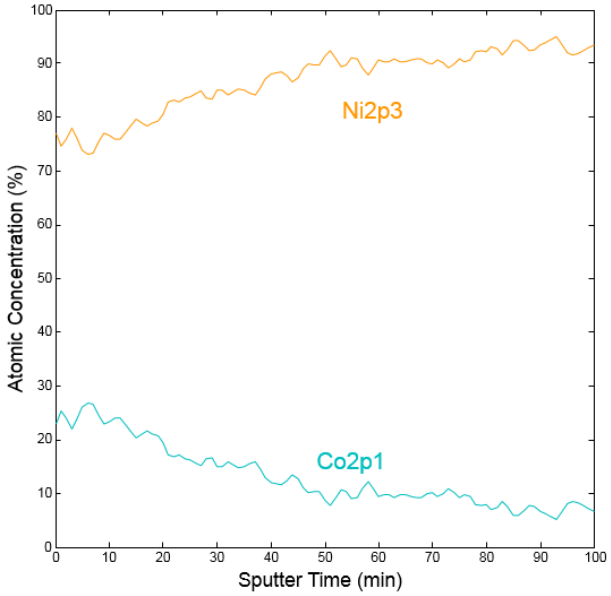

Figure 37. Depth profile (at%) of spent cathode sample using Ni $2p_{3/2}$ and Co $2p_{1/2}$ binding energies (indicated by legends Ni2p3 and Co2p1, respectively). The etching rate calibrated on Ta_2O_5 with these conditions is 4.76 nm/min.

5.4.2 Anode material

5.4.2.1 Leaching of anode

Dissolution of anode samples in 1 M ascorbic acid solutions are presented in Figure 38. The total amount of manganese in anode samples was 3.7 wt% and is mainly found in the AB_5 alloy bulk. The observation that only 4% of the total manganese content had dissolved suggests that only a little manganese (4% of 3.7 wt%) resides on the spent anode particle surfaces. This low amount makes it difficult to detect manganese compounds on the surface of the spent anode material. However, according to the observations made by Maurel et al. [72] manganese is solubilized in the electrolyte and then re-precipitates on the alloy particle surfaces as MnO(OH) (s) and $Mn(OH)_2$ (s). As previously pointed out, the reduction potential of the Mn^{3+}/Mn^{2+} pair is positive (1.54 V vs SHE) [107], and the reduction potential of ascorbic acid is negative in acidic solutions. An electrochemical cell formed from manganese (III) and ascorbic acid is therefore thermodynamically possible.

The results indicate that the physical and chemical properties of the hydrogen storage alloy particles have not been affected by the ascorbic acid treatment.

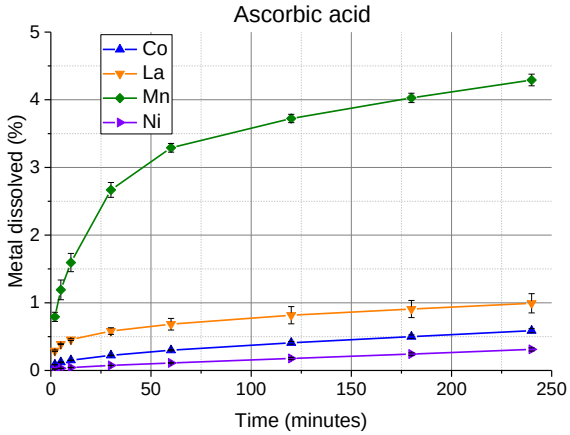

Figure 38. Dissolution of cobalt, lanthanum, manganese and nickel from anode materials using 1 M ascorbic acid solutions, at 20 °C and S/L ratio of 1/10.

5.4.2.2 Characterization of undissolved anode material

XRD analysis was performed on the collected undissolved anode samples from 1 M ascorbic acid treatment for 4 h (see Figure 39). As far as can be seen from the XRD analysis, only the $REE(OH)_3$, AB_5 alloy and Ni(s) phases can be detected. This result is in agreement with the insignificant dissolution that has been quantified through ICP-OES analysis. More importantly this result also indicates that no additional (crystalline) oxidation products have been formed during the treatment.

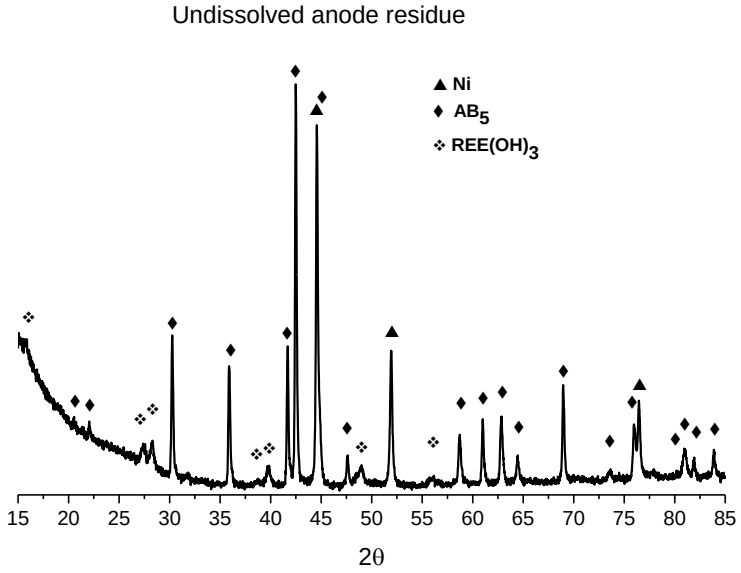

Figure 39. The figure show the relative intensities of the disposed anode material and after 4 h dissolution treatment of ascorbic acid. The suggested phases Ni, AB_5 alloy and $REE(OH)_3$ are consistent with JCPDS Card No: 01-070-1849 [126], 04-009-7537 [127] and 01-074-0665 [128], respectively.

SEM images of spent AB_5 alloy particles treated with ascorbic acid are presented in Figure 40. In agreement with XRD analysis it was possible to observe the $REE(OH)_3$ needles covering particle surfaces. Overall, the electron microscopy showed that the AB_5 particles remained in their original form. The comparison with previous SEM images (Figure 10) of unspent and spent AB_5 particles indicate that the ascorbic acid treated particles have not been completely destroyed. These results, coupled to results obtained through XRD and ICP-OES analysis, do not raise any suspicions that the ascorbic acid treatment destroys the AB_5 alloy material.

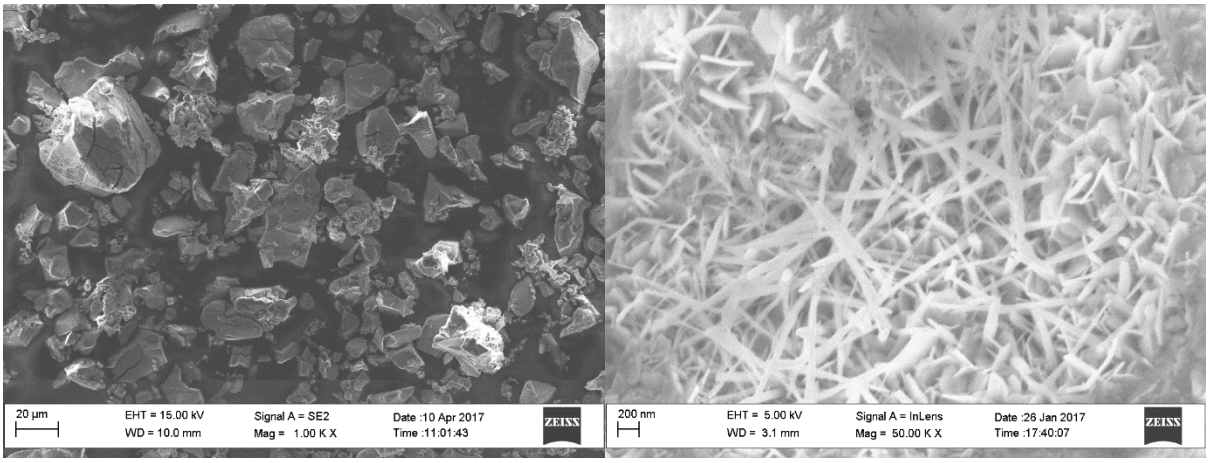

Figure 40. SEM images of anode particles treated with 1 M ascorbic acid for 4 h, using Ultra 55 FEG SEM. To the left, three different particle morphologies are observed. The particles in the background show two different morphologies, compared to the particle in focus. The right images show $REE(OH)_3$ needles at high resolution.

6. CONCLUSIONS

Recycling of NiMH batteries is important in order to recover economically and technologically important metals (Ni, Co, REEs), which can be used to sustain the needs of various markets, e.g. steel industry or new NiMH batteries. The intention of this work was to contribute to the development of sustainable recycling methods by investigating selective recovery of the components: (1) metallic nickel, (2) reusable AB_5 alloy and (3) cobalt.

6.1 Characterization of spent NiMH batteries

The aim of characterizing NiMH materials was to evaluate the feasibility of reusing some of its components. It was clearly shown from the characterization of spent bipolar NiMH batteries using ICP-OES, XRD, SEM and BET that the components did not completely degrade through battery cycling. Overall, the qualitative observations of degradation that were made are in agreement with previous investigations.

Ultimately, the feasibility of reusing some of the spent NiMH components cannot be addressed without practically testing new batteries made from recovered and regenerated components. Reusing the AB_5 alloy material from spent NiMH batteries appears most interesting. The increased surface area can be beneficial in further uses, and avoiding reproduction of this alloy from metal ingots reduces high consumption of energy. However, corrosion products such as $REE(OH)_3$ must be removed, in order to restore charge/discharge properties.

6.2 Recovery of metallic nickel

The intention of using hydrochloric acid to treat NiMH waste had the separate goals: (1) recovery of metallic nickel and (2) investigating compatibility of produced leachates with Cyanex 923 solvent extraction separation of metals.

Recovery of Ni(s) powder relies on strong chemisorption of hydrogen onto nickel surfaces, thus slowing down oxidation of nickel in acid solutions. At pH 1 the dissolution rate of Ni(s) powder is slower than the corresponding dissolution of the AB_5 alloy and nickel hydroxide components. Ni(s) powder can therefore be recovered by using a well-chosen leaching time. This is economically favorable for two reasons. Firstly, less acid is consumed while a relatively pure (96.6 wt%) Ni(s) powder fraction can be recovered. Secondly, extensive time to dissolve the Ni(s) powder can be avoided.

Compatibility of chloride leachates, with different levels of acidity, with Cyanex 923 was investigated. The results of this work re-confirmed that Cyanex 923 is useful for the separation of metals (Zn, La, Ce, Pr, Nd, Al, Mn, Co) from nickel, as has been stated previously by Larsson et al. [93]. It was demonstrated that excess addition of acid in the dissolution step will result in inhibited extraction of rare earth elements (La, Ce, Pr, Nd) and aluminum. Controlling the acidity of the produced leachate solution is therefore important, because extracting agent is consumed through preferential extraction of acid [114].

6.3 Recovery of reusable AB_5 alloy

This work set out to test carboxylic acids for the recovery of reusable AB_5 alloy, as had been previously proposed [115]. The results from this investigation indicated that the chemical separation of cathode and anode (including AB_5 alloy) was possible at 50 °C, using 1 M maleic acid for 60 min. However, much (50%) of the AB_5 alloy was also dissolved. Therefore, for practical recycling applications the uses of carboxylic (malonic, maleic, acetic and citric) acids are limited. Avoiding oxidation of AB_5 alloy in aqueous solutions is difficult, due to the AB_5 alloys electrochemical reactions with acid and water.

Another intention of using carboxylic acids was to slow down the dissolution of the anode material, in order to remove corrosion products without dissolving significant amount of the AB_5 bulk. The conclusions drawn from dissolution experiments as well as from XRD and SEM analyses were that it is possible to selectively remove $REE(OH)_3$ corrosion products using acetic or citric acid.

6.4 Recovery of cobalt

The aim of using ascorbic acid was to investigate if cobalt could be recovered selectively from cobalt-enriched surface layers on cathode nickel hydroxide particles. In a relatively short time (60 min) the dissolution of these layers was complete. The pH of the solutions did not influence the dissolution rate. Selective dissolution of cobalt-enriched surface layers is possible because the cobalt oxidation state(s) are higher than 2 (+2.7, +3 or a mix thereof), which is different compared to those of the other metallic or hydroxide components.

At a high S/L ratio (0.5 kg cathode material/L 1 M ascorbic acid solution) a concentrated leachate solution (249 mmol/L Co) was produced. It was also found that precipitation of cobalt, nickel, zinc and manganese compounds occurred in concentrated leachate solutions.

An interesting result was that manganese contamination, which had been detected in the spent cathode materials, was indicated to exist in the outermost layers of the nickel hydroxide particles. Complete dissolution of manganese was obtained after 40 min, in 1 M ascorbic acid solution.

The spent anode material was not affected by the ascorbic acid treatment, and therefore this treatment can be used as a pre-step in a method to recover useable AB_5 alloy.

7. FUTURE WORK

The work presented in the current thesis has suggested three different methods of extracting different valuable materials (Ni(s), AB_5 alloy and Co) from spent NiMH electrodes. These three methods are interesting to further investigate in order to develop and/or optimize practical recycling methods.

The feasibility of separating particles of metallic nickel from mixed electrode waste was demonstrated using hydrochloric acid. For recycling purposes, it is necessary to further investigate a practical method to control the amount of added acid. It is important to either completely dissolve the solid materials or control the acidity of the leachate solution. Addition of oxidation agents, such as hydrogen peroxide, may be useful to achieve complete Ni(s) dissolution. The effect of added chemicals to subsequent separation and steps needs to be considered. Controlling the acidity would be another alternative, which involves developing a practical method of measuring the rate of acid consumption.

Recovery of AB_5 alloy using aqueous method is challenging due to oxidation of AB_5 alloy through hydrogen reduction from water or acid. It is necessary to inhibit the surface oxidation. Nitrogen containing compounds (i.e. amines) have a high base strength and the free electron pairs on nitrogen can associate and bind to the metal surface. Potentially, amines can inhibit oxidation more than similar oxygen-containing compounds (i.e. carboxylic acids).

To separate cobalt using ascorbic acid in practical recycling it is recommended that further investigations of this system focus on the aqueous system perspectives (i.e. complex solubility). This recommendation is made due to observations of precipitation of cobalt, nickel, zinc and manganese in some leachate solutions, while attempting to scale up this method. It is also recommended that further investigations are designed to further evaluate the type of cobalt complex that is formed, in order to develop leachate treatment methods, e.g. solvent extraction.

8. ACKNOWLEDGEMENTS

There are many that have contributed to this work and the author would like to thank:

The Swedish Energy Agency for funding this work (project P37720-1: Process development for reuse and/or recycling of Nickel metal hydride batteries).

The battery manufacturer Nilar AB, through Stina Starborg and Erika Widenkvist Zetterström, for good cooperation, introduction to battery chemistry and production, and supplying batteries and materials.

Supervisor Britt-Marie Steenari for all her time, patience, support and guidance.

Assistant supervisors Martina Petranikova and Burcak Ebin for useful ideas and support through practical work.

The Examiner (Prof. Christian Ekberg) and Reviewers.

Stellan Holgersson for help with BET measurements.

Anders Kvist, Stefan Gustafsson and Britt-Marie for SEM introduction.

Britt-Marie and Burcak for help with XRD measurements.

Yu Cao for performing XPS analysis and data interpretations.

Rikard Ylmén for help with AAS, suggestions and computational contributions.

Fredrik Nyhlén for your good lab work and interesting ideas.

My current and former great colleagues at NC/IMR who helped to make this work possible.

My office-mate Toni Gutknecht for putting up with me and bringing laughter to the office space.

My whole family and all my friends who made this work possible.

My dear girlfriend Elin Hidebring for all your love and support.

Thank You All,
Filip Holmberg

Gothenburg, Sweden
May 2017

9. BIBLIOGRAPHY

1. Köhler, U., C. Antonius, and P. Bäuerlein, *Advances in alkaline batteries.* Journal of Power Sources, 2004. **127**(1-2): p. 45-52.
2. Biendicho, J.J., et al., *In situ investigation of commercial Ni(OH)2 and LaNi5-based electrodes by neutron powder diffraction.* Journal of Materials Research, 2015. **30**(3): p. 407-416.
3. Sato, N. and K. Yagi, *Thermal behavior analysis of nickel metal hydride batteries for electric vehicles.* JSAE review, 2000. **21**(2): p. 205-211.
4. Taniguchi, A., et al., *Development of nickel/metal-hydride batteries for EVs and HEVs.* Journal of Power Sources, 2001. **100**(1-2): p. 117-124.
5. Taheri, P., M. Yazdanpour, and M. Bahrami, *Analytical assessment of the thermal behavior of nickel–metal hydride batteries during fast charging.* Journal of Power Sources, 2014. **245**: p. 712-720.
6. *Battery module produced at Nilar AB*. www.nilar.com.
7. The European Commisson. *Directive 2006/66/EC of the european parliament and of the council*. 2006 [cited 2015 02-10]; Available from: ec.europa.eu.
8. European Rare Earths Compentency Network. *Strengthening the european rare earths supply-chain*. 2015; Available from: http://ec.europa.eu/.
9. Umicore. Available from: www.umicore.com.
10. Nickel-Hütte Aue GMBH. Available from: http://www.nickelhuette.com/.
11. Lin, S.-L., et al., *Characterization of spent nickel–metal hydride batteries and a preliminary economic evaluation of the recovery processes.* Journal of the Air & Waste Management Association, 2016. **66**(3): p. 296-306.
12. Shanghai Metals Market. 2017-02-10]; Available from: www.metal.com.
13. Eckelman, M.J., *Facility-level energy and greenhouse gas life-cycle assessment of the global nickel industry.* Resources, Conservation & Recycling, 2010. **54**(4): p. 256-266.
14. The European Commisson, *Report on critical raw materials for the EU*. 2014: ec.europa.eu.
15. U.S. Department of Energy. *Critical Materials Strategy*. 2010 [cited 2016 11-12]; Available from: energy.gov.
16. Binnemans, K., et al., *Recycling of rare earths: a critical review.* Journal of Cleaner Production, 2013. **51**(0): p. 1-22.
17. Alonso, E., et al., *Evaluating rare earth element availability: A case with revolutionary demand from clean technologies.* Environmental Science and Technology, 2012. **46**(6): p. 3406-3414.
18. Sullivan, J.L. and L. Gaines, *Status of life cycle inventories for batteries.* Energy Conversion and Management, 2012. **58**: p. 134-148.
19. *A review of battery life-cycle analysis: State of knowledge and critical needs*. 2011. p. 91-133.
20. Majeau-Bettez, G., T.R. Hawkins, and A.H. StrØmman, *Life cycle environmental assessment of lithium-ion and nickel metal hydride batteries for plug-in hybrid and battery electric vehicles.* Environmental Science and Technology, 2011. **45**(10): p. 4548-4554.
21. Ye, Z., et al., *Metal hydrides for high-power batteries.* MRS Bulletin, 2013. **38**(6): p. 504-508.
22. Ye, Z., et al., *Oxygen and hydrogen gas recombination in NiMH cells.* Journal of Power Sources, 2012. **208**: p. 232-236.
23. Bäuerlein, P., et al., *Progress in high-power nickel–metal hydride batteries.* Journal of Power Sources, 2008. **176**(2): p. 547-554.
24. Reddy, T., *Linden's Handbook of Batteries (4th Edition)*. 2010: McGraw-Hill Professional Publishing.
25. Fetcenko, M.A., et al., *Recent advances in NiMH battery technology.* Journal of Power Sources, 2007. **165**(2): p. 544-551.
26. Encyclopædia Britannica. *lanthanoid contraction*. 2011 [cited 2017 02-15]; Available from: https://global.britannica.com/science/lanthanoid-contraction.
27. Kleperis, J., et al., *Electrochemical behavior of metal hydrides.* Journal of Solid State Electrochemistry, 2001. **5**(4): p. 229-249.

28. Percheron-Guégan, A. and J.-M. Welter, *Preparation of intermetallics and hydrides*. Hydrogen in Intermetallic Compounds I, ed. L. Schlapbach. 1988: Springer.
29. Schlapbach, L., et al., *Surface effects and the formation of metal hydrides.* Journal of The Less-Common Metals, 1980. **73**(1): p. 145-160.
30. Khaldi, C., et al., *Corrosion effect on the electrochemical properties of LaNi 3.55Mn0.4Al0.3Co0.75 and LaNi 3.55Mn0.4Al0.3Fe0.75 negative electrodes used in Ni-MH batteries.* Materials Science and Engineering B: Solid-State Materials for Advanced Technology, 2010. **175**(1): p. 22-28.
31. MCBreen, J. and J.J. Reilly, *Synthesis and characterization of metal hydride electrodes*. 1995, Division of chemical sciences: New York.
32. Bode, H., K. Dehmelt, and J. Witte, *Zur kenntnis der nickelhydroxidelektrode—I. Über das nickel (II)-hydroxidhydrat1.* Electrochimica Acta, 1966. **11**(8): p. 1079-1087.
33. Hall, D.S., et al., *Nickel hydroxides and related materials: a review of their structures, synthesis and properties.* PROCEEDINGS OF THE ROYAL SOCIETY A-MATHEMATICAL PHYSICAL AND ENGINEERING SCIENCES, 2015. **471**(2174): p. 20140792-20140792.
34. Bode, H., K. Dehmelt, and J. Witte, *Zur kenntnis der nickelhydroxidelektrode—I.Über das nickel (II)-hydroxidhydrat.* Electrochimica Acta, 1966. **11**(8): p. 1079-IN1.
35. Besenhard, J.O., *Handbook of battery materials*. 1999, Weinheim: Wiley-VCH.
36. Chen, J., et al., *The effect of Zn(OH)(2) addition on the electrode properties of nickel hydroxide electrodes.* Journal of Materials Research, 1999. **14**(5): p. 1916-1921.
37. Leblanc, P., *MECHANISM OF ALLOY CORROSION AND CONSEQUENCES ON SEALED NICKEL-METAL HYDRIDE BATTERY PERFORMANCE.* Journal of the Electrochemical Society, 1998. **145**(3): p. 860-863.
38. Li, L., F. Wu, and K. Yang, *Degradation analysis of nickel/metal hydride battery and its electrode materials.* Trans. Nonferrous Met. Soc. China, 2004. **14**(3).
39. Shinyama, K., et al., *Deterioration mechanism of nickel metal-hydride batteries for hybrid electric vehicles.* Journal of Power Sources, 2005. **141**(1): p. 193-197.
40. Mavis, B., *Homogeneous Precipitation of Nickel Hydroxide Powders*. 2009.
41. Liu, L.P., Z.T. Zhou, and C.H. Peng, *Sonochemical intercalation synthesis of nano gamma-nickel oxyhydroxide: Structure and electrochemical properties.* Electrochimica Acta, 2008. **54**(2): p. 434-441.
42. Hu, B., et al., *Controllable Synthesis of Zinc-Substituted α- and β-Nickel Hydroxide Nanostructures and Their Collective Intrinsic Properties.* Chemistry – A European Journal, 2008. **14**(29): p. 8928-8938.
43. Dou, S.X., J.B.D.H. Chen, and H.K. Liu, *Nickel hydroxide as an active material for the positive electrode in rechargeable alkaline batteries.* Journal of the Electrochemical Society, 1999. **146**(10): p. 3606-3612.
44. Pickett, D.F. and J.T. Maloy, *MICROELECTRODE STUDIES OF ELECTROCHEMICALLY COPRECIPITATED COBALT HYDROXIDE IN NICKEL HYDROXIDE ELECTRODES.* Journal of the Electrochemical Society, 1978. **125**(7): p. 1026-1032.
45. Ratke, L., et al., *Growth and Coarsening: Ostwald Ripening in Material Processing*. Vol. 1. 2002, Berlin, Heidelberg: Springer Berlin Heidelberg.
46. Peng, M.-x., et al., *Template growth mechanism of spherical Ni(OH)2.* Journal of Central South University of Technology, 2007. **14**(3): p. 310-314.
47. Van Bomme, A. and J.R. Dahn, *Analysis of the growth mechanism of coprecipitated spherical and dense nickel, manganese, and cobalt-containing hydroxides in the presence of aqueous ammonia.* Chemistry of Materials, 2009. **21**(8): p. 1500-1503.
48. Chang, Z., et al., *Influence of preparation conditions of spherical nickel hydroxide on its electrochemical properties.* Journal of Power Sources, 1998. **74**(2): p. 252-254.
49. Tsai, I.C., Y.Y. Wang, and C.C. Wan, *Effect of synthesis method on the properties of Ni(OH)(2) for Ni/MH batteries.* JOURNAL OF NEW MATERIALS FOR ELECTROCHEMICAL SYSTEMS, 2001. **4**(2): p. 99-106.

50. Shangguan, E.B., et al., *Comparative structural and electrochemical study of high density spherical and non-spherical Ni(OH)(2) as cathode materials for Ni-metal hydride batteries.* Journal of Power Sources, 2011. **196**(18): p. 7797-7805.
51. Shangguan, E., et al., *Effects of different Ni(OH)(2) precursors on the structure and electrochemical properties of NiOOH.* International Journal of Hydrogen Energy, 2011. **36**(16): p. 10057-10064.
52. Li, L., et al., *Recovery of Ni, Co and rare earths from spent Ni–metal hydride batteries and preparation of spherical Ni(OH)2.* Hydrometallurgy, 2009. **100**(1–2): p. 41-46.
53. Zhang, W., et al., *Effect of nickel hydroxide composition on the electrochemical performance of spherical Ni(OH)2 positive materials for Ni–MH batteries.* International Journal of Hydrogen Energy, 2009. **34**(1): p. 473-480.
54. Oshitani, M., et al., *Development of a pasted nickel electrode with high active material utilization.* Journal of the Electrochemical Society, 1989. **136**(6): p. 1590-1593.
55. Ying, T., *Surface modification of nickel hydroxide particles by micro-sized cobalt oxide hydroxide and properties as electrode materials.* Surface & Coatings Technology, 2005. **200**(7): p. 2376-2379.
56. Chang, Z., H. Tang, and J.G. Chen, *Surface modification of spherical nickel hydroxide for nickel electrodes.* Electrochemistry Communications, 1999. **1**(11): p. 513-516.
57. Wang, X.Y., et al., *Electrochemical characteristics of nickel hydroxide modified by electroless cobalt coating.* International Journal of Hydrogen Energy, 1998. **23**(10): p. 873-878.
58. Wang, X., et al., *Surface modification and electrochemical studies of spherical nickel hydroxide.* Journal of Power Sources, 1998. **72**(2): p. 221-225.
59. Benson, P., G.W.D. Briggs, and W.F.K. Wynne-Jones, *The cobalt hydroxide electrode-I. Structure and phase transitions of the hydroxides.* Electrochimica Acta, 1964. **9**(3): p. 275-280.
60. Ye, Z., et al., *Ni-MH battery electrodes made by a dry powder process.* Journal of the Electrochemical Society, 1995. **142**(12): p. 4045-4050.
61. Naboychenko, S.S., I.B. Murashova, and O.D. Neikov, *Production of Cobalt and Cobalt-Alloy Powders*. 2009, Elsevier Science & Technology. p. 399-408.
62. Capus, J.M., *Chapter 5 - Technical overview — Metal powder production*, in *Metal Powders (Fourth Edition)*, J.M. Capus, Editor. 2005, Elsevier Science: Oxford. p. 153-165.
63. Lancashire, R.J. *Nickel Chemistry*. 2010 [cited 2015 02-15]; Available from: wwwchem.uwimona.edu.jm/courses/nickel.html.
64. Mond, L., C. Langer, and F. Quincke, *Action of carbon monoxide on nickel.* Journal of the Chemical Society, Transactions, 1890. **57**: p. 749.
65. *Possible selective solar photothermal absorber: Ni dendrites formed on Al surfaces by the CVD of Ni (Co) 4. (USA).* Vacuum, 1978. **28**(8): p. 377-377.
66. Beattie, J.K., A.F. Masters, and J.T. Meyer, *Nickel carbonyl cluster complexes.* Polyhedron, 1995. **14**(7): p. 829-868.
67. Monnier, J., et al., *Identification of a new pseudo-binary hydroxide during calendar corrosion of (La, Mg).sub.2Ni.sub.7-type hydrogen storage alloys for Nickel-Metal Hydride batteries.* Journal of Power Sources, 2014. **266**: p. 162.
68. Ruiz, F.C., et al., *Effect of electrolyte concentration on the electrochemical properties of an AB5-type alloy for Ni/MH batteries.* International Journal of Hydrogen Energy, 2013. **38**(1): p. 240-245.
69. Zhou, X., et al., *Degradation mechanisms of high-energy bipolar nickel metal hydride battery with AB5 and A2B7 alloys.* Journal of Alloys and Compounds, 2013. **580**(1): p. S373-S377.
70. Hu, W.K., et al., *Effect of long-term overcharge and operated temperature on performance of rechargeable NiMH cells.* Journal of Power Sources, 2006. **159**(2): p. 1478-1483.
71. Ikoma, M., et al., *Effect of alkali-treatment of hydrogen storage alloy on the degradation of Ni/MH batteries.* Journal of Alloys and Compounds, 1999. **284**(1): p. 92-98.

72. Maurel, F., B. Knosp, and M. Backhaus-Ricoult, *Characterization of corrosion products of AB5-type hydrogen storage alloys for nickel-metal hydride batteries.* Journal of the Electrochemical Society, 2000. **147**(1): p. 78-86.
73. Iwakura, C., et al., *Self-discharge mechanism of nickel-hydrogen batteries using metal hydride anodes.* Journal of the Electrochemical Society, 1989. **136**(5): p. 1351-1355.
74. Wang, C.S., et al., *Corrosion behaviour of AB5-type hydride electrodes in alkaline electrolyte solution.* Journal of Applied Electrochemistry, 2003. **33**(3): p. 325-331.
75. Li Li, W.F., Yang Kai, Wang Jing, Chen., *Electrochemical performance of nickel／metal hydride batteries under unconventional conditions and degradation analysis.* Transactions of Nonferrous Metals Society of China, 2004. **14**(1): p. 208-214.
76. Kong, L., et al., *Effects of Al- and Mn-contents in the negative MH alloy on the self-discharge and long-term storage properties of Ni/MH battery.* Journal of Power Sources, 2012. **213**: p. 128-139.
77. Shinyama, K., et al., *Investigation into the deterioration in storage characteristics of nickel-metal hydride batteries during cycling.* Journal of Power Sources, 2005. **143**(1): p. 265-269.
78. Young, K., et al., *Microstructures of the oxides on the activated AB2 and AB5 metal hydride alloys surface.* Journal of Alloys and Compounds, 2014. **606**: p. 97-104.
79. Sherif, S.A., et al., *Handbook of Hydrogen Energy*. 2014, Boca Raton: CRC Press.
80. Guerlou-Demourgues, L., C. Denage, and C. Delmas, *New manganese-substituted nickel hydroxides.* Journal of Power Sources, 1994. **52**(2): p. 269-274.
81. Mantuano, D.P., et al., *Analysis of a hydrometallurgical route to recover base metals from spent rechargeable batteries by liquid-liquid extraction with Cyanex 272.* Journal of Power Sources, 2006. **159**(2): p. 1510-1518.
82. Pietrelli, L., et al., *Characterization and leaching of NiCd and NiMH spent batteries for the recovery of metals.* Waste Management, 2005. **25**(2): p. 221-226.
83. Junmin, N., et al., *Dismantling, Recovery, and Reuse of Spent Nickel-Metal Hydride Batteries.* Journal of the Electrochemical Society, 2006. **153**(1): p. A101-A105.
84. Zhang, P., et al., *Recovery of metal values from spent nickel–metal hydride rechargeable batteries.* Journal of Power Sources, 1999. **77**(2): p. 116-122.
85. Zhang, P., et al., *Hydrometallurgical process for recovery of metal values from spent nickel-metal hydride secondary batteries.* Hydrometallurgy, 1998. **50**(1): p. 61-75.
86. Rodrigues, L.E.O.C. and M.B. Mansur, *Hydrometallurgical separation of rare earth elements, cobalt and nickel from spent nickel–metal–hydride batteries.* Journal of Power Sources, 2010. **195**(11): p. 3735-3741.
87. Wu, F., et al., *Recovery of valuable metals from anode material of hydrogen-nickel battery.* Transactions of Nonferrous Metals Society of China, 2009. **19**(2): p. 468-473.
88. Pietrelli, L., et al., *Rare earths recovery from NiMH spent batteries.* Hydrometallurgy, 2002. **66**(1–3): p. 135-139.
89. Fernandes, A., J.C. Afonso, and A.J.B. Dutra, *Separation of nickel(II), cobalt(II) and lanthanides from spent Ni-MH batteries by hydrochloric acid leaching, solvent extraction and precipitation.* Hydrometallurgy, 2013. **133**(0): p. 37-43.
90. Tzanetakis, N. and K. Scott, *Recycling of nickel–metal hydride batteries. I: Dissolution and solvent extraction of metals.* Journal of Chemical Technology & Biotechnology, 2004. **79**(9): p. 919-926.
91. Innocenzi, V. and F. Vegliò, *Recovery of rare earths and base metals from spent nickel-metal hydride batteries by sequential sulphuric acid leaching and selective precipitations.* Journal of Power Sources, 2012. **211**: p. 184-191.
92. Larsson, K., C. Ekberg, and A. Ødegaard-Jensen, *Dissolution and characterization of HEV NiMH batteries.* Waste Management, 2013. **33**(3): p. 689-698.
93. Larsson, K., et al., *Using Cyanex 923 for selective extraction in a high concentration chloride medium on nickel metal hydride battery waste: Part II: Mixer-settler experiments.* Hydrometallurgy, 2013. **133**: p. 168-175.

94. Provazi, K., et al., *Metal separation from mixed types of batteries using selective precipitation and liquid–liquid extraction techniques.* Waste Management, 2011. **31**(1): p. 59-64.
95. Tzanetakis, N. and K. Scott, *Recycling of nickel–metal hydride batteries. II: Electrochemical deposition of cobalt and nickel.* Journal of Chemical Technology & Biotechnology, 2004. **79**(9): p. 927-934.
96. Innocenzi, V. and F. Veglio, *Separation of manganese, zinc and nickel from leaching solution of nickel-metal hydride spent batteries by solvent extraction.* Hydrometallurgy, 2012. **129-130**: p. 50-58.
97. Nayl, A.A., *Extraction and separation of Co(II) and Ni(II) from acidic sulfate solutions using Aliquat 336.* Journal of hazardous materials, 2010. **173**(1): p. 223-230.
98. Juang, R.-S. and H.-C. Kao, *Extraction separation of Co(II)/Ni(II) from concentrated HCl solutions in rotating disc and hollow-fiber membrane contactors.* Separation and Purification Technology, 2005. **42**(1): p. 65-73.
99. Rice, N., H. Irving, and M. Leonard, *Nomenclature for liquid-liquid distribution (solvent extraction)(IUPAC Recommendations 1993).* Pure and applied chemistry, 1993. **65**(11): p. 2373-2396.
100. Bard, A.J., et al., *Electrochemical Dictionary*. 1. Aufl. ed. 2008, Berlin, Heidelberg: Springer Berlin Heidelberg.
101. Lupi, C. and D. Pilone, *Ni–MH spent batteries: a raw material to produce Ni–Co alloys.* Waste Management, 2002. **22**(8): p. 871-874.
102. Nan, J., et al., *Recovery of metal values from a mixture of spent lithium-ion batteries and nickel-metal hydride batteries.* Hydrometallurgy, 2006. **84**(1–2): p. 75-80.
103. Dixini, P.V.M., et al., *Recycling of the anode from spent Ni-MH batteries for synthesis of the lanthanide oxysulfide/oxysulfate compounds used in an oxygen storage and release system.* Journal of Power Sources, 2014. **260**(0): p. 163-168.
104. Bertuol, D.A., A.M. Bernardes, and J.A.S. Tenório, *Spent NiMH batteries—The role of selective precipitation in the recovery of valuable metals.* Journal of Power Sources, 2009. **193**(2): p. 914-923.
105. Jones, D.A., *Principles and prevention of corrosion*. Vol. 2. 1996, Englewood Cliffs, N.J: Prentice Hall.
106. Atkins, P.W. and L. Jones, *Chemical principles: the quest for insight*. Vol. 4. 2008, New York: W.H. Freeman.
107. Vanýsek, P., *CRC Handbook of Chemistry and Physics*. 87 ed. 2006, Boca Raton, Florida: CRC Press.
108. Christmann, K., et al., *Adsorption of hydrogen on nickel single crystal surfaces.* The Journal of Chemical Physics, 1974. **60**(11): p. 4528-4540.
109. Konvalinka, J., P. Vanoeffelt, and J. Scholten, *Temperature programmed desorption of hydrogen from nickel catalysts.* Applied Catalysis, 1981. **1**(3-4): p. 141-158.
110. McCafferty, E., *Introduction to corrosion science*. 2010, New York: Springer.
111. Speight, J., et al., *Lange's Handbook of Chemistry*. Vol. 16th,Anniversary,Special,Revis;16th;. 2004, Blacklick;New York;: McGraw-Hill Professional Publishing.
112. Rydberg, J., ed. *Solvent extraction principles and practice*. 2004, Marcel Dekker Inc.
113. Larsson, K., *Hydrometallurgical treatment of NiMH batteries*. 2012, Chalmers University of Technology: Göteborg.
114. Alguacil, F.J. and F.A. López, *The extraction of mineral acids by the phosphine oxide Cyanex 923.* Hydrometallurgy, 1996. **42**(2): p. 245-255.
115. Smith, W.N. and S. Swoffer, *Process for the Recovery of AB5 Alloy from Used Nickel/Metal Hydride Batteries*. 2014, Google Patents.
116. Martell, A.E. and R.M. Smith, *Critical stability constants: Vol. 3, Other organic ligands*. 1977, Ney York: Plenum.

117. Amin, M.A., H. Shokry, and E.M. Mabrouk, *Nickel Corrosion Inhibition in Sulfuric Acid-Electrochemical Studies, Morphologies, and Theoretical Approach.* Corrosion, 2012. **68**(8): p. 699.
118. Ferreira, E.S., et al., *Evaluation of the inhibitor effect of l-ascorbic acid on the corrosion of mild steel.* Materials Chemistry and Physics, 2004. **83**(1): p. 129-134.
119. Amin, M.A., et al., *The inhibition of low carbon steel corrosion in hydrochloric acid solutions by succinic acid.* Electrochimica Acta, 2007. **52**(11): p. 3588-3600.
120. Tizpar, A. and Z. Ghasemi, *The corrosion inhibition and gas evolution studies of some surfactants and citric acid on lead alloy in 12.5 M H2SO4 solution.* Applied Surface Science, 2006. **252**(24): p. 8630-8634.
121. Du, J., J.J. Cullen, and G.R. Buettner, *Ascorbic acid: Chemistry, biology and the treatment of cancer.* Biochimica et Biophysica Acta - Reviews on Cancer, 2012. **1826**(2): p. 443-457.
122. Borsook, H. and G. Keighley, *Oxidation-reduction Potential of Ascorbic Acid (Vitamin C).* Proceedings of the National Academy of Sciences of the United States of America, 1933. **19**(9): p. 875-878.
123. Buettner, G.R. and B.A. Jurkiewicz, *Catalytic Metals, Ascorbate and Free Radicals: Combinations to Avoid.* Radiation Research, 1996. **145**(5): p. 532-541.
124. Li, L., et al., *Ascorbic-acid-assisted recovery of cobalt and lithium from spent Li-ion batteries.* Journal of Power Sources, 2012. **218**: p. 21-27.
125. Casas-Cabanas, M., Rodriguez-Carvajal, J., Canales-Vazquez, J., Palacin, M. J., *New insights on the microstructural characterization of nickel hydroxides and correlation with electrochemical properties.* Mater. Chem. 16, 2925 (2006).
126. *Construction et mise a point d`une chambre de precision pour siagrammes de rayons X a haute temperature.* Diament, R. Met. Corros.-Ind. 31, 167 (1956).
127. Chartouni D., K.N., Otto A., Guther V., Nutzenader C., Zuttel A., *Influence of the alloy morphology on the kinetics of AB5-type metal hydride electrodes.* Alloys Compd. 293, 292 (1999).
128. Mullica, D.F., Oliver, J.D., Milligan, W.O., *Cerium Trihydroxide.* Acta Crystallogr. Sec. B: Struct. Crystallogr. Cryst. Chem. 35, 2668 (1979).
129. Bomben, K.D., et al., *Handbook of x-ray photoelectron spectroscopy. A reference bookof standard spectra for identification and interpretation of xpsdata*. 1995, Eden Prairie, MN: Physical Electronics.
130. Grosvenor, A.P., et al., *New interpretations of XPS spectra of nickel metal and oxides.* Surface Science, 2006. **600**(9): p. 1771-1779.
131. *Joint Committee of Powder Diffraction Standards*, JCPDS-ICCD, Editor. 2010: Philadelphia, USA.
132. Brunauer, S., P.H. Emmett, and E. Teller, *Adsorption of gases in multimolecular layers.* Journal of the American Chemical Society, 1938. **60**(2): p. 309-319.

APPENDIX I: ANALYSIS TECHNIQUES

I. A Qualitative analysis of crystalline compounds by X-ray diffraction (XRD)

Solid samples were analyzed using X-ray diffraction (XRD) instrument Bruker AXS. The samples were exposed to characteristic Cu K_α irradiation and the diffracted X-rays were detected with a scintillation detector. Identification of crystalline compounds was made by comparison with standards in the Joint Committee of Powder Diffraction Standard database [131].

I. B Scanning electron microscope (SEM) imaging of particles

Imaging of solid sample surfaces was carried out using an Ultra 55 field emission gun (FEG) scanning electron microscope (SEM) and Quanta 200 FEG environmental SEM (ESEM). Both these instruments were equipped with Oxford Inca energy dispersive X-ray (EDX) detectors. Acceleration voltages were between 5 and 15 kV.

I. C Elemental composition using inductively coupled plasma optical emission spectroscopy (ICP-OES)

An inductively coupled plasma optical emission spectrometer (iCAP6500) was used for determining concentrations of elements in solutions. Samples were diluted in 0.7 M suprapure nitric acid (65 wt%, Sigma Aldrich) and compared to external calibration, prepared from standard stock solutions (1000 ppm, Ultra Scientific). The limit of quantification was determined as 10σ of the standard deviation of the blank (matrix) solution.

I. D Solid sample surface area measurement using Brunauer-Emmett-Teller (BET) method

The specific surface area (m^2/g) of samples was measured using the Brunauer-Emmett-Teller (BET) method [132]. Nitrogen gas was used for adsorption determination, kept isothermal at 77 K using liquid nitrogen, using a Micrometrics ASAP 2020. The temperature was ramped with 10 °C/min to 100 °C, and kept at this temperature for 60 min under vacuum (300 µmHg).

I. E X-ray photoelectron spectroscopy (XPS) analysis of surface species

The X-ray photoelectron spectroscopy (XPS) analyses were carried out using a PHI 5000 VersaProbe III instrument. The AlK_α (1486.6 eV) X-ray source using monochromator was used to generate photoelectrons. Acquisition conditions for the survey spectra (0-1100 eV) were 140 eV pass energy, 45° take off angle with 0.5 eV/step. Selected region spectra were recorded covering the Ni $2p_{3/2}$, Co $2p_{3/2}$ and C 1s photoelectron peaks. The acquisition conditions were then 26 or 55 eV pass energy, 45° take off angle and 0.1 eV/step. The samples were mounted on a removable tape and flooded with low energy electrons and argon ions, in order to compensate for charge. C 1s (284.8 eV) was used for reference.

The depth profiling was carried out by successive ion etchings and XPS analyses using Ni $2p_{3/2}$ and $Co2p_{1/2}$ peaks, using an argon beam of 2kV over an area of 2x2 mm^2. The etching rate calibrated on Ta_2O_5 with these conditions is 4.76 nm/min.